SHIBAURA INSTITUTE OF TECHNOLOGY

Cylinder Pressure-Based Adaptive Air-Fuel Ratio Control and Compression Heat Transfer Analysis

by

Chanyut Khajorntraidet

A thesis submitted in partial fulfillment for the
degree of Doctor of Philosophy

in the
Functional Control Systems
Graduate School of Engineering and Science

September 2016

Declaration of Authorship

I, Chanyut Khajorntraidet, declare that this thesis titled, 'Cylinder Pressure-Based Adaptive Air-Fuel Ratio Control and Compression Heat Transfer Analysis' and the work presented in it are my own. I confirm that:

- This work was done wholly or mainly while in candidature for a research degree at this University.

- Where any part of this thesis has previously been submitted for a degree or any other qualification at this University or any other institution, this has been clearly stated.

- Where I have consulted the published work of others, this is always clearly attributed.

- Where I have quoted from the work of others, the source is always given. With the exception of such quotations, this thesis is entirely my own work.

- I have acknowledged all main sources of help.

- Where the thesis is based on work done by myself jointly with others, I have made clear exactly what was done by others and what I have contributed myself.

Signed:
_____

Date:
_____

"This Page Intentionally Left Blank"

SHIBAURA INSTITUTE OF TECHNOLOGY

Abstract

Functional Control Systems
Graduate School of Engineering and Science

Doctor of Philosophy

by Chanyut Khajorntraidet

This thesis presents cylinder pressure-based adaptive air-fuel ratio control and compression heat transfer analysis. In the first main part, we focus on the air-fuel ratio (AFR) estimation and control. The static AFR calculation model based on in-cylinder pressure data and on the adaptive AFR control strategy is presented. The model utilizes the intake manifold pressure, engine speed, total heat release, and the rapid burn angle, as input variables for the AFR computation. The combustion parameters, total heat release, and rapid burn angle, are calculated from in-cylinder pressure data. This proposed AFR model can be applied to the virtual AFR sensor for the feedback control system. In practical applications, simple adaptive control (SAC) is applied in conjunction with the AFR model for port-injected fuel control. The experimental results show that the proposed model can estimate the AFR, and the accuracy of the estimated value is applicable to the feedback control system. Additionally, the adaptive controller with the AFR model can be applied to regulate the AFR of the port injection SI engine. For the second part, we present an estimation method for the compression heat transfer and its application. Based on the first law of thermodynamics, ideal gas law, and some assumptions, the state-space model for the compression process can be derived. During the compression stroke, the heat transfer to, or from, the cylinder walls can be computed using the least squares regression. The identification results show that the proposed method can estimate the amount of heat transfer and its direction. Additionally, these results can be applied to evaluate the polytropic exponent variation, which is affected by heat transfer. This variation is mainly attributed to both the quantity and direction of heat transfer. Moreover, we also discuss the analysis methodology and possible ways for improvement of the heat transfer estimation method.

Acknowledgements

Contents

List of Figures

List of Tables

Abbreviations

AFR	Air Fuel Ratio
BDC	Bottom Dead Center
CAD	Crank Angle Degree
DIS	Direct Injection System
DOHC	Double Over Head Camshaft
ECU	Engine Control Unit
EFI	Electronic Fuel Injection
EGO	Exhaust Gas Oxygen
HCCI	Homogeneous Charge Compression Ignition
HRR	Heat Release Rate
HR	Heat Release
HHV	High Heating Value
LHV	Low Heating Value
RGF	Residual Gas Fraction
RSS	Residual Sum of Squares
SAC	SimpleAdaptive Control
SI	Spark Ignition
TDC	Top Dead Center
TWC	Three Way Catalytic converter
VVT	Variable Valve Timing

Physical Constants

Specific heat of air at volume constant	c_v	$=$	718 J/(kg·K)
Specific heat of air at pressure constant	c_p	$=$	1005 J/(kg·K)
Low heating value of gasoline	Q_{LHV}	$=$	43.45 MJ/kg
Gas constant of air	R	$=$	287 J/(kg·K)
Specific heat ratio of air	γ	$=$	1.4
Density of Gasoline	$\rho_{gasoline}$	$=$	748.9 kg/m^3
Density of Air	ρ_{air}	$=$	1.22 kg/m^3

Symbols

I	identity matrix	-
J	moment of inertia	kg·m/rad
k	complexity parameter	-
k_{e_y}	error adaptation gain	-
k_{u_m}	input signal adaptation gain	-
k_{x_m}	state adaptation gain	-
m	mass	kg
N	speed	rev/min
p	pressure	Pa
p_c	in-cylinder pressure	Pa
p_m	intake manifold pressure	Pa
p_{amb}	ambient pressure	Pa
Q_{tot}	total heat release in one working cycle	J
T	temperature	K
T_{amb}	ambient temperature	K
U	internal energy	J
V	volume	m^3
W	work	J
Y	output vector	-
α	fuel factor	-
α_0	model constant offset	-
$\Delta\theta$	rapid burn angle	Degree

ϵ	parameter vector	-
γ_P	adjustable gain for adaptation rate	-
γ_I	adjustable gain for adaptation rate	-
λ_0	stoichiometric air-fuel ratio	-
ϕ	throttle angle	Degree
Φ	regressor matrix	-
τ_e	engine torque	N·m
τ_L	load torque	N·m
θ	crank angle	Degree

For my family

Chapter 1

Introduction

The aim of this chapter is to introduce methodologies for spark ignition (SI) engines control and analysis based on in-cylinder pressure measurement. The content will begin with the historical view of SI engine control and follow by the brief review of in-cylinder pressure based air-fuel ratio (AFR) control. Then, literature of adaptive control on engine control application will be presented. Subsequently, an introduction of heat transfer analysis based on in-cylinder pressure measurement will be addressed. The objectives and contribution of this thesis including its overview are then explained. Finally, the list of publications related to this thesis is presented.

1.1   Historical View of Spark Ignition Engine Control

SI engines have been known as fundamental power sources of vehicles for a long time. This kind of engine system contains a large number of control loops. There are many main objectives for the design of these feedforward and feedback control systems. First, the driver's demand for instant torque response, good drivability, and low fuel consumption must be satisfied. Second, the engine system must be kept in a safe operating region. For example, damage to or fatigue of the material should be avoided, knocking must be prevented, the catalytic converter must not overheat, etc. Finally, the emission regulations must be met. In the vehicle equipped with SI engines, it requires a rapid light-off of the catalytic converter, precise stationary AFR control, and good compensations of the transient phenomena [1]. A general engine management system is based on the calibrated open-loop control including the feedback compensation. Many technologies have been introduced for improvement of engine performance and emission, for

example, downsized boosting, cylinder pressure sensing, and dilute combustion. With increasing demand on emissions and driving performance, high efficiency controller is required.

Nowadays, the majority of modern passenger cars are still equipped with port (indirect) injection SI gasoline engines. The torque of a stoichiometric SI engine is controlled by the quantity of air/fuel mixture in the cylinder during each stroke. Typically, this quantity is varied by changing the intake pressure, and hence, the density of the air/fuel mixture. Most SI engines used in passenger cars are equipped with three-way catalytic (TWC) converter. The introduction of the TWC in after treatment system caused a revolution in the combustion engine industry and research community. In order to get high conversion efficiency for all three pollutants, the ratio of the masses of air and fuel in the combustion chamber has to stay within a very narrow band surrounding the stoichiometric ratio [2]. Due to the TWCs ability to store oxygen and carbon monoxide on its surface, short excursions of the AFR can be tolerated as long as they do not exceed the remaining storage capacity and the mean deviation is kept below 0.1 %. These two observations require the AFR control system to comprise both an approximate but fast feedforward control to handle transients as well as a slow but precise feedback control-loop to ensure the required high steady-state accuracy. The ratio of air to fuel is very important for the combustion process of internal combustion engines. The AFR control system is improved by the introduction of the exhaust gas oxygen sensor (EGO), and electronic fuel injection (EFI). The EGO sensor can provide a feedback signal which indicate lean or rich condition of the AFR in the exhaust system.

Regarding control system development, mathematical models play an important role in advanced engine control. They will be used for model based control and analysis, and also be the basis for sensor fusion, adaptive control, and supervision. The demands of reduced emission and advanced diagnosis functionality are steadily increased by legislators and customers. The key areas that help meeting the increased demands are the development of control and diagnosis functions in the control units [3]. Moreover, the reduction of measured sensors leads to an important improvement of the feedback control system price and complexity. The most important transducer should be satisfied both for measurement and analysis. Therefore, an in-cylinder pressure is considered for this task.

To meet emission legislation, some effective strategies of closed loop control will be required. In-cylinder pressure is a fundamental variable, which characterizes the combustion process. Monitoring the cylinder pressure in each cylinder allows the engine to

be operated at optimum conditions. With this measured signal, combustion parameters and AFR can be calculated. Additionally, the AFR control can be performed without AFR sensor.

1.2 AFR Estimation and Control Based In-Cylinder Pressure Data

Rassweiler and Withrow [4] have presented the first attempt at a cylinder pressure based model of combustion in an internal combustion engines. They develop an empirical model, which states that the amount of mass burnt, is proportional to the difference between the measured cylinder pressure, and the cylinder pressure obtained from polytropic compression and expansion. Subsequently, in the work of Blizard and Keck [5], the flame propagation in a spark ignition engine is predicted by using thermodynamics, a turbulence model, and chemical kinetics. The predictions are compared with cylinder pressure measurements. In the research presented by Gatowski et al. [6], a one-zone model based on the first law of thermodynamics is used to compute the heat release in a spark ignition engine from crank angle resolved cylinder pressure measurements. In practical applications, the in-cylinder pressure has been considered as a dominant indicator of combustion performance in internal combustion engines. Therefore, the combustion control and analysis can be performed on the basis of in-cylinder pressure data. In many studies, in-cylinder pressure is utilized for combustion analysis and control of SI engines [7–10].

The combustion control and analysis can be performed based on the in-cylinder pressure measurement, for example, crank angle position at 50% of mixture is burned (CA50), knocking and AFR control. In addition, the combustion efficiency can be analyzed by using the cylinder pressure signal. However, this signal cannot be applied directly because it includes the offset and effects of heat transfer. Hence, there are some required conditioning processes that should be proceed carefully such as offset compensation and filter design for noise reduction. Moreover, mismatching between crank angle and cylinder pressure data leads to some calculation errors of combustion parameters.

For the application on AFR estimation, many researches have presented the method for AFR estimation based on in-cylinder pressure data. For example, Gilkey and Powell [11] have applied a cylinder pressure moment approach for AFR estimation. They developed an empirical relationship between various moments of crank angle resolved cylinder

pressure traces and cylinder AFR. Patrick [12] has developed a model based method of estimating AFR from cylinder pressure. Using molecular weight approach, the model relies on the fact that the number of moles in the cylinder increases with combustion. The ratio of the number of moles before and after combustion can be obtained from cylinder pressure and temperature before and after combustion by applying the ideal gas law. Since the mass in the cylinder stays the same throughout compression, combustion, and expansion, this ratio is the same as the ratio of average molecular weights after compared to before combustion. Therefore, estimated AFR can be determined from the average molecular weights of burned and unburned charge at chemical equilibrium. Leisenring and Yurkovich [13] have utilized an equivalent heat release duration approach which is interpreted as the crank angle at which instantaneous release of Q Joules of heat would result in a heat release moment of M, and is thus a measure of the combustion duration. AFR estimation model is obtained from the equivalent heat release duration correlated with cylinder AFR through experiments.

The estimation of AFR is quite challenging in the application in AFR control system for a feedback control signal. This is because of many reasons such as low accuracy, high variation, and limitation of working condition. Moreover, based on cylinder pressure data, the variation of combustion affects directly to estimated value of AFR. Consequently, the improvement of AFR model has been interested.

1.3 Literature Review on Applications of Adaptive Control

The words adaptive systems and adaptive control have been used as early as 1950 [14, 15]. This generic definition of adaptive systems has been used to label approaches and techniques in a variety of areas. Adaptive control specific definition can be defined as follows: Adaptive control is the combination of a parameter estimator, which generates parameter estimates online, with a control law in order to control classes of plants whose parameters are completely unknown and/or could change with time in an unpredictable manner. Adaptive control as defined above has also been referred to as identifier-based adaptive control in order to distinguish it from other approaches referred to as non-identifier-based, where similar control problems are solved without the use of an online parameter estimation [16]. An adaptive controller is formed by combining an on-line parameter estimator, which provides estimates of unknown parameters at each instant, with a control law that is motivated from the known parameter case. The parameter

estimator is combined with the control law gives rise to two different approaches. In the first approach, referred to as indirect adaptive control, the plant parameters are estimated on-line and used to calculate the controller parameters. This approach has also been referred to as explicit adaptive control, because the design is based on an explicit plant model. In the second approach, referred to as direct adaptive control, the plant model is parameterized in terms of the controller parameters that are estimated directly without intermediate calculations involving plant parameter estimates. This approach has also been referred to as implicit adaptive control because the design is based on the estimation of an implicit plant model [17].

Research in adaptive control has a long history of intense activities. Model reference adaptive control was suggested by Whitaker et al. in [18, 19] to solve the autopilot control problem. The sensitivity method and the MIT rule was used to design the adaptive laws of the various proposed adaptive control schemes. An adaptive pole placement scheme based on the optimal linear quadratic problem was suggested by Kalman in [20]. The adaptive control is one of an effective control methodologies which is very useful for control various dynamic systems. Model reference adaptive control (MRAC) has been utilized for many control applications see also [21–23]. Many results have already been reported on the applications of MRAC. Some researches have applied MRAC for the engine control applications, for example, [24].

The simplified adaptive control methodology, called simple adaptive control (SAC), shows that practical adaptive control can be both simple and robust under certain conditions. In particular, SAC has been developed to avoid the use of identifiers, observer-based controllers and, in general, to avoid using higher order adaptive controllers in the control loop. This controller can be modified such that both perfect asymptotic tracking in ideal conditions and robustness in non-ideal conditions can be guaranteed [25]. SAC methodology requires the controlled plant to satisfy a so-called almost strictly positive realness (ASPR) condition [26]. Because most plants may not satisfy this condition, various forms of parallel feedforward configurations have been developed to satisfy the condition, thus extending SAC applicability to almost all practical applications. This adaptive control performs perfect tracking even when the linear time-invariant solution does not exist. It is shown that the adaptation performs a steepest descent minimization of the errors, ultimately ending with the appropriate set of control gains that fit the particular input command and initial conditions [27].

1.4 Heat Transfer Analysis Based In-cylinder Pressure Measurement

Heat transfer in internal combustion engine is also the important losses which have highly effects in combustion analysis. This part of heat losses is mainly caused by convection to the combustion chamber walls. The effects of combustion heat transfer have been studied for improvement of combustion processes and emissions. This issue is highly challenging because of the limitation of combustion information obtained from measurement. Several papers have researched on the effects of heat transfer in internal combustion engines, for example, [28–32]. This heat loss is an important part of the energy balance, which influences gas temperature and pressure, piston work, engine performance, and emissions as presented in [33]. Heat transfer becomes more important as the combustion process ends and average gas temperature peak. The combination of the loss mechanisms, crevice effect and heat transfer, also makes it hard to identify the separate effects [34]. The estimation of heat transfer during the compression and combustion strokes allows representing the system during the combustion. However, the heat transfer model contains strong nonlinearities and is difficult to implement in the heat release modeling. Therefore, this part of energy losses is always neglected in the heat release calculation process.

Because of important effects of heat transfer, there are many efforts for estimation and analysis of heat transfer. This analysis contains many effects of combustion, for example, unburned loss, crevice effect, and heat transfer. Especially, effects of combustion heat transfer have been studied for improvement of combustion processes and emissions. This issue is highly challenging because of the limitation of combustion information obtained from measurements. In practical applications, the effects of heat transfer during compression are separated from the heat release during combustion. Then, it is possible to identify the compression heat transfer and its direction by using in-cylinder information. This amount of heat transfer affects the variation of polytropic exponent which is used for calculation of the pressure offset value. Hence, this is reasonable to use the compression heat transfer for the calculation improvement. Moreover, if the heat transfer effects are compensated precisely, we can improve the combustion parameters calculation using accurate compensated pressure. However, the estimation of the compression heat transfer is highly challenging because of limitations of measured data.

1.5   Contributions and Thesis Outline

Two applications of in-cylinder pressure for the AFR control of a port injection SI engine and the compression heat transfer analysis are organized as follows:

In the first part, this thesis presents the possible method to estimate and control AFR of a port injection SI engine using an in-cylinder pressure sensor. We have proposed the AFR estimation model using in-cylinder pressure data that can replace the AFR sensor in the engine control system. Using the regression technique, we can identify the AFR model parameters and also adjust the coefficients of the proposed model properly. There are many benefits obtained from this identification technique such as solving the singular problem and shrinking model parameters. The proposed model can estimate AFR accurately at the identified conditions. The precise model can be replaced with the AFR sensor in feedback loop. Hence, this model has been utilized for AFR calculation in an application of the simple adaptive control system. For the control application, we have introduced the simple adaptive control which is an efficient control method for control the dynamic system. It shows high performance to track controlled output to the desired reference and reject the system disturbance. Based on the introduced method, the experimental results show that the adaptive controller with the proposed AFR model can regulate the AFR of port injection SI engine. However, because of combustion variation, the cycle moving average is required. This reason leads to some delay time in the estimated AFR response. Especially, the response is quite slow under transient operating conditions. Hence, we also discuss on the control performance of the proposed system.

For the second part, we explain the compression heat transfer estimation as an analyzed application. On the basis of in-cylinder pressure measurement, the compression heat transfer estimation strategy is addressed. We apply the heat transfer model included some assumptions for identification of the heat transfer. The off-line calculation with some experimental data show that the proposed method can identify the amount of compression heat transfer and its direction. Additionally, using the estimated heat transfer, we can evaluate the variation of polytropic exponent cycle-by-cycle. This results can be utilized for combustion analysis of SI engine. However, because of limitations of measuring data and some ideal assumptions, the possible ways for the model improvement are also discussed.

The arrangements of this thesis are as follows.

In chapter 2, we presented the SI engine basics which contain the detail of a basic SI engine modeling. In this modeling, air subsystem, fuel subsystem, crank shaft subsystem, and a problem formulation are expressed. Then, we explain the combustion process model of SI engine and some phenomena happening during combustion. Subsequently, the relationship between in-cylinder pressure and AFR is introduced by consideration of the theoretical model. Additionally, the performance of this model is investigated. Finally, the thermodynamic model and the simplified compression heat transfer model for compression heat transfer estimation are expressed.

Subsequently, in chapter 3, thermodynamic analysis of SI combustion and in-cylinder pressure measurement are expressed. The combustion variation in SI engine is then discussed. Next, for in-cylinder pressure measurement, the experimental set-up, measurement procedure, pressure offset identification, and results validation are expressed. Also, method for combustion parameters calculation which will be used in AFR estimation model is included in this chapter. Finally, some examples of in-cylinder pressure application will be presented.

Next, in chapter 4, first, we will introduce the AFR estimation method and its control application. Second, the AFR estimation model, the AFR model identification and model validation are explained. Third, the design of a simple adaptive controller for AFR control is presented. This adaptive controller have implemented with the proposed AFR model. Fourth, some important phenomena in fueling control have considered. Then, the experimental results on the controller performance and the effects of controller parameters are investigated. Finally, the controller performance analysis is discussed.

Then, in chapter 5, the application of in-cylinder pressure for compression heat transfer estimation is introduced. Subsequently, the compression heat transfer modeling, the model identification which composes of data collection, identification procedure, identification results, and model validation are expressed. Then, the application of estimated heat transfer is explained. Finally, all results are discussed.

Finally, in chapter 6, we present the conclusion of this thesis including AFR estimation model and performance of SAC controller. Then, we conclude the results of the compression heat transfer analysis and its application. Additionally, future works on AFR estimation model, controller performance improvement, heat transfer analysis, are discussed.

For the detail of in-cylinder pressure compensation and the stability proof of the SAC controller, they are explained in appendixes.

A flow chart of the dissertation is presented in Fig. 1.1.

- -

Chapter 2: Spark Ignition Engine Basic and System Modeling

Spark Ignition Engine Geometry

| Spark Ignition Engine Modeling | | Spark Ignition Combustion |

| Compression Heat Transfer Model | | Air-fuel Ratio Estimation Model |

- -
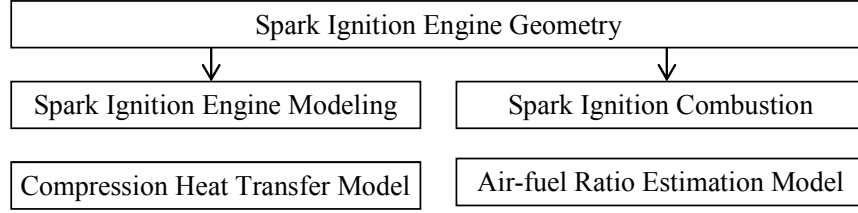
Chapter 3: Thermodynamic Analysis and Cylinder Pressure Measurement

| Thermodynamic Analysis | | In-cylinder Pressure Measurement |

| Possible Applications of In-Cylinder Pressure Based |

- -

Chapter 4: Air-Fuel Ratio Estimation and Control

| Adaptive Control Design | | Air-Fuel Ratio Estimation |

| Adaptive Fueling Control based Cylinder Pressure Data |

- -
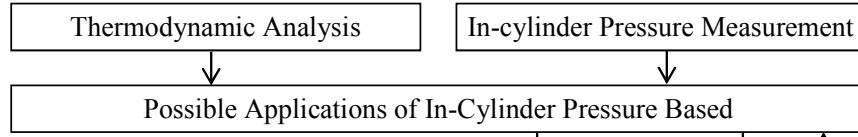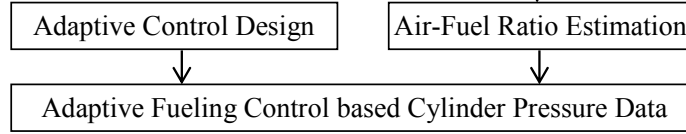
Chapter 5: Compression Heat Transfer Estimation

| Compression Heat transfer Estimation |

| Polytropic Exponent Variation |
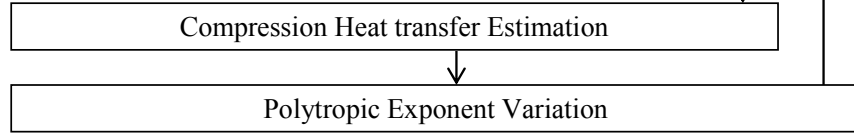
FIGURE 1.1: Flow chart of the dissertation

1.6 Publications

The main contributions of this thesis are the subject of the following publications:

[Chapter 4]

- C. Khajorntraidet and K. Ito, Simple Adaptive Air-fuel Ratio Control of a Port Injection SI Engine with a Cylinder Pressure Sensor, Journal of Control Theory and Technology, Vol. 13, No. 2, pp.141-150, May 2015.

- C. Khajorntraidet, K. Ito and T. Shen, Improvement of Air Fuel Ratio Model using a Least Absolute Shrinkage and Selection Operator, Proceeding of the MSAM 2015, August 23-24, 2015, Phuket, Thailand.

- C. Khajorntraidet, K. Ito and T. Shen, Adaptive Time Delay Compensation for Air-Fuel Ratio Control of a Port Injection SI Engine, Proceeding of the SICE Annual Conference 2015, July 27-30, 2015, Hangzhou, China.

[Chapter 5]

- C. Khajorntraidet and K. Ito, An Application of In-Cylinder Pressure for Compression Heat Transfer Estimation, Proceedings of the 8th IFAC Symposium on Advances in Automotive Control-AAC 2016, June 20-23, 2016, Kolmarden Wildlife Resort, Sweden.

- C. Khanjorntraidet and K. Ito, An Application of the Parameter-Influence Technique for a Reduced Heat Transfer Model Identification, Proceedings of the10th SEATUC Symposium 2016, OS-A2-05, February 22-24, 2016, SIT, Japan.

Chapter 2

Spark Ignition Engine Basics and System Modeling

In this chapter, first, the geometry of SI engine is explained. The SI engine modeling which consists of, intake manifold subsystem, fuel subsystem, crank shaft subsystem, and problem formulation are then presented. Subsequently, the basis of SI engine combustion and some effects from combustion are expressed. The theoretical relation of in-cylinder pressure and AFR is then expressed. Finally, the thermodynamic model for compression process are presented.

2.1 Introduction

The basis of system model obtained from physical system is a fundamental knowledge for control engineering. The fundamental system modeling of engines always consider mean-value model for controller design. This kind of system model can represent the average behavior of the considered system. We focus on the basic system of the SI engine which can be used for AFR control. The important parts are intake manifold, fuel path, and sensor dynamics. For the crank shaft dynamics, it is important for power generation and speed control. The AFR estimation model using in-cylinder pressure data obtained from theoretical relation is also reviewed. This model is designed based on the available measurement data and the in-cylinder information. Additionally, the thermodynamic model for compression process is explained. This model will be applied for compression heat transfer estimation in the second part of this research.

2.2 SI Engine Geometry

This section presents some basic geometrical relationships and the parameters of a reciprocating engine. From Heywood [35], the parameters defined the basic geometry of a reciprocating engine is illustrated in Fig. 2.1. The compression ratio is defined as
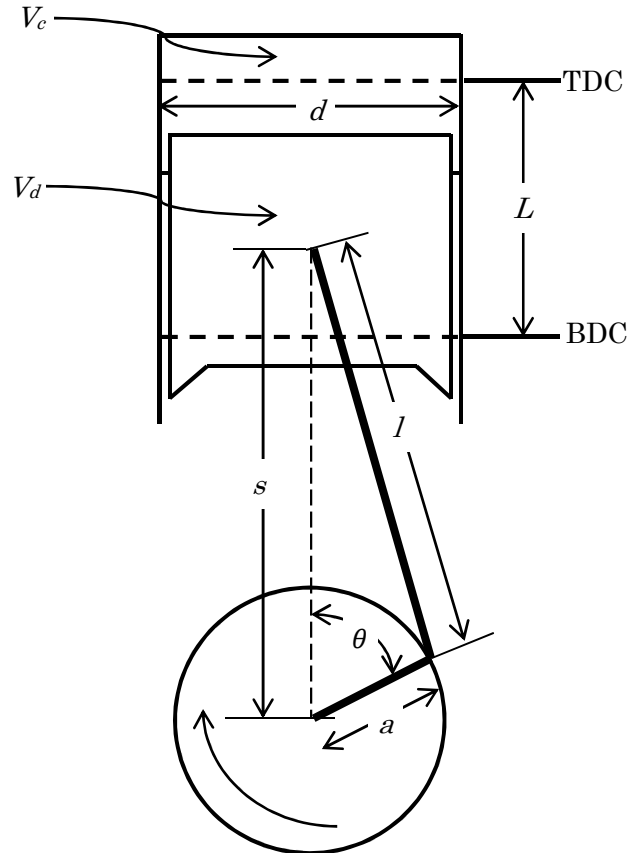
FIGURE 2.1: Geometry of cylinder (Heywood, 1988)

$$r_c = \frac{V_d + V_c}{V_c} \tag{2.1}$$

where V_d is the displaced or swept volume and V_c is the clearance volume. Ratio of cylinder bore to piston stroke:

$$R_{ds} = \frac{d}{L} \tag{2.2}$$

Ratio of connecting rod length to crank radius:

$$R = \frac{1}{a} \tag{2.3}$$

The stroke and crank radius are related by

$$L = 2a \tag{2.4}$$

Typical values of these parameters for SI engines are: $r_c = 8$ to 10; $d/L = 0.8$ to 1.2 and $R = 3$ to 4 for small and medium size engines. The cylinder volume V at any crank position θ is

$$V = V_c + \frac{\pi d^2}{4}(l + a + s) \tag{2.5}$$

where s is the distance between the crank axis and the piston pin axis (see Fig. 2.1) and is given by

$$s = a\cos\theta + \left(l^2 - a^2\sin^2\theta\right)^{1/2} \tag{2.6}$$

The angle θ, defined as shown in Fig. 2.1, is called the crank angle. The above equation can be rearranged:

$$\frac{V}{V_c} = 1 + \frac{1}{2}(r_c - 1)\left(R + 1 - \cos\theta - \left(R^2 - \sin^2\theta\right)^{1/2}\right) \tag{2.7}$$

The combustion chamber surface area A at any crank position θ is given by

$$A = A_{ch} + A_p + \pi d \left(l + a - s\right) \tag{2.8}$$

where A_{ch} is the cylinder head surface and A_p the piston crown surface area. For flat-topped pistons, $A_p = (\pi d^2)/4$, Using (2.6), (2.8) can be rewritten:

$$A = A_{ch} + A_p + \frac{\pi dL}{2}\left(R + 1 - \cos\theta - \left(R^2 - \sin^2\theta\right)^{1/2}\right) \tag{2.9}$$

An important characteristic speed is the mean piston speed $\bar{S}_p$:

$$\bar{S}_p = 2LN \tag{2.10}$$

where N is the rotational speed of the crank shaft. Mean piston speed is often a more appropriate parameter than crank rotational speed for correlating engine behavior as a function of speed. For example, gas flow velocities in the intake and the cylinder all scale with $\bar{S}_p$. The instantaneous speed piston velocity S_p is obtained from

$$S_p = \frac{ds}{dt} \tag{2.11}$$

The piston velocity is zero at top dead center (TDC), reaches maximum near the middle of the stroke, and decreases to zero again at bottom dead center (BDC). Differentiation

of (2.6) and substitution yields

$$\frac{S_p}{\bar{S}_p} = \frac{\pi}{2} \sin \theta \left(1 + \frac{\cos \theta}{\left(R^2 - \sin^2 \theta \right)^{1/2}} \right) \tag{2.12}$$

Resistance to gas flow into the engine or stresses due to the inertia of the moving parts limit the maximum mean piston speed to with in the range 8 to 15 (Heywood, 1988).

2.3 SI Engine Modeling

In this section, three parts of engine mean-value model subsystem, intake manifold, port injection and crank shaft subsystem, are presented. The simplified system of the SI engine is shown in Fig. 2.2.
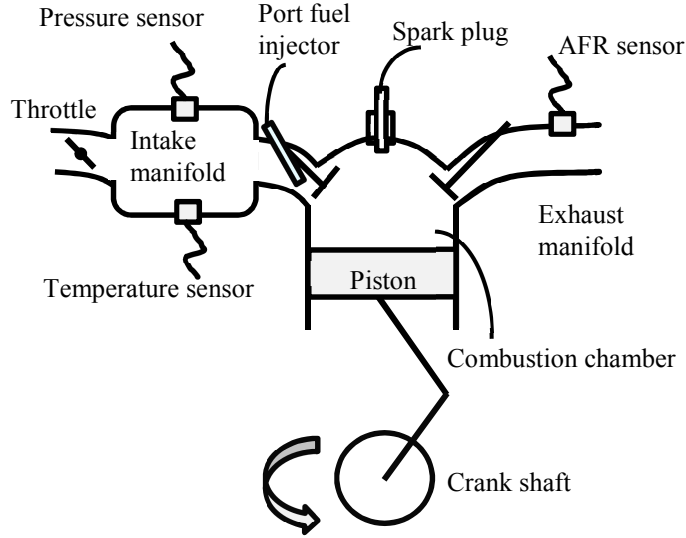
FIGURE 2.2: Simplified sketch of SI engine.

2.3.1 Intake Manifold Subsystem

The intake manifold can be modeled as a receiver. The inputs and outputs are the mass and energy flows, the reservoirs store mass and thermal energy, [36] and the level variables are the pressure and temperature. If one assumes that no heat or mass transfer through the walls and that no substantial changes in potential or kinetic energy in the flow occur, then the following two coupled differential equations describe such a receiver [1]. The throttle angle, temperature, pressure and other factors affect the mass flow

rate of air mass going into the combustion chamber. Assuming that the fluids can be modeled as ideal gases. Dynamics of air path can be estimated by the equation

$$
\begin{aligned}
\dot{p}_m &= c_0(\dot{m}_{ai} - \dot{m}_{ao}) \\
\dot{m}_{ao} &= c_m p_m \omega_e \\
\dot{m}_{ai} &= c_p u_{th}
\end{aligned}
\tag{2.13}
$$

with $c_0 = \frac{RT_m}{V_m}$, $c_m = \frac{\rho_a V_c \eta}{4\pi p_a}$, $c_p = s_0 \frac{p_a}{\sqrt{RT_a}} \Psi(p_m/p_a)$, $u_{th} := (1 - \cos\phi)$, where R is the gas constant, T_m the manifold temperature, V_m the manifold volume, ρ_a, T_a, p_a are density, temperature, and pressure of the ambient air, respectively. The total volume of engine combustion chamber is denoted by V_c, the volumetric efficiency is denoted by η. The parameter ω_e is the engine speed, s_0 is the throttle area, u_{th} is throttle control signal related to the throttle angle ϕ, and $\Psi(\cdot)$ is the flow function.

2.3.2 Fuel Injection Subsystem

The fuel path provides the cylinder with the necessary fuel for the combustion process. Both indirect and direct fuel injection systems are in use [37]. The indirect injection can be realized as port injection in SI engines. Most SI engines are equipped with a port injection configuration. In this section, only port-injected SI gasoline engine systems will be discussed. For port injection system, the liquid fuel is injected through a solenoid on-off valve in the intake port, which is usually located directly in front of the intake valve. Since the difference of the injection pressure to the pressure in the intake manifold generally is kept constant by a dedicated control loop, the injected fuel mass is approximately proportional to the injection times. Because of communication with the electronic engine controller, it causes delays in the fuel injection transmission path of this kind of injection system.

One of the most important dynamic effects in the fuel path is caused by the wall-wetting phenomena. The liquid fuel injected into the intake port only partially enters the cylinder in the next intake stroke. The wall-wetting phenomena have important effects on the fuel path of the AFR control system. The utilized mean-value model in the control design accounts for the impingement and the evaporation processes of the injected fuel on the walls [38]. An empirical model, defined in [39], has been utilized to express the port injection path dynamics.

$$\dot{m}_f = \epsilon u_{fi} + \dot{m}_{ff}$$

$$\tau_f \ddot{m}_{ff} + \dot{m}_{ff} = (1 - \epsilon) u_{fi} \tag{2.14}$$

where u_{fi} denotes the fuel injection command as the commanded fuel mass flow rate, $\dot{m}_f$ the fuel mass flow rate entering the combustion chamber, $\dot{m}_{ff}$ the fuel mass flow rate going into the cylinder from the fuel puddle, ϵ the portion of fuel that enters the cylinder directly as vapor and τ_f the fuel lag time constant, respectively.

2.3.3   Crank Shaft Subsystem

The main objective of the engine control is to produce the mechanical power. The engine torque is a function of many variables, such as fuel injection mass, AFR, engine speed, and ignition timing. The crank shaft rotational dynamics is described as

$$J\dot{\omega}_e = \tau_e - D\omega_e - \tau_L \tag{2.15}$$

where J and D are the moment of inertia and damping coefficient of the crank shaft, respectively. τ_e is the engine torque and τ_L the load torque. The mean-value computation of engine torque is presented in [40, 41] as follows:

$$\tau_e = a \frac{\dot{m}_{ao}}{\omega_e} f_\lambda(\lambda) f_s(u_s) = c_T p_m(t) \tag{2.16}$$

with $c_T = \frac{\rho_a \eta V_c \eta_f Q}{4\pi p_a}$, where η_f is engine efficiency per cycle and Q the heat release from unit air with complete combustion, $f_\lambda(\lambda) \in [0,1]$ and $f_s(u_s) \in [0,1]$ denote the normalized influences of the AFR ($\lambda = \dot{m}_{ao}/\dot{m}_f$) and the spark advance command u_s on the mean-value engine torque, respectively. Additionally, the constant a represents the maximum torque capacity when $f_\lambda(\lambda) = 1$ and $f_s(u_s) = 1$.

2.3.4 Control Problem Formulation

The dynamics of engine consisting of the subsystems (2.13)-(2.16), can be rewritten as follows:

$$
\begin{aligned}
\dot{p}_m &= c_0(\dot{m}_{ai} - c_m p_m \omega_e) = c_0(c_p u_{th} - c_m p_m \omega_e) \\
J\dot{\omega}_e &= \tau_e - D\omega_e - \tau_L \\
\dot{m}_f &= -\frac{1}{\tau_f}\dot{m}_f + \epsilon\dot{u}_{fi} + \frac{1}{\tau_f}u_{fi} \\
\lambda &= \frac{\dot{m}_{ao}}{\dot{m}_f} = \frac{c_m p_m \omega_e}{\dot{m}_f}
\end{aligned}
\tag{2.17}
$$

Based on this SI engine mean-value model, we can investigate the generated torque response, the speed control performance, and design the AFR controller. However, the model parameters are unknown and contained nonlinearities. Additionally, the above equations represent only the basic system model which can only use for fundamental study. Therefore, the control strategy that can deal with the unknown time varying system parameters and disturbance rejection is required.

2.4 Spark Ignition Engine Combustion

General gasoline engines in one working cycle consist of four strokes which are intake, compression, combustion, and exhaust. Nowadays, injection system both port and direct injection have been used for most of vehicle gasoline engines. These injection systems lead to high performance fuel injection control both injection time and amount of injection. For the air path, amount of air flow is controlled by throttle. Another important part is the spark plug which is used for spark ignition. Additionally, with new technologies such as variable valve timing (VVT) and turbocharger, the engine combustion efficiency and emissions have been improved. All actuators in the engine systems are controlled by the engine control unit (ECU).

2.4.1 Mixture Formation

The process of mixture formation of port injection engine starts from intake air to the intake manifold which control by throttle. The design details of intake manifolds determine to a large extent the volumetric efficiency and the transient characteristics of the SI engine. The fuel injection position is at the combustion chamber inlet closed to intake valves. Then, air-fuel mixture pass through the cylinder. The injection amount

and quality are mainly important for combustion. In case of liquid fuel enters the cylinder in large droplets and ligaments, evaporates only partially, and causes abnormally high local in-cylinder unburned hydrocarbon concentrations.

2.4.2 Combustion Formation

After air-fuel mixture enters the combustion chamber and finish the intake process, the compression process will start. After some crank angle of compression process, the ignition is given then the combustion is started. The combustion process in SI engines can be divided into four main stages [42]: spark and flame initiation, initial flame kernel development, turbulent flame propagation and flame termination. For SI engine combustion, we can consider the burning process of gasoline which mainly compose of isooctane. A reference fuel is isooctane C_8H_{18}, which is used when determining the octane number of a fuel. The oxidizing reaction of a fuel releases heat, for example isooctane and oxygen gives [43]:

$$C_8H_{18} + 12.5O_2 \rightarrow 8CO_2 + 9H_2O + Heat$$
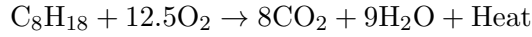
The energy that is released as heat from a fuel can be determined using, for example, a bomb calorimeter. Two fuel properties that are frequently used to quantify the amount of heat release are the higher heating value Q_{HHV} and the lower heating value Q_{LHV} of the fuel. The higher heating value is the amount of energy that the combustion of one unit of fuel can generate when the water among the combustion products is condensed to liquid phase. The lower heating value is the amount of energy that the combustion of one unit of fuel can release when the water in the products is in gaseous phase. In practical applications, the lower heating value is always considered. It is mean that the lower heating value is used to describe the available energy in the fuel.

For the AFR calculation, the AFR is defined as the ratio between mass of air m_a and mass of fuel m_f. A stoichiometric combustion reaction, between a general hydrocarbon fuel C_aH_b and air, produces only water and carbon dioxide and is written

$$C_aH_b + \left(a + \frac{b}{4}\right)(O_2 + 3.773N_2) \rightarrow aCO_2 + \frac{b}{2}H_2O + 3.773\left(a + \frac{b}{4}\right)N_2 \qquad (2.18)$$
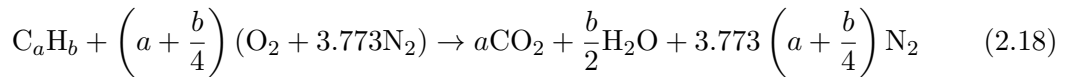
This combustion reaction defines the stoichiometric proportions of air and fuel. By denoting the relative contents of hydrogen and carbon in the fuel $y = b/a$ and using the molecular weights for carbon, hydrogen, oxygen, and nitrogen we can derive an

expression for the stoichiometric AFR

$$AFR_{stoi} = \left(\frac{m_a}{m_f}\right)_{stoi} = \frac{34.56(4+y)}{12.011 + 1.008y} \tag{2.19}$$

The stoichiometric AFR for gasoline which mostly compose of isooctane is about 14.7. Usually the AFR is normalized with the stoichiometric mixture, and this is called the air/fuel equivalence ratio λ

$$\lambda = \frac{AFR}{AFR_{stoi}} \tag{2.20}$$

Another quantity is the fuel-air ratio (FAR), which is the inverse of the AFR, and its normalized fuel/air equivalence ratio is denoted

$$\frac{1}{\lambda} = \frac{FAR_{stoi}}{FAR} \tag{2.21}$$

When there is excess air in the combustion ($\lambda > 1$) the mixture is referred to as lean, and conversely, excess fuel in the combustion ($\lambda < 1$) the mixture is referred to as rich. Under rich conditions the amount of air is insufficient for complete combustion of the fuel and the combustion efficiency decreases. In the lean operation, the combustion efficiency will increase and reduce after some value of λ because of misfire.

2.5 The Relationship Between AFR and In-cylinder Pressure

Cylinder pressure has long been considered as an important indicator of combustion performance in internal combustion engines. Nowadays, the cylinder pressure sensor efficiency and cost have been improved. The complex combustion process in SI engines can be explained using the analysis of the in-cylinder pressure data and some combustion parameters. For the AFR calculation, combustion parameters of interest include the total heat release (Q_{tot}) and the rapid burn angle ($\Delta\theta_b$). A prior literature publication [44] presented the relation between the AFR and the in-cylinder pressure data. In their work, Tunestal et al. [44] indicated that the rate with which fuel was consumed with respect to the crank angle could be modeled as a function of the inlet pressure (p_m), temperature (T_m), engine speed (N), and AFR. The resulting function is expressed as follows:

$$\frac{dm_f}{d\theta} = bp_m^{1+\mu}T_m^{\beta-1}N^{-\eta}AFR^{-1} \tag{2.22}$$

where b, μ, β and η are unknown constants, which have to be determined from experiments. Additionally, subject to some assumptions on the flame geometry, the cylinder's AFR is proportional to the heat release rate during the rapid burn phase of combustion. During this phase, the heat release rate is almost constant in the crank angle domain. Therefore, when the bulk of the combustion event is considered, the heat release rate can be approximately obtained as

$$\frac{dm_f}{d\theta} \approx \frac{\Delta m_f}{\Delta \theta_b} = \frac{1}{Q_{LHV}} \frac{Q_{tot}}{\Delta \theta_b} \tag{2.23}$$

where Q_{LHV} is the lower heating value of gasoline. Finally, Tunestal et al. [44] obtained the AFR as the function of the engine speed, inlet pressure of air entering into the cylinder, inlet temperature, total heat release, and rapid burn angle;

$$AFR = c\frac{\Delta \theta_b}{Q_{tot}} p_m^{1+\mu} T_m^{\beta-1} N^{-\eta} \tag{2.24}$$

where c is an unknown constant, which has to be determined by experiments. However, when the AFR calculated from the model yields a high variation and the root-mean-square (RMS) of the average estimation error exceeds about 4.1%, the model cannot be applied directly to feedback control systems.

We have investigated the results of the AFR model indicated by (2.24). The experimental results following this AFR model and its identification process [44] at 1000 rpm and the torque of 60 N·m are shown in Fig. 2.3(a). Moreover, the AFR estimation error is exhibited in Fig. 2.3(b). The results indicated in Fig. 2.3 show high variation of the estimated AFR cycle-by-cycle. This variation is caused by the model structure which use the inputs powered by some identified model coefficients. Actually, the estimated output variation can be reduced by the application of cycle moving average window but the problem related to model offset and estimation delay should be considered. Additionally, the model requires the in-cylinder temperature as one of model inputs. Hence, based on the results, we can conclude that this model is not directly suitable for generating the AFR feedback signal.

2.6 Thermodynamic Model for Compression Process

The combustion chamber of the internal combustion (IC) engines is considered to be an open system, and with a uniform in-cylinder pressure, in the single-zone thermodynamic model. During the compression process, there is no mass transfer through the intake and

(a)

(b)
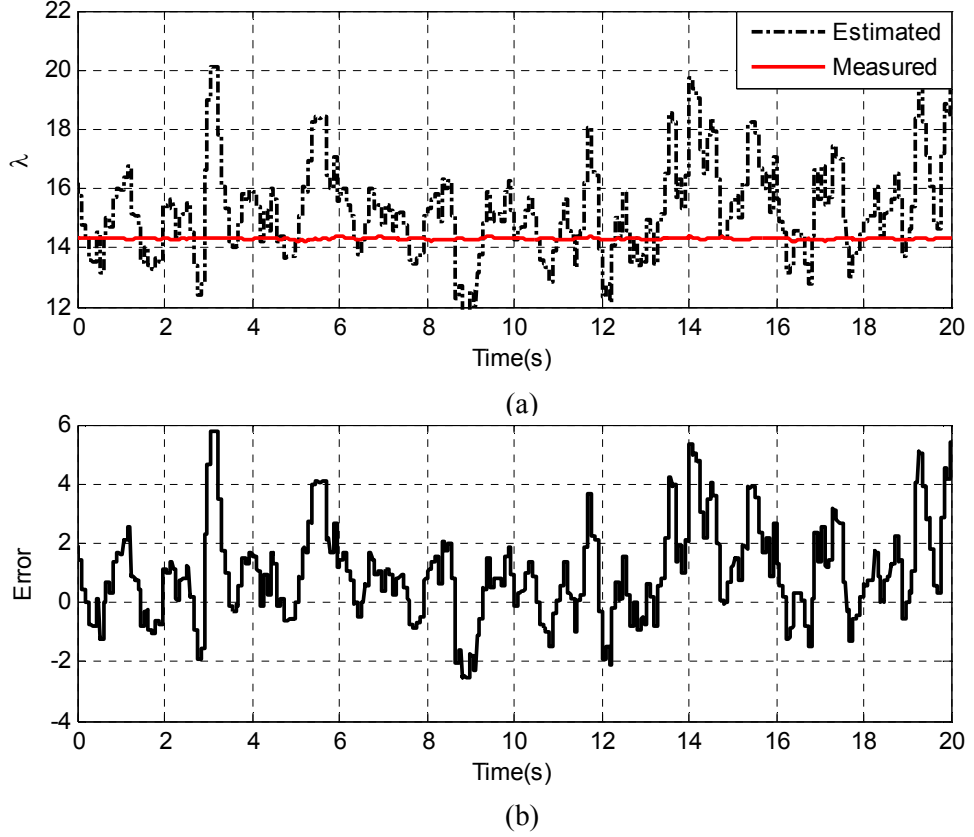
FIGURE 2.3: The comparison between raw pressure data and pressure with cycle moving average

exhaust valves. Additionally, small crevice effects are ignored. Hence, the combustion chamber can be regarded as a closed system with a constant mass. Based on the model presented by Rivas et al. [45], the energy equation for the cylinder is inferred from the first thermodynamic principle,

$$dU(t) = -\delta Q_{th}(t) - p_c(t)dV(t) \tag{2.25}$$

where $U(t)$ is the internal energy of the gas mixture, $Q_{th}(t)$ the heat transfer of the mixture to the surroundings, $p_c(t)$ the in-cylinder pressure, and $dV(t)$ the cylinder volume derivative. Assuming that the specific heat at constant volume, c_v is constant, the left-hand side of (2.25) can be written as:

$$dU(t) = mc_v dT(t) \tag{2.26}$$

where m is the total mass of the mixture in the cylinder, and $T(t)$ corresponds to the gas temperature. Solving equations (2.25) and (2.26) for $T(t)$,

$$dT(t) = \frac{1}{mc_v}\left(-\delta Q_{th}(t) - p_c(t)dV(t)\right) \tag{2.27}$$

where $V(t)$ is the cylinder volume. The ideal gas law is used to determine the dynamics of $p_c(t)$:

$$p_c(t)V(t) = mRT(t) \tag{2.28}$$

where R is the specific gas constant. Taking the derivative of (2.28) leads to:

$$dp_c(t) = \frac{mRdT(t)}{V(t)} - \frac{mRT(t)dV(t)}{V(t)^2} \tag{2.29}$$

With the use of the equations listed above, the model can be represented in the state-space form with two state variables.

$$\begin{aligned}
\dot{p}_c(t) &= -\left(\frac{R}{c_v} + 1\right)\frac{\dot{V}(t)}{V(t)}p_c(t) - \frac{R}{c_v V(t)}\delta Q_{th}(t) \\
\dot{T}(t) &= -\frac{R}{c_v}\frac{\dot{V}(t)}{V(t)}T(t) - \frac{R}{c_v V(t)}\frac{T(t)}{p_c(t)}\delta Q_{th}(t)
\end{aligned} \tag{2.30}$$

Note that all derivatives presented in (2.30) denote time derivatives. The convective heat transfer from the gases in the combustion chamber to the cylinder walls is given by:

$$\delta Q_{th}(t) = h_c(t)A_w(t)\left(T(t) - T_w\right) \tag{2.31}$$

where T is the in-cylinder temperature, T_w the cylinder-wall temperature, and A_w the heat transfer area. In this model, the heat transfer area is considered as

$$A_w(t) = \frac{\pi}{2}d^2 + 4\frac{V(t)}{d} \tag{2.32}$$

where d is the constant cylinder bore. The convective heat transfer coefficient is always computed from Woschni's equation [30]

$$h_c(t) = \alpha_{th}d^{-0.2}p_c(t)^{0.8}T(t)^{-0.53}\left(C_1 S_p + C_2\frac{V_d T_1}{p_1 V_1}\left(p_c(t) - p_0(t)\right)\right) \tag{2.33}$$

where V_d is the displacement volume, α_{th} and C_1 are calibration constant and C_2 is the tuning parameter, p_1 and T_1 represent the know state of the working gas related to the instantaneous cylinder volume V_1, (e.g. at intake valves closure), S_p is the piston speed, and $p_0(t)$ is the motored pressure (without combustion). Because the model

presented by (2.33) consists of non-linear terms and it is quite difficult to implement in the compression heat transfer model. Hence, the simplified model is required in actual implementation. The simplified model for the convective heat transfer coefficient is defined as

$$h_{c,re}(t) = p_c(t)\omega \tag{2.34}$$

Subsequently, the reduced heat transfer model is introduced, and the convective heat transfer rate to the combustion chamber walls can be calculated from the relation:

$$\delta Q_{th,re}(t) = p_c(t)\omega A_w(t)\left(k_1 T(t) - k_0 T_w\right) \tag{2.35}$$

where ω is the engine speed in rad/s. There are two parameters in the convective heat transfer model, namely, k_0 and k_1. These parameters are assumed to be constant during one considered period.
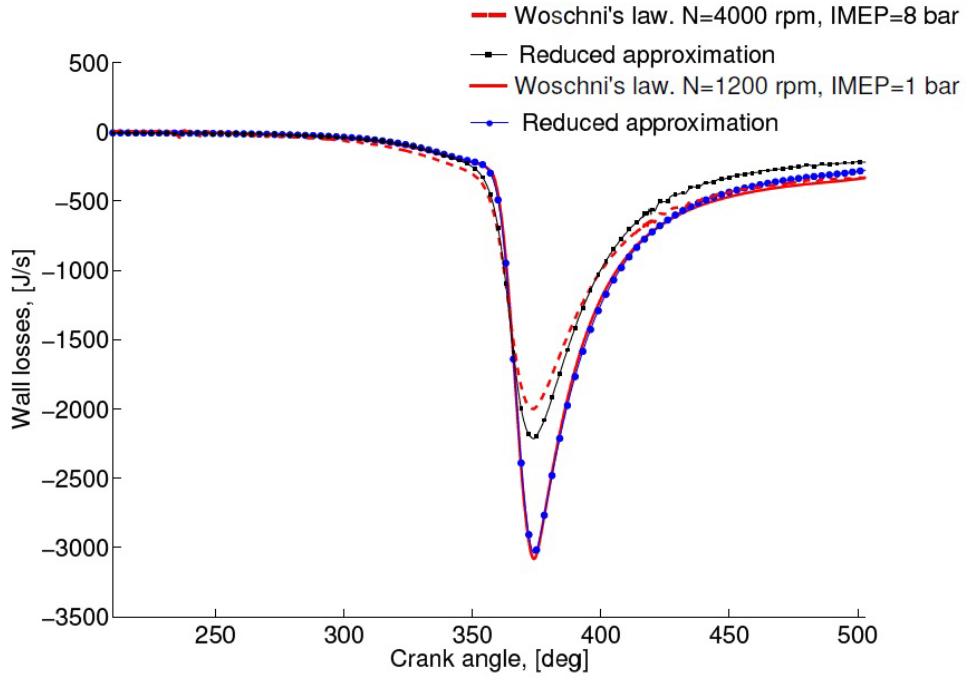
FIGURE 2.4: Reduced model output comparison (Rivas, 2012)

In application, we use this simplified model as an example of the numerical model which can be represented the behavior of the heat transfer rate. However, the structure of this model is different from the model obtained from Newtons law of cooling. This simplified model is proposed and validated with respect to Woschni's approximation by Rivas [45] and the satisfactory results are obtained. In Fig. 2.4, two examples for different operating conditions of the validation of the wall losses reduced model are presented.

The results show that this numerical model can represent the behavior of the original model with low error. In this work, the constant parameters of this simplified model are identified using the available experimental data and some assumptions.

Chapter 3

Thermodynamic Analysis of SI Combustion and In-cylinder Pressure Measurement

In this chapter, we will explain the important background on thermodynamic analysis of SI engines and combustion parameter calculation based on in-cylinder pressure data. Subsequently, the in-cylinder pressure measurement and signal conditioning are described. Additionally, the possible applications in engine control and analysis will then be presented.

3.1 Introduction

The cylinder pressure is the primary source of combustion information which caused by chemical reaction inside the cylinder. We can obtain the pressure data by using piezoelectric pressure transducers. The output from the piezoelectric transducer is in the form of a charge which can be converted to a voltage output by connecting to a charge amplifier. An important effect associated with all pressure transducers is the time varying pressure offset. This is caused by the charge amplifier electrical circuit. There are many methods for the offset compensation. In this thesis, the author have applied the method presented by Tunestal [46]. For the detail of the pressure offset calculation, please see Appendix A.

For the heat release and combustion parameter calculation, we can apply the fundamental thermodynamics to derive a differential equation. This equation represents the progress of combustion process related to the measured in-cylinder pressure. The model is considered as a single-zone model which assumes homogeneous conditions throughout the combustion chamber. For the SI engines, the combustion is not exactly homogeneous as in a homogeneous charge compression ignition (HCCI). Hence, applying a two-zone model which considers burned zone and unburned zone separately should be more appropriate. However, in the two-zone model, the heat transfer between the two zone must be modeled, and this requires a model for the surface area of the two-zone interface. Because these reasons, the two-zone model are very difficult to obtain correctly because of the turbulent of combustion in an SI engine. Therefore, using the one-zone model approach is still a good approximation. Moreover, the lower computational load of the single-zone model leads to easily real time control applications.

3.2 Thermodynamic Analysis of SI Combustion

The thermodynamics of combustion in an internal combustion engines is the gas trapped in the combustion chamber during compression, combustion, and expansion. This gas is a mixture of air, gaseous fuel, and residual gas fraction. Using in-cylinder pressure data, a major advantage is that the pressure changes can be related directly to the amount of fuel chemical energy released by combustion. The first law of thermodynamics for the system states

$$\delta Q_{ch} = dU + \delta W + \delta Q_{th} + \Sigma h_i dm_i \tag{3.1}$$

where δQ_{ch} represents the chemical energy released by combustion, dU the changing of internal energy of the charge, δW the piston work and equal to $p_c dV$, δQ_{th} the heat transfer to the cylinder walls, the last term stands for crevice effects which compose of enthalpy h and the changing of crevice mass dm. The total energy that include all effects in (3.1) is called gross heat release.

Engine crevices consist of small spaces within the combustion chamber, filled with unburned mixture, whose characteristic dimension does not allow a flame to penetrate. For example, the head gasket crevice is composed of the gaps between the head gasket and cylinder liner and the head gasket and head. Also, the piston ring-pack crevice consists of the top land volume, the side and back top ring volume, and the volume between the first and second rings [47]. A crevice becomes a source of inefficiency and hydrocarbon

emissions when the unburned mixture trapped within escapes primary combustion. This occurs when the entrance to said crevice is geometrically such that a flame cannot enter.

The effects of heat transfer is very important in the combustion process. A methodology for heat transfer calculation is quite complex and requires some information. The accuracy of heat transfer estimation using some models is not very effective because of limitations of measured data. Moreover, the model requires a proper calibration process and the model parameters depends on considered engine system. Therefore, the heat transfer and crevice effects are difficult to be obtained precisely by measurement then in our study they are omitted. When the energy release is not combined with heat transfer and crevice terms, the remaining combination terms called net heat release. The net heat release $\delta Q_{ch,net}$ can be calculated from

$$\delta Q_{ch,net} = dU + \delta W \tag{3.2}$$

The changing of internal energy is given by

$$dU = mc_v dT \tag{3.3}$$

where m is the mass of charge, c_v the specific heat at volume constant, and dT the changing of the charge temperature. Using ideal gas law

$$p_c V = mRT \tag{3.4}$$

where p is the cylinder pressure, V the cylinder volume, and R the gas constant of the mixture. Then considering the derivative of (3.4), yields

$$p_c dV + V dp_c = mRdT \tag{3.5}$$

Note that the mass of charge in the cylinder is not change because intake and exhaust valves are closed. Moreover, the crevice effects which affect to the changing of mass inside the control volume is ignored. Substituting (3.5) and (3.3) into (3.2), we get

$$\delta Q_{ch,net} = \left(\frac{c_v}{R} + 1\right) p_c dV + \left(\frac{c_v}{R}\right) V dp_c \tag{3.6}$$

Now, assuming that crank angle (θ) resolved measurements of p_c are available, (3.6) can be rewritten on a form where the crank angle dependence is explicit. Including the

relations $R = c_p - c_v$ and $\gamma = \frac{c_p}{c_v}$, yield

$$\frac{dQ_{ch,net}}{d\theta} = \left(\frac{\gamma}{\gamma - 1}\right) p_c dV + \left(\frac{1}{\gamma - 1}\right) V dp_c \tag{3.7}$$

This formula is utilized to compute the net heat release rate (HRR) and heat release (HR) from combustion. This heat release can be applied to calculate the combustion parameters which have many advantages for combustion control and analysis.

3.2.1 Definitions of Heat Release Based Cycle Parameter

Total heat release, $Q_{tot,cyl}$, represents the increase in $Q_{ch,net}(\theta)$ due to combustion, and is approximately equal to the amount of chemical energy which is converted to pressure (measurable quantity) during combustion. The definition defining here means total energy release in one cycle from pressure data this is because the pressure signal obtained from sensor is not include some losses.

$$Q_{tot,cyl} = Q_{\max} - Q_{\min} \tag{3.8}$$

where $Q_{\max}$ and $Q_{\min}$ represent the minimum and maximum of $Q_{ch,net}(\theta)$, respectively.

$$Q_{\min} = \min_{\theta} \left[Q_{ch,net}(\theta)\right] \tag{3.9}$$

$$Q_{\max} = \max_{\theta} \left[Q_{ch,net}(\theta)\right] \tag{3.10}$$

The crank angle of 10% burnt (or 10% heat release), $CA10$, approximately represents the crank angle from the combustion starts to 10% heat release.

$$CA10 = Q_{\min} + 0.1 \cdot Q_{tot,cyl} \tag{3.11}$$

Similarly, the crank angle of 50% heat release $CA50$, is defined by

$$CA50 = Q_{\min} + 0.5 \cdot Q_{tot,cyl} \tag{3.12}$$

The crank angle of 90% heat release $CA90$ indicates the end of combustion in the same way that can be defined as

$$CA90 = Q_{\min} + 0.9 \cdot Q_{tot,cyl} \tag{3.13}$$

Finally, the heat release duration, $\Delta\theta_b$, represents the duration of the combustion event in crank angle degrees.

$$\Delta\theta_b = CA90 - CA10 \qquad (3.14)$$

The definition of the combustion duration in the form of $\Delta\theta_b$ denotes the period from 10% to 90% of the mixture burnt. This is because the detection of combustion starting is quite difficult. At the beginning of combustion, the cylinder pressure is very low compared with the maximum cylinder pressure then the signal from the transducer suffers from noise effects. In addition, at the end of combustion period, the low pressure signal is happen again. This situation leads to difficult sensing of the end of combustion point. Hence, most researches have considered only the $\Delta\theta_b$ and used this value for combustion control and analysis.

3.2.2 Effects of Cycle-to-Cycle Variation in SI Engine Combustion

The main important data in this research is in-cylinder pressure which is affected by cyclic variation. Therefore, the basic knowledge on combustion cyclic variation should be investigated. The combustion process in a spark ignition engine is not repetitive from engine cycle to engine cycle. This can be easily noted if the pressure trace in the cylinder is measured. The peak pressure obtained can change about 30% from cycle-to-cycle in a well functioning engine [48]. The cylinder pressure has been used to measure the fluctuations. This has led to the use of pressure related parameters to quantify the fluctuation intensity. The maximum pressure and its crank angle location are frequently used parameters [35]. In some researches, the variation in indicated mean effective pressure (IMEP) produced per engine cycle is also a well-used parameter. Many researches have reported on the effects of cycle-by-cycle variation of combustion [49–52].

For the AFR control, the combustion variation is very important especially during lean burn operation. Lean combustion in spark-ignition engines has long been recognized as a means of reducing both exhaust emissions and fuel consumption. However, problems associated with cycle-by-cycle variations in flame initiation and development limit the range of lean-burn operation [53]. Under high dilution levels, a lean limit is reached where combustion becomes unstable, significantly deteriorating drivability and engine efficiency, thus limiting the full potential of lean combustion [54]. Cyclic variability has long been recognized as limiting the range of operating conditions of spark ignition engines, in particular, under lean and highly diluted operation conditions [55]. In practical application, the AFR control system for lean burn combustion requires another control

loop for spark advance (SA) regulation. Without SA control, the AFR cannot increase so high because of safety conditions defining by manufacturer. Additionally, the SA control based on mapping implemented in ECU is not designed for very rich or very lean combustion. It means that the design conditions only consider at stoichiometric AFR and the variation around this point. Moreover, the operational range of AFR sensor is limited and it shows non-linear behavior both in very low and very high AFR. Therefore, the study on AFR based in-cylinder pressure control can be one of lean burn control solution.

3.3　In-cylinder Pressure Measurement and Experimental Facilities

The in-cylinder pressure measurement and experimental facilities will be expressed in this section. Including the detail of measurement process, pressure offset compensation method, and also a real time control application for engine control are presented. Moreover, the detail of engine specifications, measuring devices and control equipments are explained. There are many application of cylinder pressure for engine control and analysis. The cylinder pressure measurement including crank angle position affects directly to the combustion parameters. Most control methodologies are based on the combustion parameters calculation. Therefore, the correct cylinder pressure detection, pressure offset compensation, and the data matching are very important factors.

3.3.1　Experimental Setup

The engine test bench consists of six cylinders gasoline commercial engine with a low inertia dynamometer. Connecting with the active electric dynamometer, we can control various operating modes of the engine, for example, an idle speed mode, a constant speed mode and a constant torque mode. The experiment was conducted on the engine test bench depicted in Fig. 3.1.

The engine control systems were implemented by a dSPACE1006 rapid prototyping unit, which communicates with the real time interface (RTI) bypass system and the commercial engine ECU via controller area network (CAN) bus. This system was exploited to act as the parallel controller. Meanwhile, the control algorithm already embedded in ECU provides the free communication interface so that the control commands given by ECU itself can be overwritten by the external command. Herein, the external control
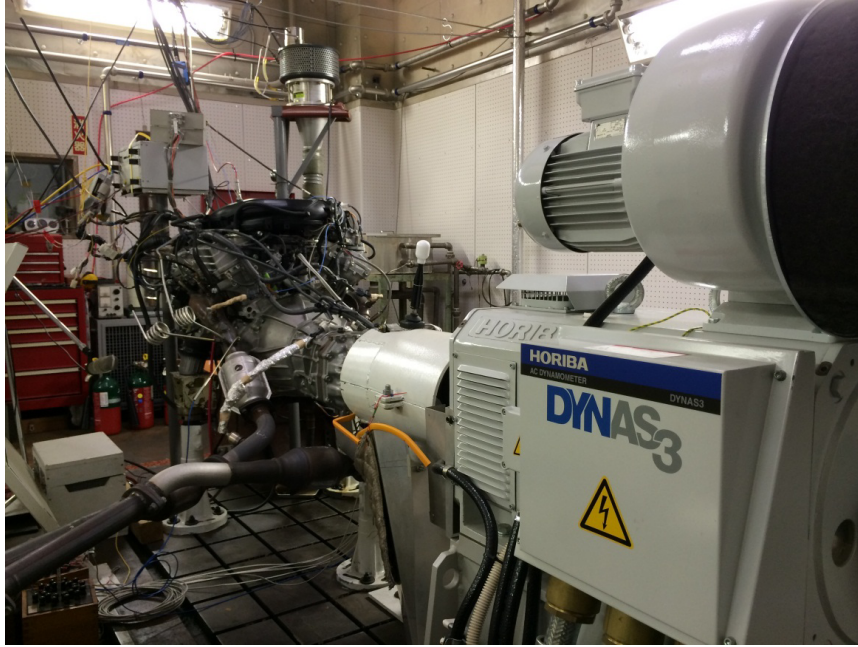
FIGURE 3.1: Engine test bench

scheme is programmed in MATLAB/Simulink platform and then it is complied in C-code and real-time executed in the dSPACE1006. Thus the dSPACE1006 achieves the control for all control-loops of the engine simultaneously, for example, fuel injection control loop, spark advance control loop, VVT control loop, etc. Actually, the data transfer via the CAN bus was assumed sufficient to be fast then the communication delay can be ignored.

In order to obtain the engine operating status, some additional sensors were installed including intake manifold pressure sensor, crank angle encoder, individual air-fuel ratio sensors, in-cylinder pressure sensor, intake and exhaust temperature sensor, and so on. All signal from sensors can be collected by the dSPACE1006 in real time. On the dynamometer side, the real-time control of the dynamometer is achieved by MicroAuto-Box II (another kind of rapid prototype controller also manufactured by dSPACE Inc.), which is connected to the controller of dynamometer (named by SPARC) via CAN bus. Similar to the dSPACE 1006, the control logic can be programmed in Simulink and implemented in MicroAutoBox II in real time. Then the external control commands form MicroAutoBox II such as desired speed or desired torque can be received and performed by SPARC. In addition, a torque sensor and speed encoder are installed in the front side of the dynamometer and the real-time signals can be provided to the MicroAutoBox II via CAN bus [56]. The sketch of experimental facilities is shown in Fig. 3.2.
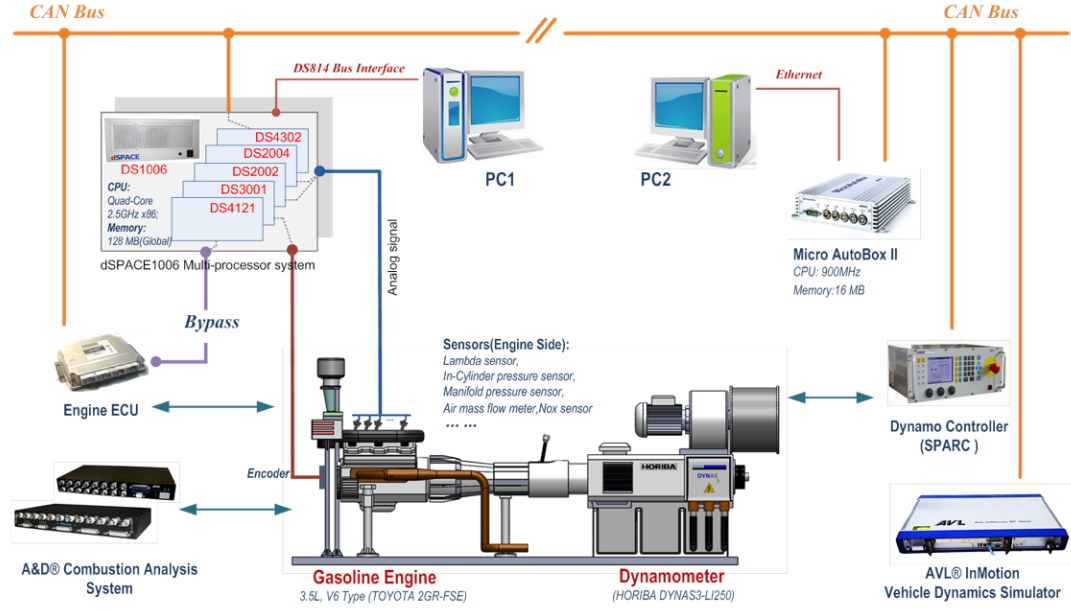
FIGURE 3.2: Experimental facilities (Kang, 2014)

The engine specifications for the control experiment are presented in Table 3.1.

TABLE 3.1: Engine specifications.

Engine system	Detail
No. of cylinders	6-cylinder
Arrangement	V-type
Valve mechanism	24-valve DOHC
Combustion chamber	Pentroof type
Manifolds	Parallel flow
Fuel system	SFI D-4S
Ignition system	DIS
Displacement (cm^3)	3456
Compression ratio	11.8:1
Maximum output	306 HP at 6400 rpm
Maximum torque	375 N·m at 4800 rpm

There are two in-cylinder pressure sensor installed on the engine test bench. For this experiment, we will focus on the cylinder pressure information obtained from the 5th cylinder. The pressure sensor (Kistler 6052C) installed on the horizontal direction on the cylinder head of the 5th cylinder. The position of the sensor on the test bench system is shown in Fig. 3.3(a). The pressure signal from the sensor will be sent to the charged amplifier and the to the dSPACE control device. Additionally, the encoder (Kistler 5064B21) is installed on the front side of the crank shaft. The detail of encoder

position is exhibited in Fig. 3.3(b). Using the encoder signal, we can obtain both the crank angle position and engine speed.

(a) (b)
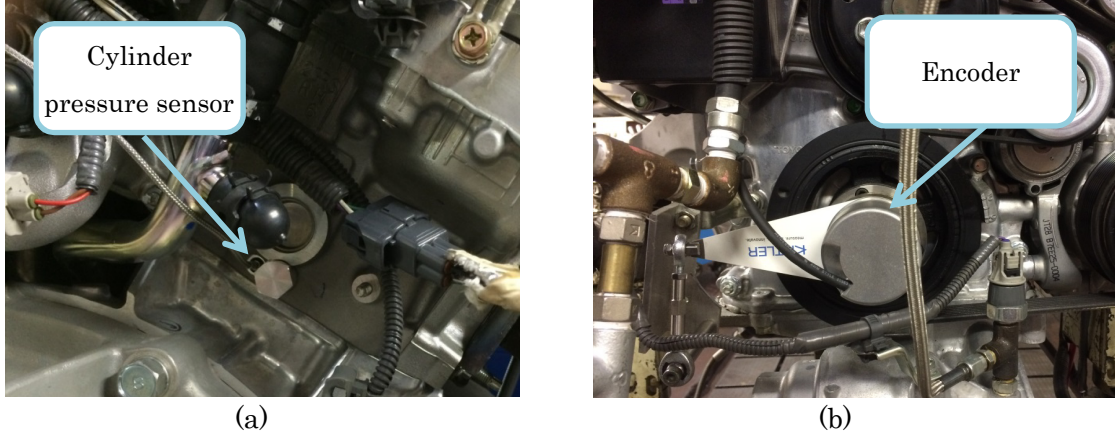
FIGURE 3.3: Position of sensors: a) in-cylinder pressure sensor and b) encoder for crank angle and engine speed measurement

Moreover, the intake manifold pressure sensor and the AFR sensor (Denso DOX-0222) at mixing point are shown in Fig. 3.4(a) and (b), respectively. The AFR sensor has linear operating range from AFR is equal 12 to 18. These sensors are necessary for AFR model input measurement and the AFR model validation. The detail of the proposed model will be expressed in chapter 4.

(a) (b)
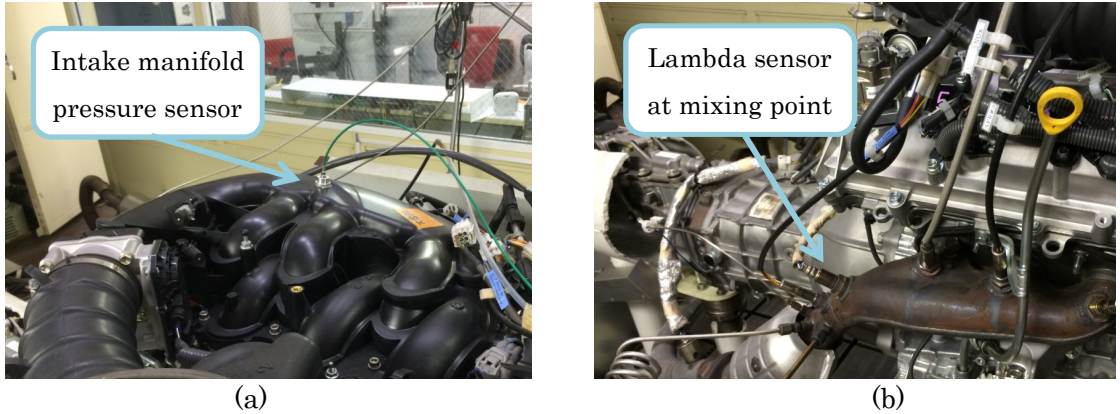
FIGURE 3.4: Position of sensors: a) intake manifold pressure sensor and b) AFR sensor at mixing point

During experiments, the engine was fully warmed, the coolant temperature was controlled at 80°C, and the lubricant oil temperature was regulated at 70°C. Other control variables such as the air-fuel ratio, spark advanced angle, fuel injection mode, and injection timing were controlled by the ECU.

3.3.2 In-cylinder Pressure Measurement

There are various kinds of transducer for crank angle resolved in-cylinder pressure measurement on internal combustion engines. The most prevalent transducers are the piezoelectric pressure sensor and the optical transducer which are available in a wide range of sizes for suitable different applications. In this work, the piezoelectric pressure transducer is selected for our pressure measurement. The sensor bandwidth limitation is adequate to capture the pressure information in the combustion chamber. An output from the transducer is in the form of charge then it must be connected to a charge amplifier for transforming the signal to voltage. Subsequently, the voltage signal passes through the dSPACE1006 and is sent to computer for calculation. The pressure transducer has also one unpleasant characteristic which is an unpredictable variable DC offset. This offset varies with time and change cycle-by-cycle. Therefore, the method for pressure offset identification is very important for obtaining the accurate cylinder pressure. Additionally, we have applied 10 moving average cycles for reduction of the cycle variation by trial and error. Based on this number of cycles, we can relieve the cycle variation and it does not strongly affect to AFR estimation in practical application. The measured in cylinder pressure with and without cycle moving average window are shown in Fig. 3.5.
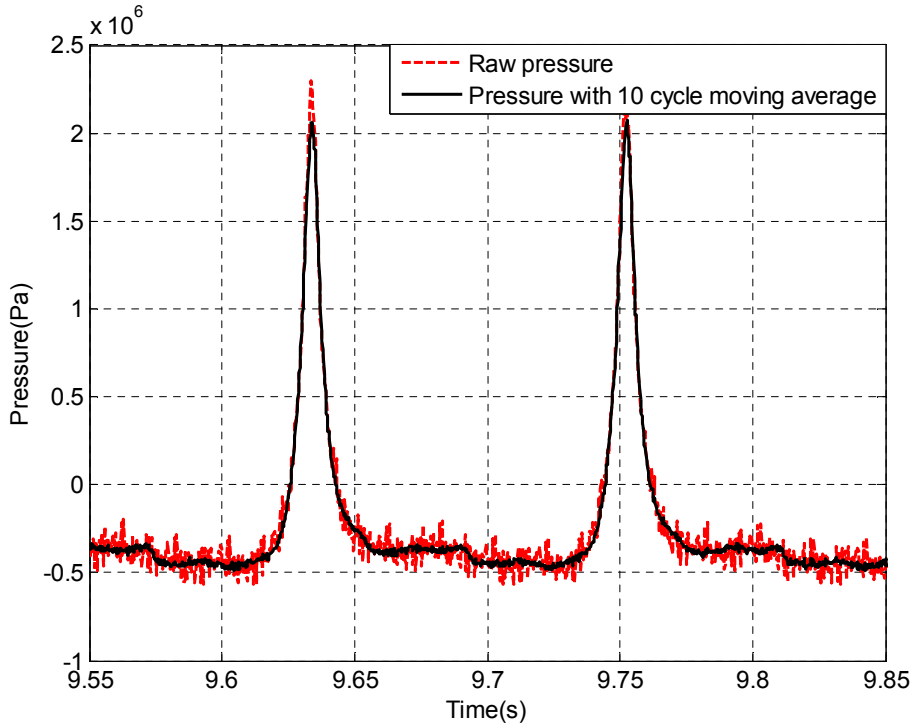
FIGURE 3.5: The comparison between raw pressure data and pressure with cycle moving average

In many studies, in-cylinder pressure data are averaged over certain number of cycles at each crank angle in order to observe the effects of the parameters. If the number of cycles included is low, then the results may be misleading due to cyclic variations of in-cylinder pressure. The desired level of accuracy can only be obtained if the number of cycles is increased with increasing cyclic variations. There is no general standard about how many cycle should be taken to obtain the average cycle to remove the effects of cyclic variations [57]. Moreover, the crank angle moving average window is required to deal with noise effects during low pressure region. The comparison between raw pressure and pressure with crank angle including cycle moving average is presented in Fig. 3.6.
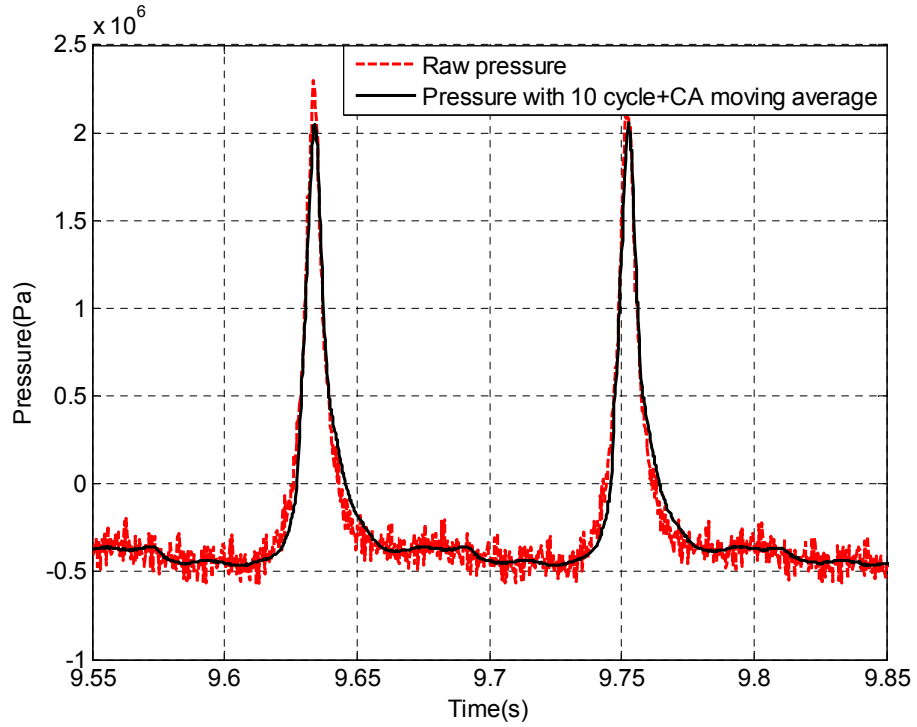
FIGURE 3.6: The comparison between raw pressure data and pressure with crank angle including cycle moving average

In this experiment, the pressure and crank angle measurement have performed using time based devices. The required resolution of pressure and crank angle data for the combustion parameters calculation is one data per one crank angle degree. Hence, the quadratic interpolation has applied for estimation of the missing measured information for both cylinder pressure and crank angle. Consequently, we can get the adequate resolution of data for combustion parameters computation. On the other hand, during high pressure region, the crank angle moving average window should be inactivated. This is because the moving affects the pressure signal delay which leads to calculated combustion parameters. Next, the important effects caused by a charge amplifier will

be considered. The pressure offset which varies with time cycle by cycle is calculated and compensated.

3.3.3 Pressure Offset Identification

The authors have applied the pressure offset identification presented by Tunestal et al. (2000). The detail of assumptions and calculation processes have been described in an Appendix A. After applying the pressure offset identification method, the identification results are depicted in Fig. 3.7.
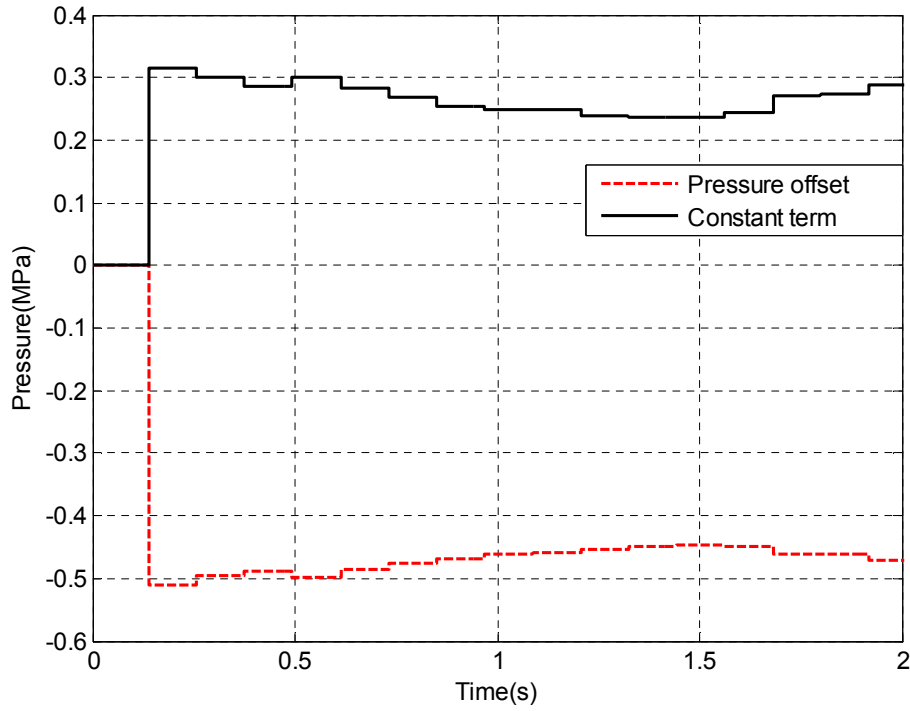
FIGURE 3.7: Identification results of a pressure data offset and a constant term.

The pressure offset is assumed to be constant in one cycle and the identification value will be updated every cycle. Also, the comparison results of data before the compensation and after offset compensation are depicted in Fig. 3.8. Subsequently, the results of the pressure offset validation are investigated. We have compared the original pressure data with the estimated results obtained from identification. Additionally, the enable signal for pressure offset calculation is also presented. The identification period is on some crank angle before ignition because the adiabatic assumption is applied. The validation results are shown in Fig. 3.9.
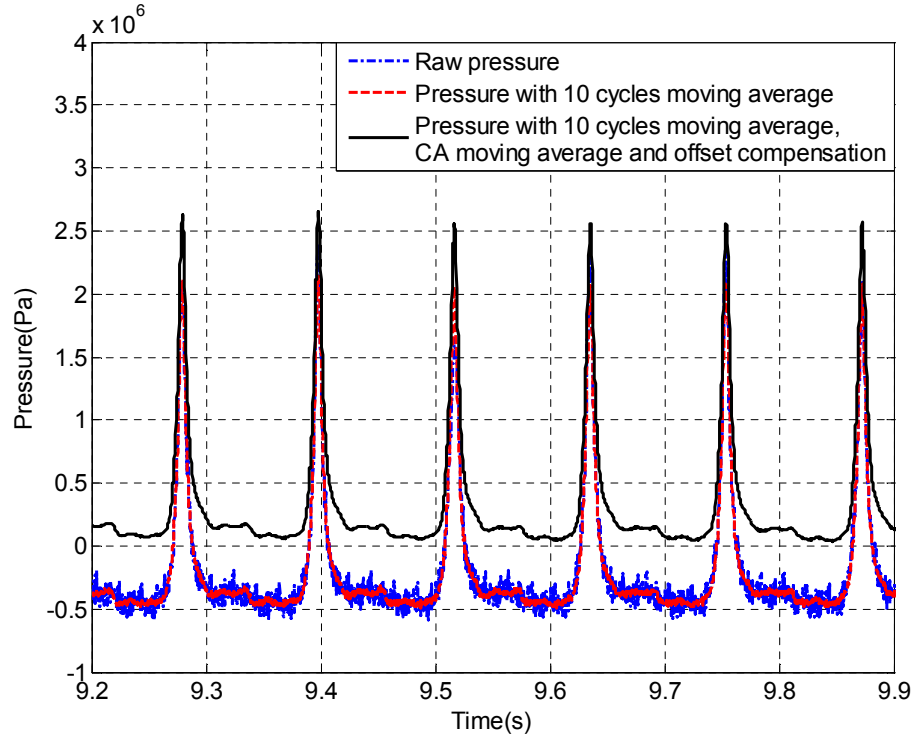
FIGURE 3.8: The comparison of the pressure data with and without offset compensation.
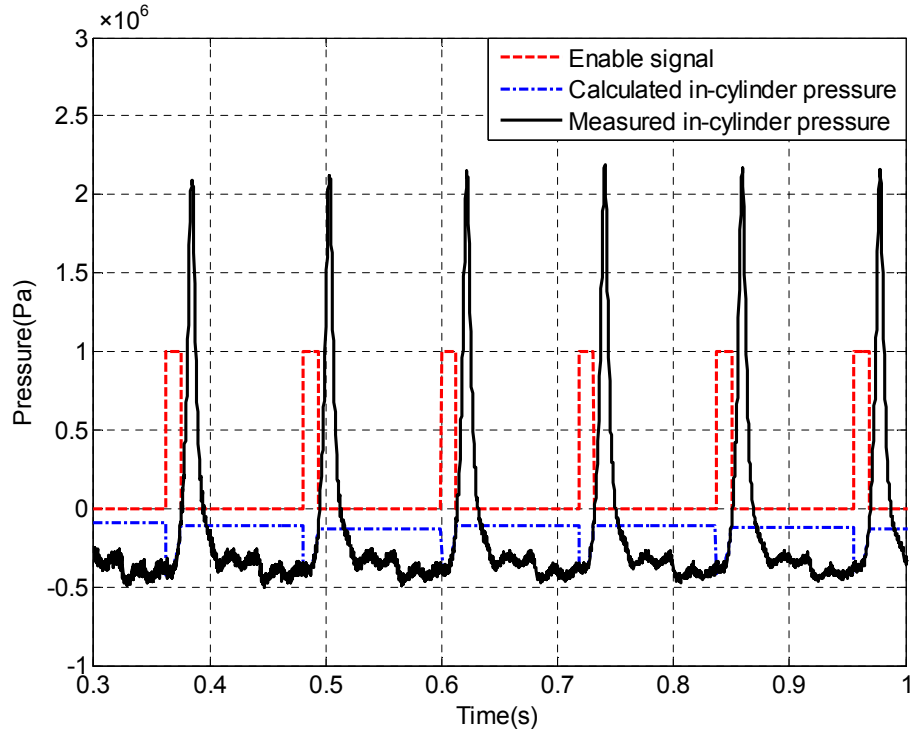
FIGURE 3.9: The comparison of measured and estimated compression pressure.

3.3.4 An Example of In-cylinder Pressure Application

We have performed in-cylinder pressure and crank angle measurement at 1000rpm and 60Nm of load torque. Additionally, the pressure offset is calculate and compensate to the measured data. The cylinder pressure and crank angle data are depicted in Fig. 3.10 (a). An example of HRR and HR calculation using in-cylinder pressure measurement is shown in Fig. 3.10 (b).
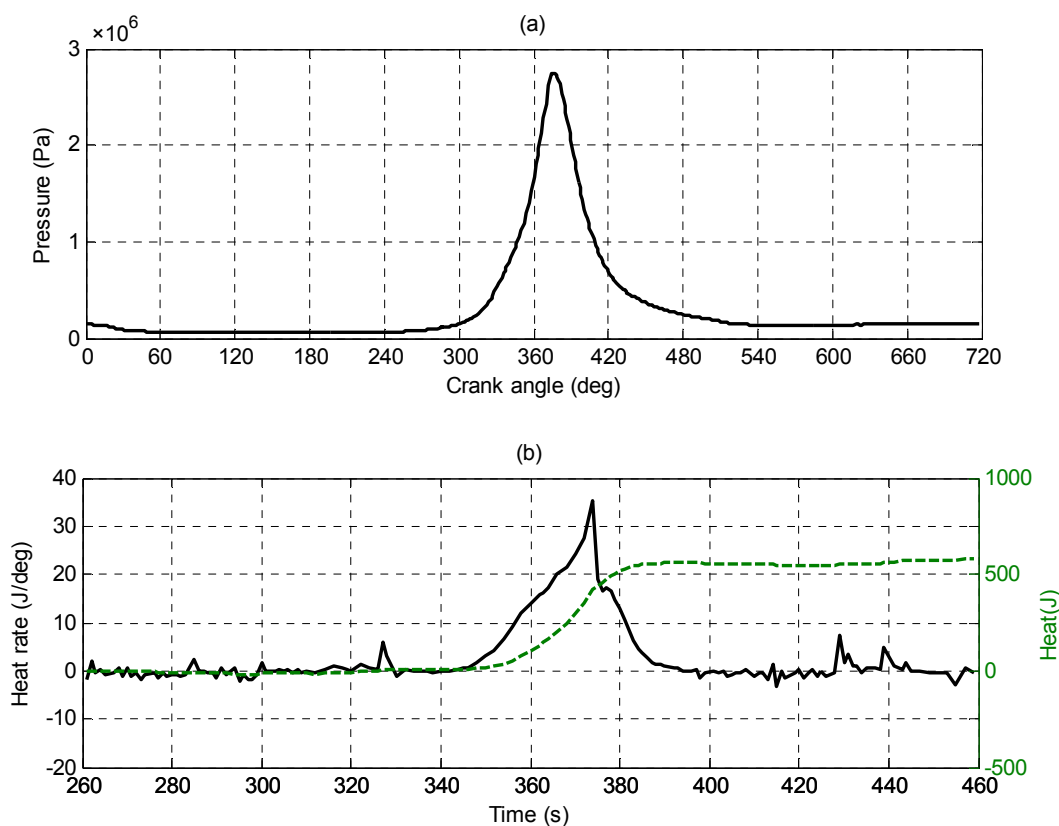
FIGURE 3.10: An example for net heat release rate and net heat release calculation

However, not only the crank angle and pressure data but also the data matching have affected the accuracy of combustion parameters calculation. So, the carefully data measurement and the accurate calculation procedure are required.

3.4 Possible Applications of In-cylinder Pressure Data

Gasoline combustion is highly influenced by many factors such as injection quantity, spark angle, and amount of air charge. All mentioned factors affects the combustion

pressure then the cylinder pressure can be applied for many control applications. In this work, we will focus on the AFR control of SI engine using some information of the cylinder pressure measurement.

The cylinder pressure contains information about the proceeding of the combustion process in the cylinder. The cylinder pressure based control of the fuel injection system will have many benefits. This information can be used to improve engine performance, emissions, and fuel consumption because the cylinder pressure feedback allows reliable engine operation. We can perform the engine load monitoring through cylinder pressure in the compression stroke. Moreover, with some methodologies, the AFR can be estimated and used for feedback control by replacing the AFR sensor. Also, the engine heat transfer analysis can be performed using in-cylinder pressure data. For the detail of this estimation and control, we will present in chapter 4.

Additionally, we also will explain the application of in-cylinder pressure data for compression heat transfer estimation in chapter 5. With this estimated heat transfer and its direction, the polytropic exponent variation can be calculated. Therefore, the combustion parameters calculation process should be improved by consideration of the heat transfer effects.

3.5   Conclusion

From the presented details in this chapter, the combustion parameter calculation requires accurate cylinder pressure, crank angle and fundamental thermodynamical formulas. Hence, the proper method and basic on cylinder pressure measurement are required. Also, there are some important phenomena which should be considered in AFR control based on in-cylinder pressure data. Based on this knowledge, we can calculate the combustion parameters accurately which will be used as inputs for AFR estimation model. Additionally, these parameters can also be utilized for combustion analysis. The detail of an application for estimation of AFR will be expressed in chapter 4. Moreover, the detail of an in-cylinder pressure application for compression heat transfer estimation and analysis are presented in chapter 5.

Chapter 4

Air-Fuel Ratio Estimation and Control using In-cylinder Pressure Data

In this chapter, first, we will present an introduction for AFR estimation and control. Second, the in-cylinder pressure based AFR model is proposed. Third, based on the proposed AFR model, the system identification and model validation are expressed. Fourth, the application of simple adaptive control with the proposed AFR model is presented. Fifth, we will express the control performance in real time control. Subsequently, the effects of feedback time delay will be discussed. Finally, the conclusion is then explained.

The main contributions presented in this chapter are the principal subject of the following publications:

- C. Khajorntraidet and K. Ito, Simple Adaptive Air-fuel Ratio Control of a Port Injection SI Engine with a Cylinder Pressure Sensor, Journal of Control Theory and Technology, Vol. 13, No. 2, pp.141-150, May 2015.

- C. Khajorntraidet, K. Ito and T. Shen, Improvement of Air Fuel Ratio Model using a Least Absolute Shrinkage and Selection Operator, Proceeding of the MSAM 2015, August 23-24, 2015, Phuket, Thailand.

- C. Khajorntraidet, K. Ito and T. Shen, Adaptive Time Delay Compensation for Air-Fuel Ratio Control of a Port Injection SI Engine, Proceeding of the SICE Annual Conference 2015, July 27-30, 2015, Hangzhou, China.

4.1 Introduction

The AFR control has been developed and improved because of demands on increased engine efficiency and emission control. For pollution control, the AFR in the combustion chamber has to vary within a very narrow range. The possibility of sensing the AFR plays an important role in the determination of the fuel injection control strategy. In practical applications, the in-cylinder pressure has been considered as a dominant indicator of combustion performance in internal combustion engines. Therefore, the combustion control and analysis can be performed on the basis of in-cylinder pressure data. There are many combustion parameters that can be obtained from cylinder pressure data, such as the heat release rate, total heat release, and the rapid burning angle, for example [35]. The calculation of these combustion parameters requires accurate in-cylinder pressure and crank angle data in practice. For instance, the inaccurate crank angle data leads to an incorrect heat release rate and to an incorrect magnitude of the total heat release calculation [58]. The control system using combustion pressure measurement can be used under cold or lean conditions when the conventional exhaust gas oxygen sensor cannot be used [59]. The AFR can be calculated from in-cylinder pressure data using an empirical model accounting for the dependence of the laminar flame speed on temperature, pressure, and AFR [44]. The model parameters are obtained from a steady state experiment at different loads, speeds, and AFR. The linear least-squares regression is used to compute the model parameters for minimization of the sum of the squares of the residuals between the measured and the estimated AFR [60]. Many approaches have been developed for determining the relationship between the cylinder pressure and the in-cylinder AFR for the estimation of the cylinder pressured-based AFR. These include, for example, the cylinder pressure moment approach [11], the molecular weight approach [12], and the equivalent heat release duration approach [13]. The challenging target of the in-cylinder pressure-based AFR calculation is its application to feedback control systems.

The main difficulties in the design of the AFR controller include the variable time delays and the uncertain plant behaviors and disturbances [61]. The model reference adaptive control (MRAC) has a high efficiency in the control of the system operating with uncertain parameters. It can also tune adaptively the controller parameters using the error signal between the plant output and the desired signal [62]. Many results have already been reported on the applications of MRAC. The simplified adaptive control methodology, called simple adaptive control (SAC), shows that practical adaptive control

can be both simple and robust under certain conditions [63]. Moreover, the stability and robustness of SAC are expressed and discussed in [64].

We introduce the cylinder pressure-based AFR model using the Taylor series expansion. The combustion parameters are calculated from in-cylinder pressure data. This pressure data is averaged using cycle moving averaging and crank angle moving averaging for noise reduction. Moreover, the cylinder pressure offset is corrected using the polytropic index pressure technique [46]. The AFR model inputs also include the intake manifold air pressure and the engine speed that affect the air mass flow rate entering the cylinder. We present the control performance of SAC with the proposed AFR model for AFR control of the port injection SI engine in practical applications. Finally, the experiments on an engine test bench indicate that the proposed control strategy can be applied for AFR control.

4.2 Air-Fuel Ratio Estimation Model

In this section, an approximation of the in-cylinder AFR model that is obtained in accordance to the basic definition of the AFR will be presented. The Taylor series approximation has been applied to calculate the AFR, based on its definition. Herein, we consider four model inputs that affect the in-cylinder AFR. The combustion parameters are the total heat release and the rapid burn angle calculated from the in-cylinder pressure. Additionally, the intake manifold pressure and the engine speed are also utilized in the model. Details of this proposed model are presented in the next section.

4.2.1 The Cylinder Pressure Based AFR Model

The detail of the AFR calculation and some required inputs are shown in Fig. 4.1. The cylinder pressure-based AFR model inputs are the rapid burn angle, total heat release, intake manifold pressure, and the engine speed. The dynamic behavior of each input is regarded as the selection of the input order in the model structure. The intake manifold pressure and engine speed have strong effects on the air mass flow rate entering into the combustion chamber. Additionally, the values of the total heat release and the rapid burn angle, are depending on the fuel mass injected into the cylinder. Therefore, the quantity of all inputs can be used to estimate the AFR of SI engines.
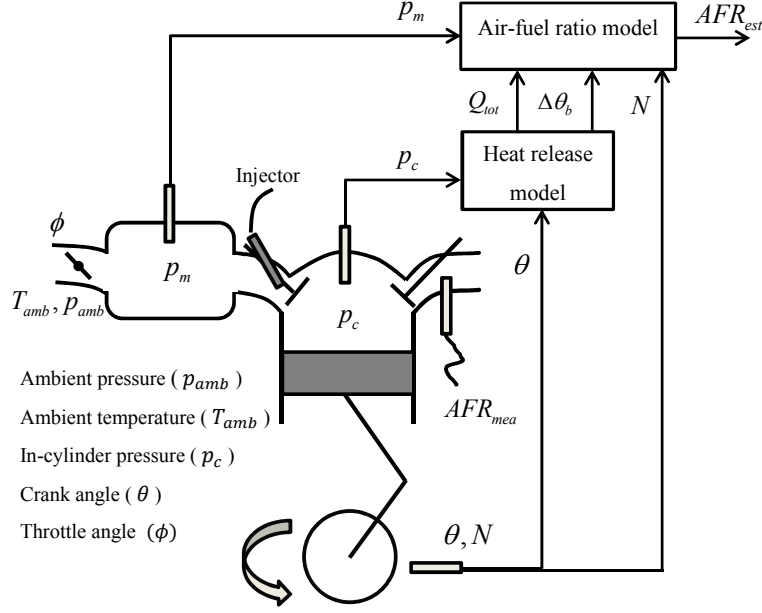
FIGURE 4.1: Air-fuel ratio (AFR) estimation model.

The total heat release for the AFR model is obtained from the integration of the heat release rate from the start to the end of combustion [35]. When crevice volumes and blow-by effects are omitted, the heat release rate can be computed from the relation

$$\frac{dQ}{d\theta} = \frac{\kappa}{\kappa - 1}\frac{p_c dV}{d\theta} + \frac{1}{\kappa - 1}\frac{V dp_c}{d\theta} + \frac{dQ_{ht}}{d\theta} \tag{4.1}$$

where Q is the gross heat release, κ the polytropic exponent, p_c the in-cylinder pressure, V the cylinder volume, θ the crank angle, and Q_{ht} the heat transfer. The rapid burning angle is defined as the crank angle interval required for burning the bulk of the charge. In general, we consider that 10% to 90% of the mass fraction is burned. The different values of all inputs compared with their values at stoichiometric ratio are considered for the AFR calculation. The introduced AFR model can be obtained with the combination of the Taylor series expansion as follows:

$$
\begin{aligned}
AFR &= f(p_m, N, \Delta\theta_b, Q_{tot}) \\
&= \lambda_0 + \alpha_1(\Delta\theta_b - \Delta\theta_{b,0}) + \alpha_2(Q_{tot} - Q_{tot,0}) + \alpha_3(\Delta\theta_b - \Delta\theta_{b,0})^2 \\
&\quad + \alpha_4(\Delta\theta_b - \Delta\theta_{b,0})(Q_{tot} - Q_{tot,0}) + \alpha_5(Q_{tot} - Q_{tot,0})^2 + \alpha_6(p_m - p_{m,0}) \\
&\quad + \alpha_7(N - N_0)
\end{aligned} \tag{4.2}
$$

where $\lambda_0 = f(p_{m,0}, N_0, \Delta\theta_{b,0}, Q_{tot,0})$, and the subscript zero of each input, refer to the initial value at stoichiometric AFR. For the model inputs, p_m is the intake manifold pressure (Pa), N the engine speed (rpm), Q_{tot} the total heat release (kJ) and $\Delta\theta_b$ the

rapid burning angle (degrees). The proposed AFR model is a static model because of the limitation of the AFR sensor. The output signal from the AFR sensor installed at the mixing point includes the delay about 200ms, therefore, we cannot obtain the value of AFR cycle-by-cycle. During the steady state operation, we can assume that the in-cylinder AFR is equal to the AFR output at the exhaust manifold. Based on the AFR model structure, this model utilizes only linear terms of the intake manifold pressure and engine speed because their dynamic behaviors are slower than the combustion parameters obtained from in-cylinder pressure data. The polynomial approximation for the rapid burning angle and the total heat release is represented the faster behavior of the combustion parameters variation. In chapter 4, the identification process for the AFR model, model validation, and an application for fuel injection control are presented.

4.3 System Identification

In this section, the system identification using ridge regression will be presented. Additionally, the cross validation of model parameters are explained.

4.3.1 Identification Using Ridge Regression

For system identification, the tests were performed on an engine test bench, which consisted of the six cylinders of the gasoline engine with a low inertia dynamometer. The air flow meter, in-cylinder pressure sensors, the intake manifold pressure sensor, universal exhaust gas oxygen (UEGO) sensors, and other components were installed on the engine system. The proposed AFR model and controller were implemented by a dSPACE rapid prototyping unit, which communicates with the real time interface (RTI) bypass system and the ECU. The engine operated under the torque control mode, the VVT system was not activated, the spark advance (SA) was fixed, and the throttle was constant while the fuel injection mass was changed. There are three constant values of throttle angles in this identification scheme for a required data set. The steady state system identification was performed and 500 working cycles of combustion are considered. Table 4.1 presented the steady state experimental data of all considered point around the operating point which used for system identification.

The implementation of the ridge regression method can overcome the singular problem caused by an experimental data set. This regression method is same as ordinary least squares except for shrinking the estimated coefficients towards zero and it also makes

TABLE 4.1: Experimental data for system identification

Operating conditions No.	$AFR_{measured}$	p_m(kPa)	N(rpm)	$\Delta\theta_b$(deg)	Q_{tot}(kJ)
1	13.49	44.477	979.25	20.25	0.4466
2	13.82	44.841	978.49	21.34	0.4451
3	14.26	44.790	977.61	21.19	0.4484
4	15.12	45.659	954.18	20.37	0.4438
5	16.27	46.827	919.29	21.38	0.4463
6	13.34	44.026	1036.20	21.08	0.4514
7	13.76	44.135	1032.30	20.43	0.4423
8	14.27	44.397	1025.10	22.82	0.4469
9	14.89	44.899	1013.90	21.15	0.4442
10	16.15	46.429	977.78	22.60	0.4487
11	13.24	43.914	1084.70	21.59	0.4262
12	13.64	43.790	1085.90	21.78	0.4233
13	14.03	43.837	1081.70	21.95	0.4228
14	14.74	44.275	1065.20	22.06	0.4236
15	15.92	45.417	1034.40	22.65	0.4259

the problem non-singular. This was the main motivation for the ridge regression when it was first introduced in statistics [65]. The design of ridge coefficient can minimize a penalized residual sum of squares. However, the ridge regression has some drawbacks such as small calculated model coefficients in the model structure. This is because the constraint defining by Euclidean norm in the penalty term in the objective function. We cannot ignore effects of these small coefficient values in the model because this will lead to AFR calculation error. Furthermore, the ridge regression technique generally affects the squared bias compared with the ordinary least squares.

We apply the ridge regression to estimate the AFR model coefficients. Ridge regression shrinks the regression coefficients by imposing a penalty on their size [66]. The ridge coefficients minimize a penalized residual sum of squares (RSS),

$$\hat{\alpha}_{Ridge} = \arg\min_{\alpha} \left\{ \sum_{i=1}^{n} \left(y_i - \alpha_0 - \sum_{j=1}^{p} x_{ij}\alpha_j \right)^2 + k \sum_{j=1}^{p} \alpha_j^2 \right\} \tag{4.3}$$

where $k \geq 0$ is a complexity parameter that controls the amount of shrinkage; the larger the value of k, the greater the amount of shrinkage. n is the number of measurements, y_i

the response at observation i, x_{ij} data, at element j of a regression vector at observation i, α_0 and α are scalar and p is the number of vector elements, respectively. α_0 is estimated by $\bar{y} = \frac{1}{n} \sum\limits_{i=1}^{n} y_i$. We can write the previous criterion in matrix form

$$RSS(k) = (Y - \Phi)^T(Y - \Phi) + k\alpha^T\alpha \qquad (4.4)$$

where Y denotes the output vector and Φ is the regression matrix.

The ridge regression is applied to this problem for estimating the model coefficients because the determinant of $\Phi^T\Phi$ is close to zero. The coefficients of the AFR model can be calculated by using the following close form solution:

$$\hat{\alpha}_{Ridge} = (\Phi^T\Phi + kI)^{-1}\Phi^TY \qquad (4.5)$$

where I is an identity matrix. k is the complexity parameter which can be designed by the application of trace plot and cross validation. The value of this complexity parameter regulated the amount of shrinkage.

Additionally, there is a high efficiency regularization method for estimation of the linear model coefficients, for example [67]. Tibshirani has presented the method which can be used for improvement of the linear model parameter estimation. This method shows effective results when the model has highly complex structure and contains many terms. However, his proposed method requires higher calculation load compared with ridge regression technique. Therefore, because of our simple model structure, we will consider only the application of ridge regression for the AFR model identification.

4.3.2 Trace Plot of Model Parameters

The regularization method has an associated tuning parameter, i.e., k for ridge regression in the penalized forms. The tuning parameter controls the amount of regularization, so choosing an appropriate value of the tuning parameter is important. We also refer to this task as model selection because each tuning parameter value corresponds to a fitted model. We might consider a good choice of tuning parameter. However, it depends on whether our goal is prediction accuracy or recovering the right model for interpretation purposes. Basically, the total variance is a monotone decreasing sequence with respect to the ridge parameter k, while the total squared bias is a monotone increasing with respect to k. Therefore, we can choose the appropriate small value of k which leads to reasonable sign and magnitude of model parameters. In this identification, the ridge

parameter k is designed at 0.06. Additionally, an alternative way of choosing k is to see how well predictions based on the bias at the value of k do at actual instances of output y. Hence, the results of model prediction output can be investigate in the model validation process. From the experimental data presented in Table 4.1, the trace plot of model parameters is performed, the results are depicted in Fig. 4.2.
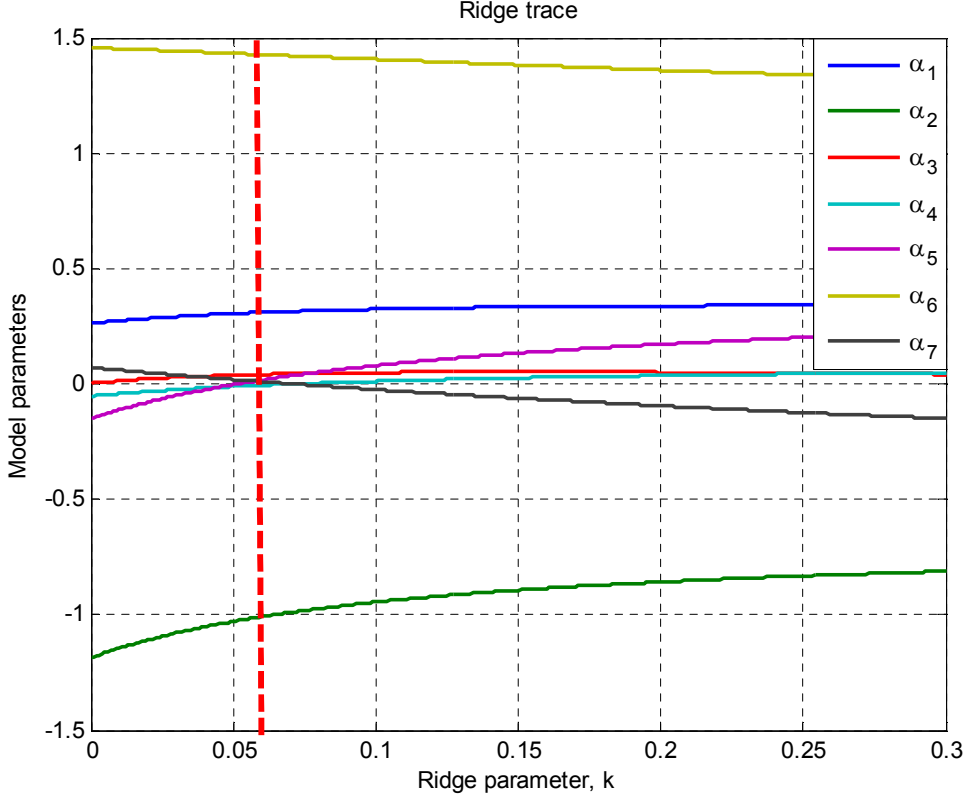
FIGURE 4.2: Trace plot of model parameters with respect to the ridge parameter

4.3.3 Cross Validation

Cross validation extends the training/test set approach. As with that approach, it estimates predictive accuracy for data that are sampled from the population in the same way as the existing data [68]. Cross validation is a simple, intuitive way to estimate prediction error. After obtaining data from experiments, we can analyze the data by applying this method. For a number K, we split the training pairs into K parts or folds (commonly $K=5$ or $K=10$). K-folds cross validation considers training on all but the l_{th} part, and then validating on the l_{th} part, iterating over $l=1,...K$. K-fold cross validation has procedure as follows:

- Divide the set of data into K subsets (i.e., folds) of rough equal size randomly.

- For $l= 1,...K$, first, consider training on (x_i, y_i), $i \notin F_l$, and validating on (x_i, y_i), $i \in F_l$. Note that, x_i is an input, y_i is output at each considered point, and $y_i = f(x_i)$. Then, for each value of tuning parameter $k \in \{k_1, ...k_m\}$, compute the estimate $\hat{f}_\theta^l$ on the training set, and record the total error on the validation set.

- For each tuning parameter value k compute the average error over all folds.

Having done this, a cross validation error curve $CV(k)$ which is a function of k are obtained. Also, the standard deviation of $CV(k)$ at each $k \in \{k_1, ...k_m\}$ are estimated. From these results, we can choose the value of complexity parameter that minimizes this curve. For increasing regularization, the value of the complexity parameter at minimum point plus one standard deviation is more appropriate. Using one standard error rule, the model with lower number of non-zero coefficients can be derived. However, the cross validation requires high calculation and all input should be normalized before calculation.

4.3.4 Identification Results

In this identification, considering a steady state AFR response, both the intake manifold pressure and the engine speed have a significant effect on the air mass flow rate. The fuel mass directly affects the total heat release and burn duration. The main AFR oscillation is caused by the total heat release and the rapid burning angle because the changing rate of the manifold pressure and the engine speed are slower compare to the variation of the combustion parameters.

The AFR values under various operating conditions are obtained from experiments by averaging over many working cycles. This is because the AFR sensors installed on the test bench have a certain delay and they cannot detect the value of AFR cycle-by-cycle. We consider both the variation of the throttle and the change of the fuel mass on the torque's constant mode. The relation between the model inputs affected by the air mass flow rate and the AFR is shown in Fig. 4.3 (a). Moreover, the connection between the combustion parameters and the AFR is exhibited in Fig. 4.3 (b).
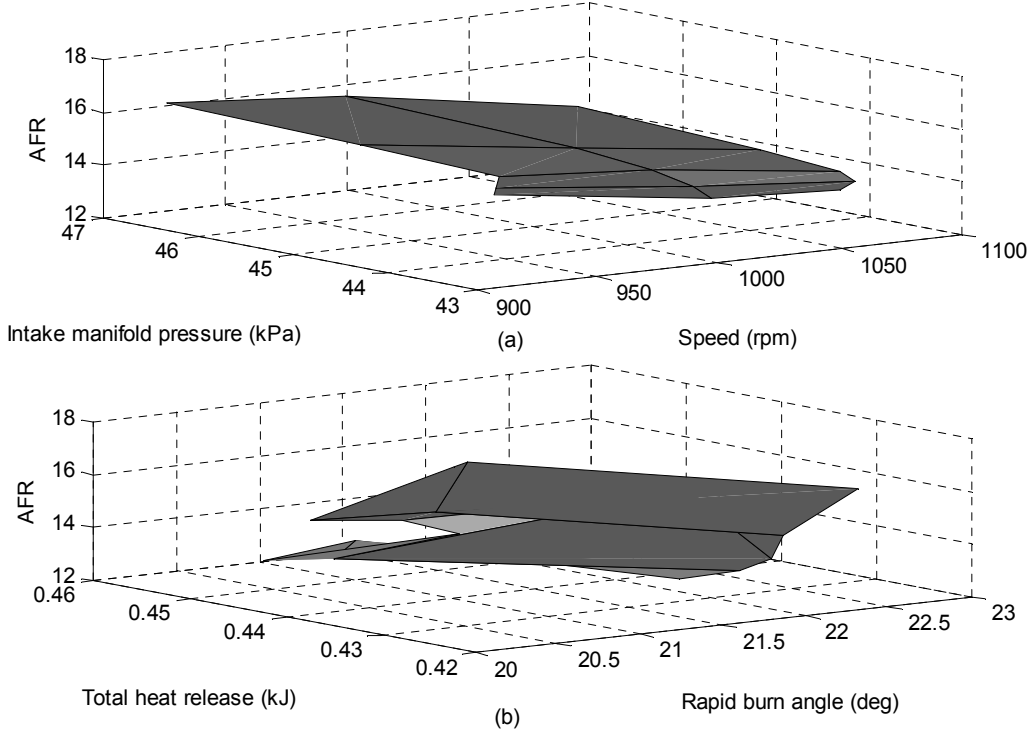
FIGURE 4.3: Relationship between model inputs and the AFR.

The polynomial parameter estimation for this model is set up as follows:

$$
\begin{aligned}
AFR - \lambda_0 = [&(\Delta\theta_b - \Delta\theta_{b,0}) \quad (Q_{tot} - Q_{tot,0}) \\
&(\Delta\theta_b - \Delta\theta_{b,0})^2 \quad (\Delta\theta_b - \Delta\theta_{b,0})(Q_{tot} - Q_{tot,0}) \\
&(Q_{tot} - Q_{tot,0})^2 \quad (p_m - p_{m,0}) \quad (N - N_0)] \cdot \\
&[\alpha_1 \quad \alpha_2 \quad \alpha_3 \quad \alpha_4 \quad \alpha_5 \quad \alpha_6 \quad \alpha_7]^T
\end{aligned}
\tag{4.6}
$$

The vector of regression is

$$
\begin{aligned}
\varphi = [&(\Delta\theta_b - \Delta\theta_{b,0}) \quad (Q_{tot} - Q_{tot,0}) \\
&(\Delta\theta_b - \Delta\theta_{b,0})^2 \quad (\Delta\theta_b - \Delta\theta_{b,0})(Q_{tot} - Q_{tot,0}) \\
&(Q_{tot} - Q_{tot,0})^2 \quad (p_m - p_{m,0}) \quad (N - N_0)]
\end{aligned}
\tag{4.7}
$$

Define the parameter vector as

$$
\alpha = [\alpha_1 \quad \alpha_2 \quad \alpha_3 \quad \alpha_4 \quad \alpha_5 \quad \alpha_6 \quad \alpha_7]^T
\tag{4.8}
$$

Therefore, the output become

$$y = AFR - \lambda_0$$
$$= f(p_m, N, \Delta\theta_b, Q_{tot}) - f(p_{m,0}, N_0, \Delta\theta_{b,0}, Q_{tot,0}) \tag{4.9}$$

An estimate for y can now be calculated from n cycles of measurements using least squares regression. The output from the measurements defined by (4.9) are collected into an output vector, Y, and the regression vectors defined by (4.7), are collected into a regression matrix, Φ.

$$Y = \begin{bmatrix} y_1 \\ y_2 \\ \vdots \\ y_n \end{bmatrix} \tag{4.10}$$

and

$$\Phi = \begin{bmatrix} \varphi_1 \\ \varphi_2 \\ \vdots \\ \varphi_n \end{bmatrix} \tag{4.11}$$

For the calculation of the estimated model parameters, we solve for the least squares estimate, $\hat{\alpha}$

$$\hat{\alpha} = (\Phi^T\Phi)^{-1}\Phi^T Y \tag{4.12}$$

However, the ridge regression is applied to this problem for estimating the regression coefficients because the determinant of $\Phi^T\Phi$ is close to zero. The parameters of the AFR model can be calculated by using the following equation:

$$\hat{\alpha} = (\Phi^T\Phi + kI)^{-1}\Phi^T Y \tag{4.13}$$

where k is the ridge parameter and I is the identity matrix. From the experimental results, the variation of AFR compares with its value at stoichiometric and the four model inputs variation are depicted in Fig. 4.4.

The AFR model parameters obtained from the system identification are shown in Table 4.2. Next, the AFR model validation will be presented in the following section.
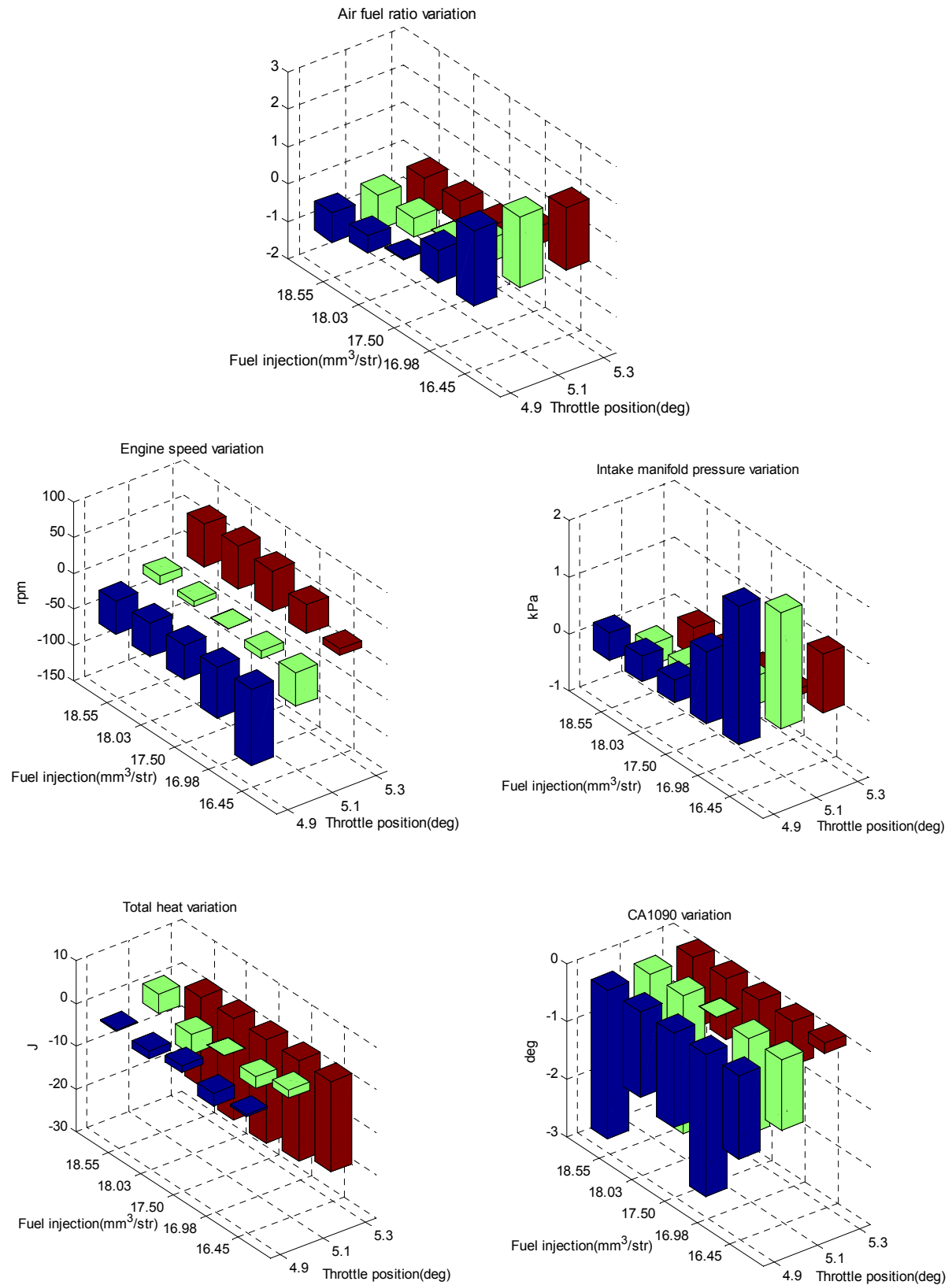
FIGURE 4.4: Input and output variation

TABLE 4.2: Air-fuel ratio model parameters.

Parameter	Value	Parameter	Value
α_1	0.3101	α_5	0.0174
α_2	-1.0081	α_6	1.4270
α_3	0.0417	α_7	0.0100
α_4	-0.0055		

4.4 Air-Fuel Ratio Model Validation

Two cases of the AFR model validation were performed, by changing the fuel-injected command during constant throttle and during the variation of the throttle under the fixed injected fuel. For the first case, the value of air mass flow rate is almost constant because the throttle is fixed. However, while the fuel injection is reduced, the engine speed and the intake manifold pressure are changed. These phenomena lead to the variation of air mass flow rate going into the combustion chamber. Fig. 4.5 shows the experimental results for the first case. The variation of the four model inputs ($N, p_m, \Delta\theta_b, Q_{tot}$) caused by the amount of the injected fuel was presented. Additionally, the changing of the fuel injection command, the estimated AFR compared with the measured AFR from the sensor at the mixing point, and the error of the AFR calculation, are all shown. The model yielded effective results in the cases of various fuel injections during constant throttle and load torque values. The RMS of the AFR error was 0.53% and the maximum absolute error was 12.30% during the transient response. These errors were calculated and compared with the stoichiometric value. Both the estimated error and the variation of the calculated AFR values were less than the values obtained from the theoretical model presented in [44].

However, the response of this model exhibited some delay compared to the reaction obtained from the sensor. This delay was mainly owing to the model inputs calculated from the in-cylinder pressure data. The estimation of the AFR had a time delay of approximately 1.0s because of the moving averaging process applied to many working cycles and the low-pass filter effects. Subsequently, the effects of the throttle changing at a constant fuel injection were examined. The air mass flow rate is changed corresponding to the throttle angle. Four model inputs, the throttle angle, and the AFR were exhibited in Fig. 4.6. The calculated AFR yielded some error, especially during the transient period. The RMS of the AFR error was 0.03% and the maximum absolute error was 12.88%. This error results from the limitation of information for the static system
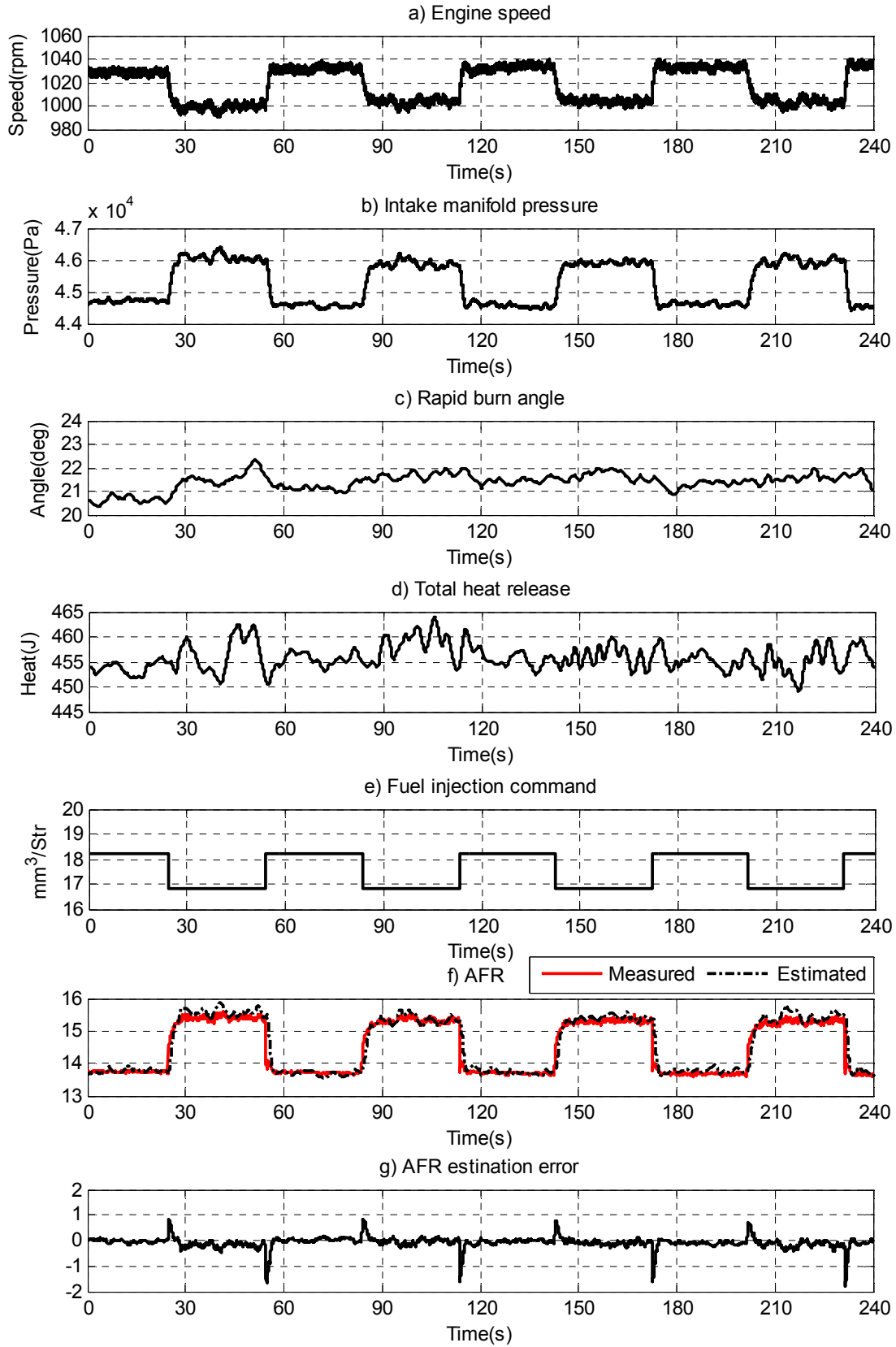
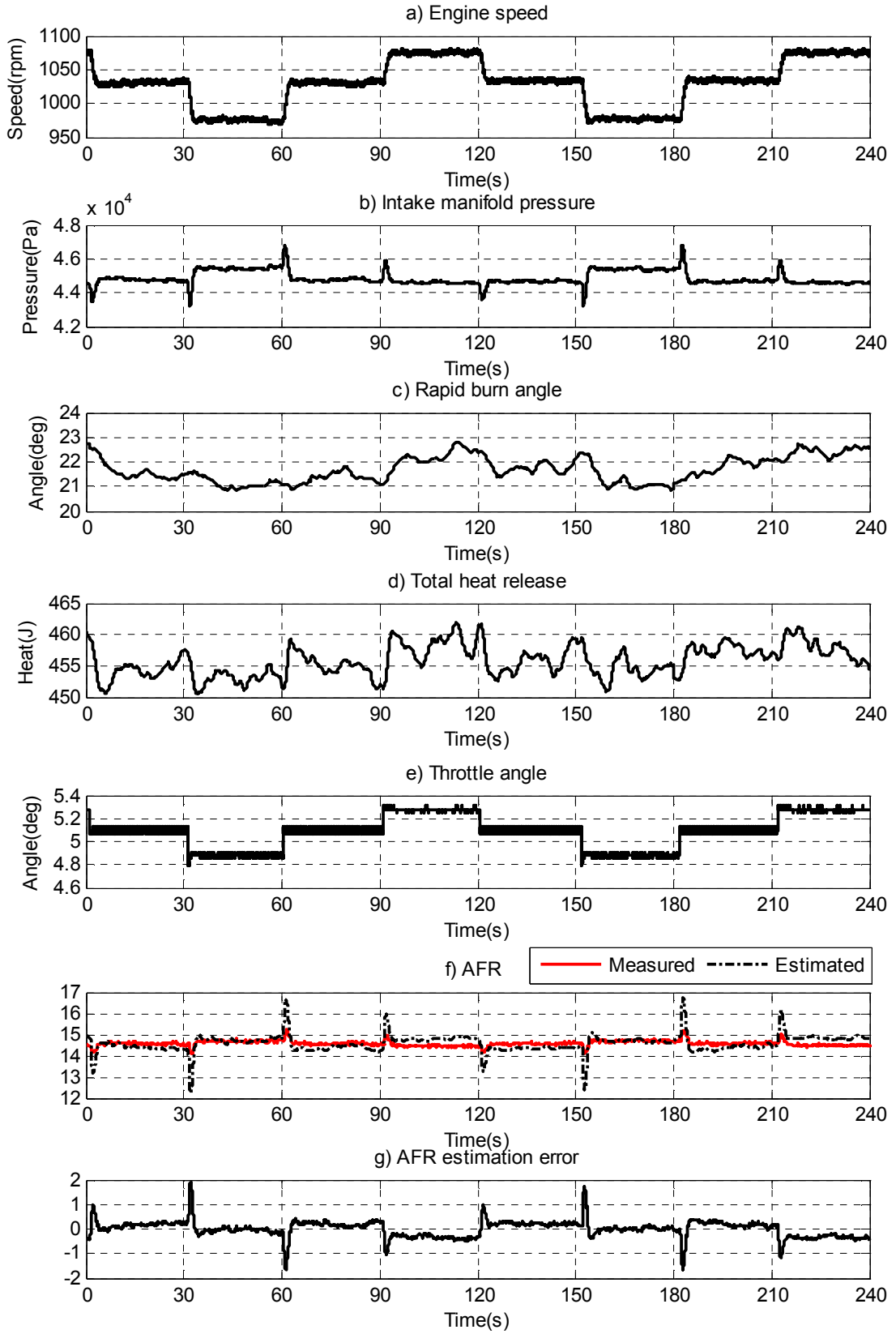FIGURE 4.5: Experimental results for the AFR model validation while the throttle is constant

FIGURE 4.6: Experimental results for the AFR model validation with a constant rate of injected-fuel

identification. The number of data points using in the case of changing the throttle is less than the number of data using in the case of changing fuel injection. The limitation of experimental data is mainly caused by the engine behavior that will stop immediately if high fluctuation torque is happened. In the torque control mode, the shift of the throttle angle yielded the main effect on the engine speed changes, while small changes in the AFR were observed during steady state. The time delay value in this case was almost the same as in the previous case.

4.5   Simple Adaptive Air-Fuel Ratio Control

In this section, we introduce some behaviors of the port injection and the system model. Subsequently, the details of the controller design with the AFR model are presented.

4.5.1   Effects of Wall-wetting on Fueling Control

The wall-wetting phenomena have important effects on the fuel path of the AFR control system. The utilized mean value model in the control design accounts for the impingement and the evaporation process of the injected fuel on the walls [38]. An empirical model, defined in [39], has been utilized to express the port injection path dynamics.

In this work, the model can be considered as a first-order system with unknown parameters. Moreover, the cooling loss and the variation of the combustion efficiency can be included as an unknown system disturbance. An adaptive controller that will be presented in the next section will control the plant with unknown parameters and reject the system disturbances.

4.5.2   Simple Adaptive Fueling Control

The simple adaptive control is applied to control the injected fuel of the port injection system. This controller uses the reference model for generating the desired signal. The control objective is to design the adaptive input making the AFR output, $\lambda_{est,fil}(t)$, track the reference input, $\lambda_d(t)$. The AFR control system using SAC, in associate with the AFR model, is shown in Fig. 4.7. Note that, the first-order filter in this case is a low pass filter, with a transfer function $1/(\tau_{fil}s + 1)$. The parameter τ_{fil} denotes the filter time constant. The measured AFR obtained from the sensor λ_s at the mixing points is only used for checking the performance of the AFR model.
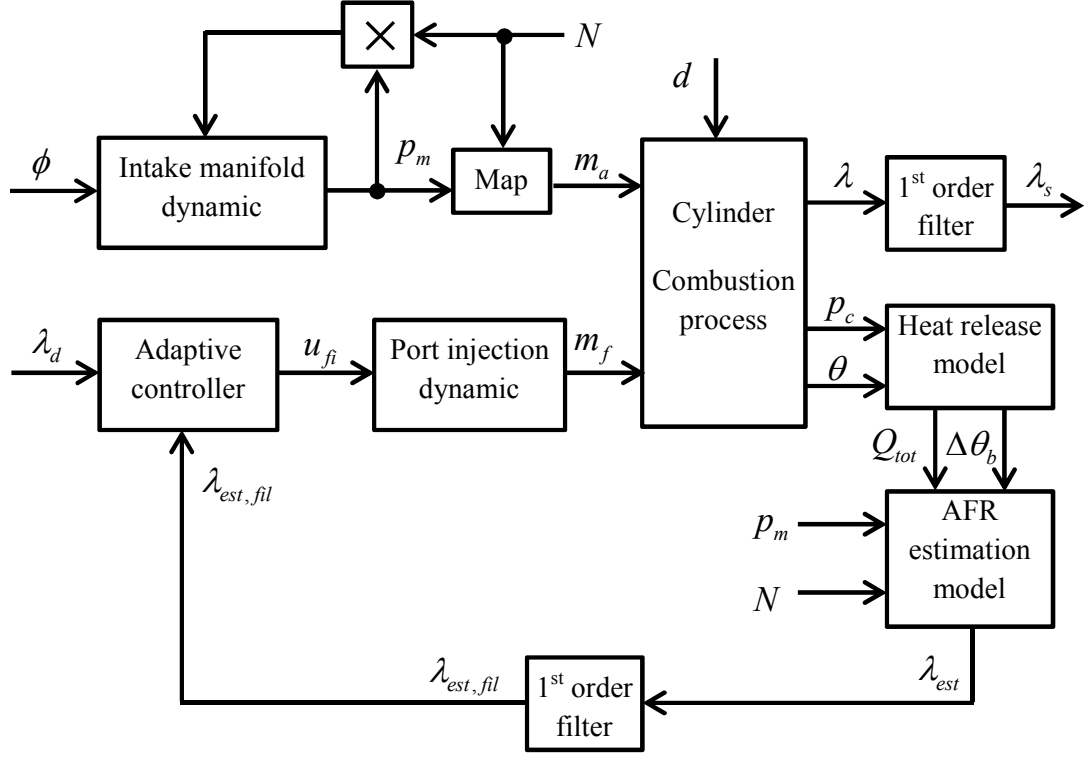
FIGURE 4.7: Block diagram of the AFR control system

In this control system, we consider mainly on the dynamic of port injection system because the experiment is conducted on steady state operation. The combustion process in the torque constant mode at steady state operation includes small variation that can be considered as the system disturbances. The proposed AFR model which is used to replace the AFR sensor for generating the output feedback signal is also the static model. Hence, the combustion process and the proposed AFR model are assumed to be only time delay.

We neglect the direct term of the wall-wetting model. In this way, the plant model is regarded as a minimum phase first-order system with a relative degree equal to one. Therefore, SAC can be applied for fuel injection control. For the design of strictly positive real system, the details have presented in [26]. The response of the controlled plant is required to follow the input-output behavior of the first-order reference model in the form of

$$\dot{x}_m(t) = -a_m x_m(t) + b_m u_m(t) \tag{4.14}$$

$$y_m(t) = c_m x_m(t) \tag{4.15}$$

where a_m, b_m, and c_m, are model parameters. We select the first-order model to generate the desired trajectory for the AFR control system and define the tracking error as

$$e_y(t) = y_m(t) - y_p(t) \tag{4.16}$$

where $y_p(t)$ is the output of the plant to be controlled. Using the values that can be measured, $e_y(t)$, $x_m(t)$, and $u_m(t)$, the following total control signal is obtained.

$$u_{fi}(t) = k_{e_y}(t)e_y(t) + k_{x_m}(t)x_m(t) + k_{u_m}(t)u_m(t) \tag{4.17}$$

where the adaptive gains, k_{e_y}, k_{x_m}, k_{u_m}, are obtained as the combination of proportional and integral gains. Firstly, an adaptation law for $k_{e_y}(t)$ is considered.

$$k_{e_y}(t) = k_{Pe_y}(t) + k_{Ie_y}(t) \tag{4.18}$$

$$k_{Pe_y}(t) = \gamma_P e_y^2(t) \tag{4.19}$$

$$\dot{k}_{Ie_y}(t) = \gamma_I e_y^2(t) - \sigma k_{Ie_y}(t) \tag{4.20}$$

We then present the adaptation law for $k_{x_m}(t)$ as

$$k_{x_m}(t) = k_{Px_m}(t) + k_{Ix_m}(t) \tag{4.21}$$

$$k_{Px_m}(t) = \gamma_P e_y(t)x_m(t) \tag{4.22}$$

$$\dot{k}_{Ix_m}(t) = \gamma_I e_y(t)x_m(t) - \sigma k_{Ix_m}(t) \tag{4.23}$$

Finally, we design the adjustment law for $k_{u_m}(t)$ in accordance to

$$k_{u_m}(t) = k_{Pu_m}(t) + k_{Iu_m}(t) \tag{4.24}$$

$$k_{Pu_m}(t) = \gamma_P e_y(t)u_m(t) \tag{4.25}$$

$$\dot{k}_{Ie_y}(t) = \gamma_I e_y(t)u_m(t) - \sigma k_{Iu_m}(t) \tag{4.26}$$

where γ_P and γ_I are parameters that affect the rate of adaptation. The σ terms following the idea of Ioannou and Tsakalis [69] in the equations are used here to avoid the divergence of the gains. The modified adaptive law with σ sacrifices the ideal stability properties in the disturbance-free case in order to achieve boundedness of all signals in the presence of disturbances. The adjustment of the controller gains corresponds to the system desired input, the model state variable, and the error between the plant and the reference model. The structure of SAC can be expressed as shown in Fig. 4.8.
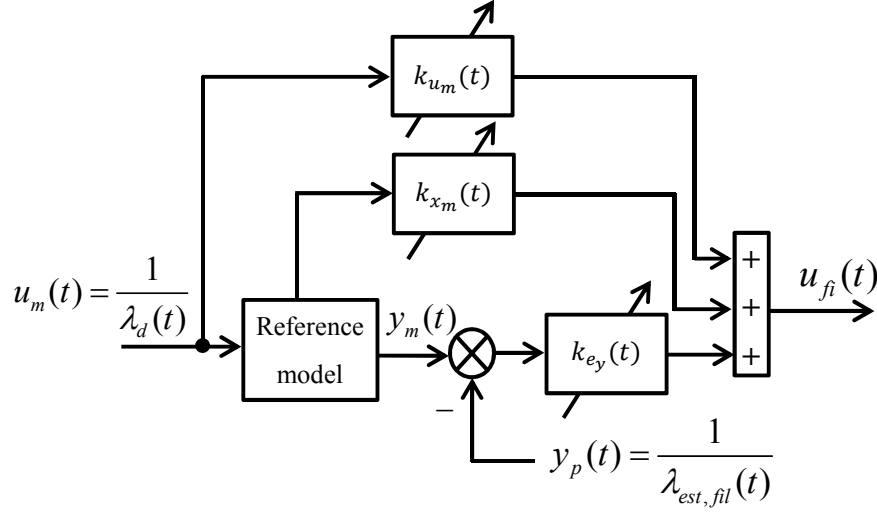
FIGURE 4.8: Schematic diagram of Simple Adaptive Control (SAC)

SAC is suitable for AFR control applications because it can deal with the unknown system parameters and the disturbances. There are some disturbances in this controlled system, such as, the variation of air mass flow rate, engine combustion efficiency and the residual burned gas, for example. Additionally, the total modeling error exists because we assume the first-order system as the plant to be controlled.

4.5.3 Air-fuel Control Experiment

The SAC control performance, tracking error, controlled fuel injection, adaptation gains, and AFR estimation efficiency, are shown in Fig. 4.9. In this case, the controller parameters are γ_P=1000, γ_I=500, and σ=0.001. These controller parameters γ_P=1000 and γ_I=500 are tuned for obtaining the effective response of the AFR. Using high value of these tuning parameters, the fast transient can be obtained but the steady response oscillation is inevitable. The sampling time in the experimental calculation program was 0.25ms, which was improper for the controller application. Therefore, a suitable trigger signal for the AFR controller was designed. This trigger signal generated the command output signal that can activate the port's fuel injection system, which also included the time delay.

In regard to the safety conditions, the injected fuel output was limited to a specified fuel mass flow rate entering the combustion chamber. The AFR calculation delay was also another important factor that affected the performance of the SAC. In this experiment, all inputs of the AFR model contain a time delay, especially the inputs obtained from the combustion parameters.
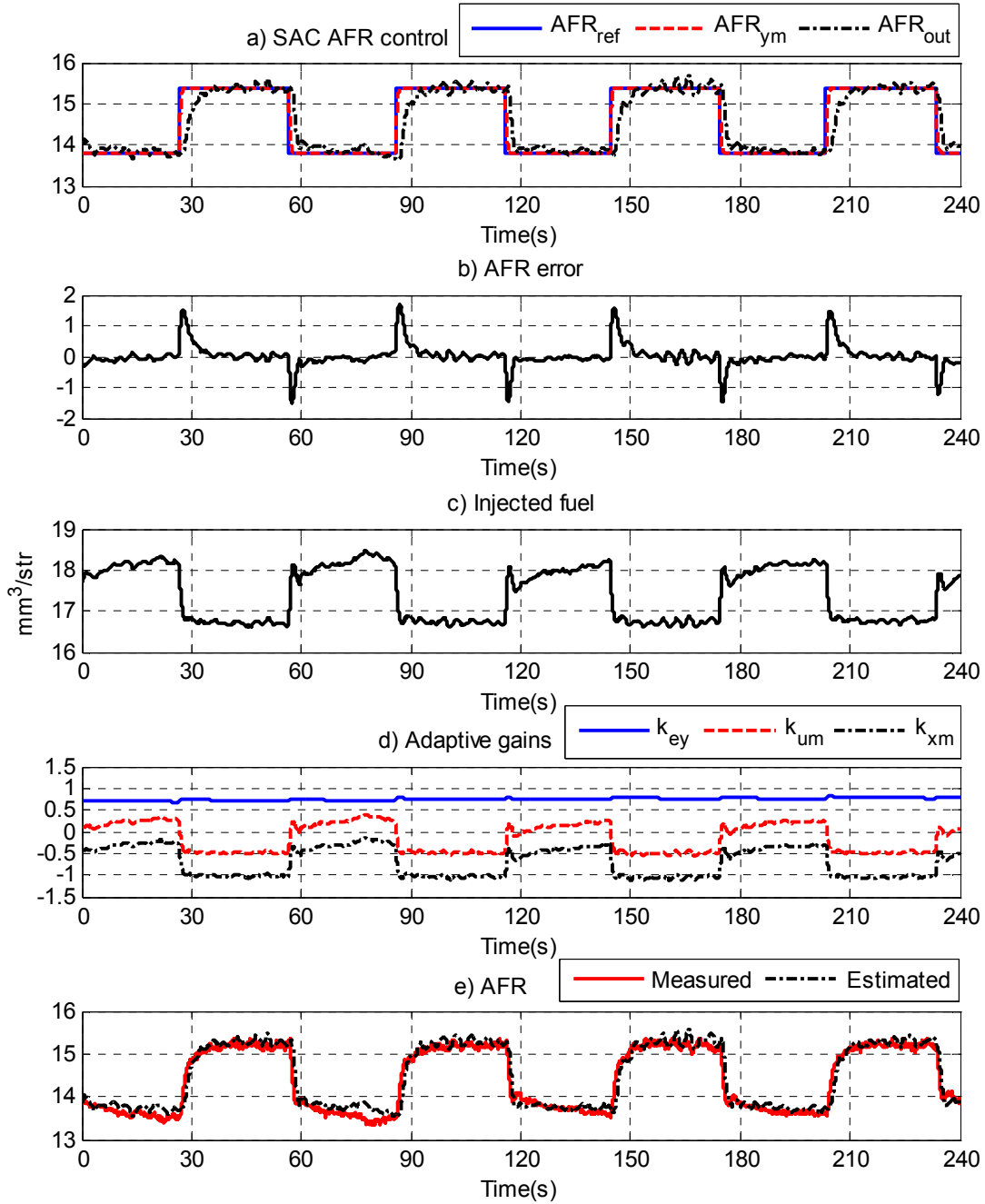
FIGURE 4.9: Experimental results for SAC control performance

This was because of the variation of the in-cylinder pressure, and the use of the moving average operator and the filter. These delays had affected the feedback signal used by SAC. Because of these reasons, the transient response of the SAC was quite slow. Therefore, this AFR model was not suitable for transient control applications. Additionally, the performance of the SAC was seriously affected by the AFR estimation error.

Furthermore, the output of the AFR model is utilized as a controller feedback signal. Additionally, the model response as a result of changes in the controller parameters was investigated. The results are shown in Fig. 4.10. In this figure, the controller parameters are as follows: (a) $\gamma_P=800$, $\gamma_I=300$ and $\sigma=0.001$, (b) $\gamma_P=900$, $\gamma_I=400$ and $\sigma=0.001$, (c) $\gamma_P=1100$, $\gamma_I=600$ and $\sigma=0.001$, and (d) $\gamma_P=1200$, $\gamma_I=700$ and $\sigma=0.001$.
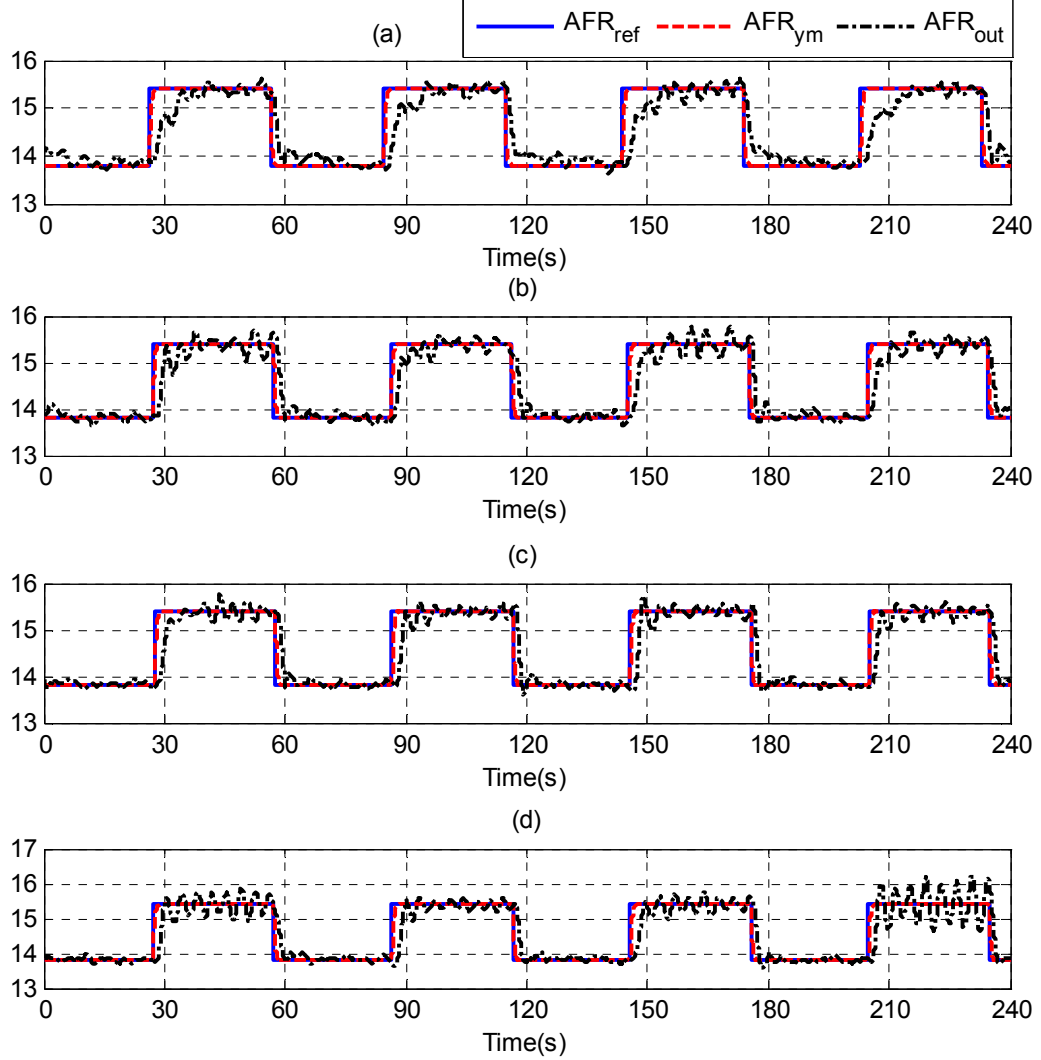
FIGURE 4.10: Effects of changing controller parameters

Stability analysis of the controlled system can be considered based on some assumptions. We omitted the dynamics of the intake manifold and the crank shaft. The time delay of the feedback was then neglected. The direct term of the plant transfer function is also ignored. Therefore, in ideal cases, we can prove the stability of the entire system using the idea presented in [64]. In practical applications, however, all these effects should be considered. We envisage pursuing this as future work.

4.6   The Control Performance Analysis

The performance analysis of the AFR control using SAC with the proposed estimated AFR model based in-cylinder pressure measurement will be investigated in this section. Generally, the AFR control system composes of two main part, feedforward and feedback loops. In this research, we have considered only one operating condition then the feedforward loop can be considered as constant fuel injection according to control lookup table. The proposed methodology is focused on the AFR control using the feedback loop. We can investigate the performance of the controller and then examine the effects of feedback signal. Additionally, this port injection system has wall-wetting dynamics behavior that must be considered.

The performance of SAC is analyzed in many literature and it can satisfy the main control requirements which are tracking the output to the desired reference and rejecting some disturbances. Moreover, it is rather insensitive to noise effects. The main part that affects directly to the AFR control system performance is the AFR estimation based on in-cylinder pressure data. This is because the variation of combustion cycle-by-cycle leads to necessary signal conditioning, for instance, cycle moving average window and crank angle moving average window. These parts can reduce the cylinder pressure variation but they generate some inevitable AFR calculation delay during the transient response.

The effects of AFR estimation delay is exhibited in Fig. 4.11 and Fig. 4.12. The figure shows that the time delay effects are obviously affected during the reference AFR changing. Additionally, the response of AFR estimation model during increasing of AFR command is different from reducing of AFR command. This is caused by the response of fuel injector system and the changing rate of AFR model inputs.

Additionally, there are some limitations of the proposed AFR model. Firstly, the identification and validation processes have considered only the steady state operating condition then the AFR model is only the static model. The transient AFR cycle-by-cycle cannot be captured because of the sensor delay. Secondly, the considered measured validation AFR are obtained from the sensor at a mixing point. The exhaust gas at this point composes of the output from the first, the third and the fifth cylinder. We have assumed that at steady state the output AFR of these three cylinder is equal. Finally, the environment also affects the AFR estimation because of day-to-day variation on the engine system. We have applied the estimated AFR using only the fifth cylinder data for control fuel injection of all cylinders. The effects of imbalance AFR happening in
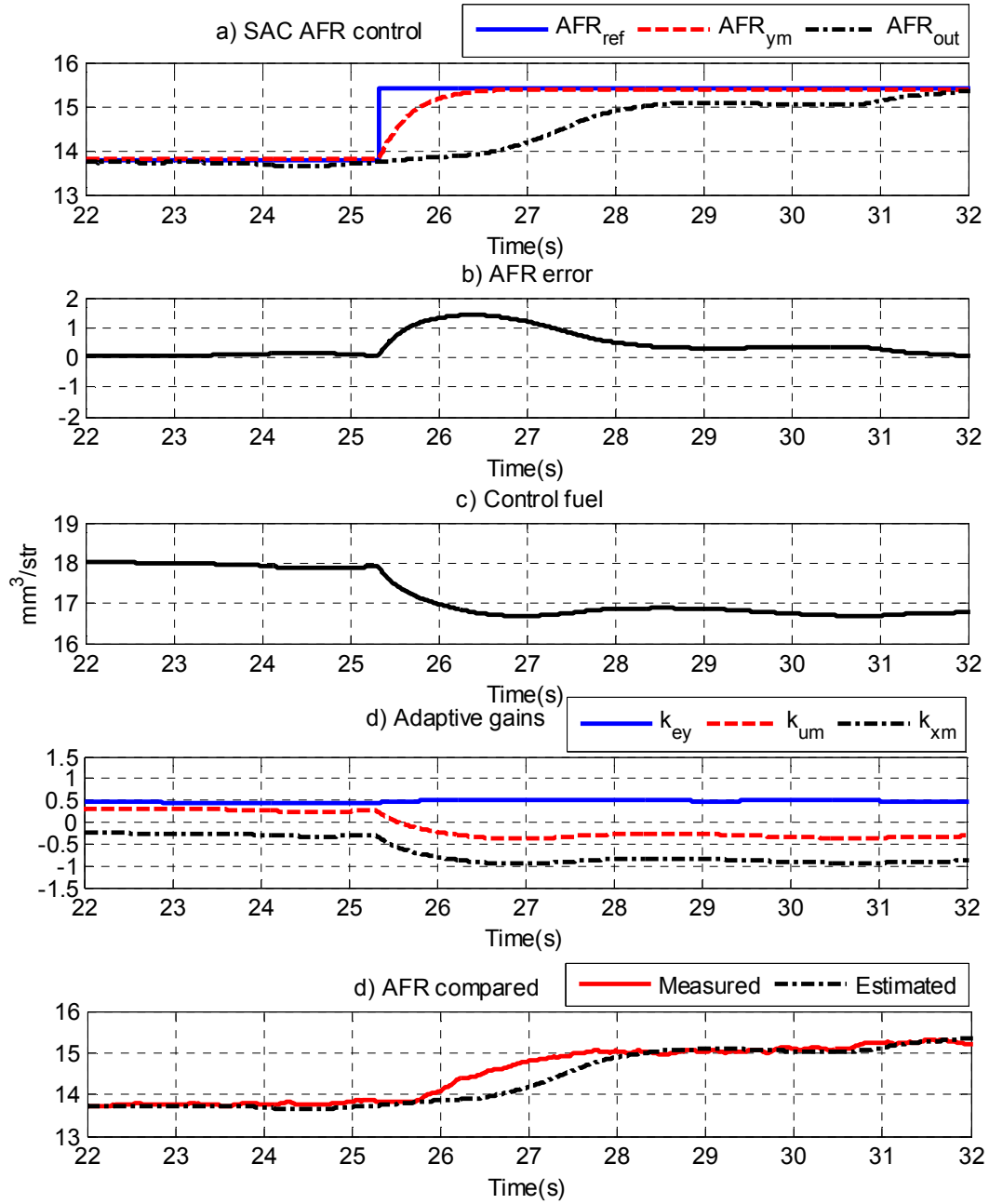
FIGURE 4.11: Effects of delay on AFR estimation while AFR is increased

all cylinders are inevitable. Additionally, the fuel injector outputs are not the same while we input the same command. Therefore, all these effects lead to the performance limitation of the proposed AFR control system.

In this experiment, the results of AFR model identification of only one operating point is investigated and implemented for AFR regulation. However, we have considered other operating conditions for the AFR estimation. The proposed model can work well but the
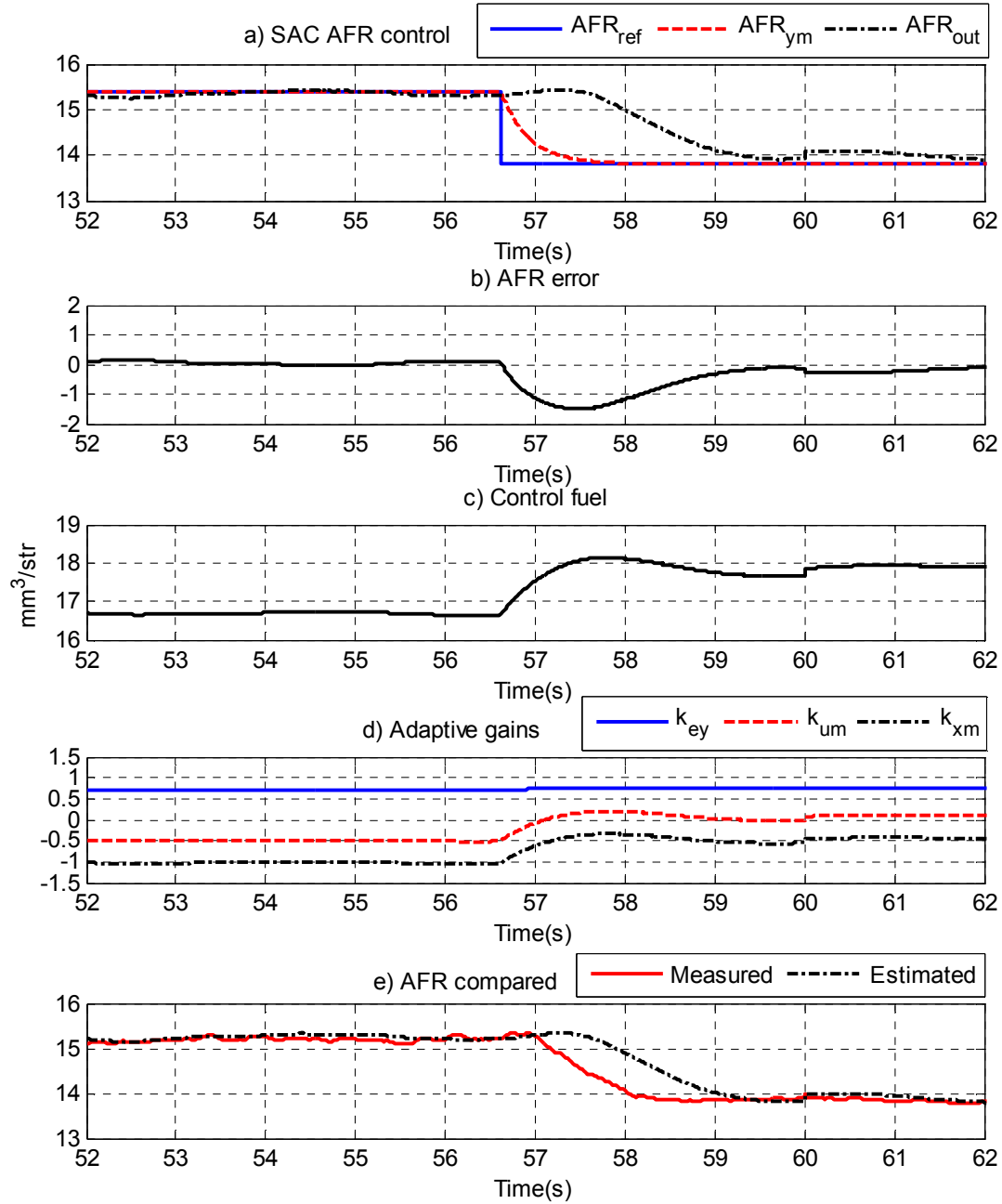
FIGURE 4.12: Effects of delay on AFR estimation while AFR is decreased

difficult issue is the operating conditions for model identification. During identification experiment, some information on torque constant mode and on lean combustion conditions are required. Under lean burn condition the engine cannot provide high torque output. Therefore, the implementation of the proposed model is limited only on the low load region. At high load condition, the model identification cannot be performed.

4.7   Conclusion

Based on the experimental results of this study, we can conclude that the proposed model shows effectiveness in calculating the AFR of the SI engine using information from the in-cylinder pressure. In addition, the SAC with the cylinder pressure-based AFR sensor can be applied to control the AFR of the port injection gasoline engine. However, the AFR model response elicits a delay because of the use of the cylinder pressure data. It also gave some important effects in AFR control applications, especially during the transient period.

Chapter 5

An Application of In-cylinder Pressure to Compression Heat Transfer Estimation

In this chapter, first, the calculation method for in-cylinder pressure offset is explained. The thermodynamic model for compression heat transfer estimation and the polytropic exponent evaluation are then introduced. Subsequently, the model identification which consists of data collection, identification procedure, identification results, and model validation are expressed. Moreover, the evaluation results of polytropic exponent caused by heat transfer is presented. Finally, all results are discussed and concluded.

The main contributions presented in this chapter are the principal subject of the following publications:

- C. Khajorntraidet and K. Ito, An Application of In-Cylinder Pressure for Compression Heat Transfer Estimation, Proceedings of the 8th IFAC Symposium on Advances in Automotive Control-AAC 2016, June 20-23, 2016, Kolmarden Wildlife Resort, Sweden.

- C. Khanjorntraidet and K. Ito, An Application of the Parameter-Influence Technique for a Reduced Heat Transfer Model Identification, Proceedings of the10th SEATUC Symposium 2016, OS-A2-05, February 22-24, 2016, SIT, Japan.

5.1 Introduction

The effects of heat transfer on the SI engine combustion have been considered in many researches. Heat transfer becomes more important as the combustion process ends and average gas temperature peaks because it will affects the heat transfer in the next working cycle. Additionally, the knocking problem is strongly depending on the amount of heat transfer because it affects ignition timing, combustion duration, and rate of pressure rise, which are correlated to knock; as presented by [70] and [71]. In the study of Woschni [30], an empirical law was proposed, where the heat transfer coefficient depends on the pressure, temperature, and engine speed. According to [72], the increased heat transfer to the cylinder walls during combustion and the expansion process makes the polytropic exponent greater than the corresponding specific heat ratio. Moreover, The combination of the loss mechanisms, crevice effect and heat transfer, also makes it difficult to identify separate effects, as indicated by [73].

The estimation of heat transfer during the compression and combustion strokes allows representing the system during the combustion. However, the heat transfer model contains strong nonlinearities and difficult to implement in the heat release modeling. Hence, in the work of [45], the reduced heat transfer model was proposed. In fact, the heat transfer to the combustion chamber walls is quite difficult to estimate. Many studies focus on the heat transfer estimation but the challenged issue is the accuracy of the heat transfer model parameters.

The combustion analysis should be more accurate than the assumed adiabatic case if the effects of heat transfer are included in the calculation. In practical applications, we can apply the estimated compression heat transfer for correction of the pressure offset calculation. This result affects the heat release calculation which can be applied for combustion control and analysis, as shown in [74]. Moreover, the estimated compression heat transfer can be considered in the case of the sensitive combustion control such as homogeneous charge compression ignition (HCCI). Many researchers study on the heat transfer in HCCI engines, including those by [75] and [76].

This work addresses the heat transfer estimation using the in-cylinder pressure data and some information during the compression stroke. The off-line calculations with the experimental data show that the heat transfer model parameters and its direction can be identified. The results of compression heat transfer can be used to compute the variation of the polytropic exponent. The polytropic exponent during the compression cycle of a reciprocating internal combustion engine depends on the instantaneous values for

pressure and volume, as well as on their variations. This dependency makes it possible to solve uncertainties typical of the engine experimental tests, such as the synchronization of pressure and volume signals. The wall temperature also affects the calculated value of polytropic exponent such as those reported in [77]. However, the proposed method requires some improvements. This is because of the limitations of the measurement data and the assumptions imposed that may not be precisely determined in practical applications. Hence, we also present the model analysis and possible ways for the model improvements.

5.2 In-cylinder Pressure Offset Calculation Using Inlet Pressure Referencing Method

In this chapter, the inlet pressure referencing method is applied based on the basic assumption of the unknown constant pressure offset during one working cycle which indicated by (A.1) in appendix A.
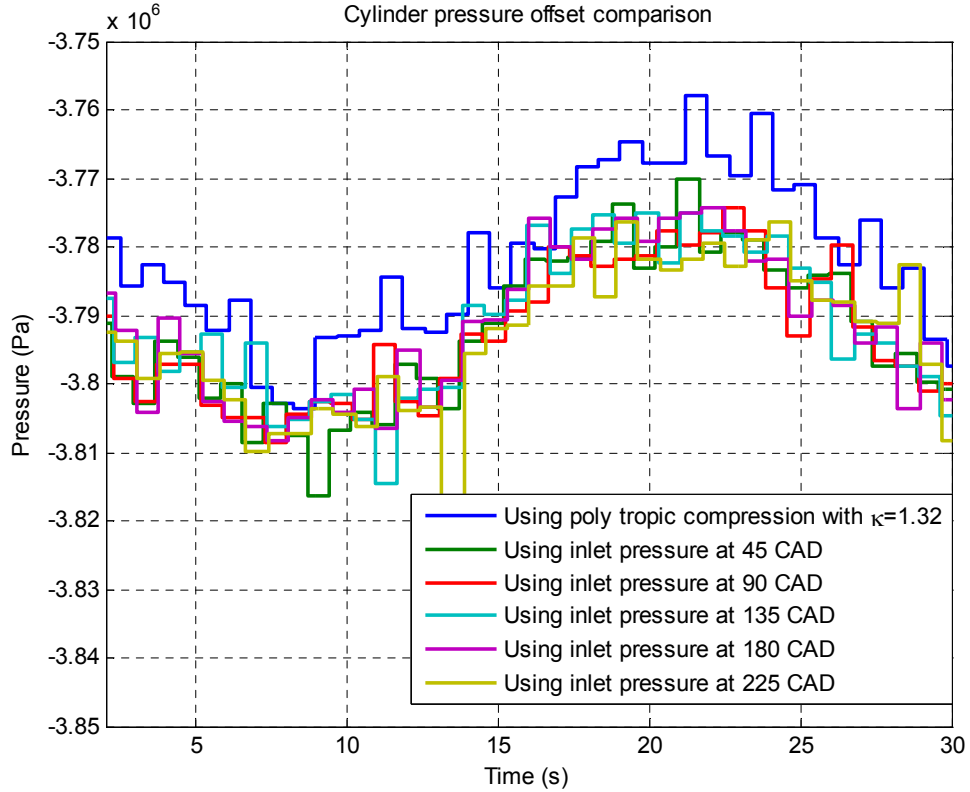
FIGURE 5.1: Effects of referencing point on the pressure offset calculation

The basic idea of the inlet pressure referencing method is to use the absolute pressure data at the inlet of the combustion chamber for the pressure offset compensation. This method sets the cylinder pressure at some points during intake valves opening equal to the intake manifold pressure. This is a very accurate procedure in an unturned intake system or at very low speeds in a turned system. This is because the variation of the pressure during the intake valve opening affects directly to the pressure referencing value. Additionally, measurement noise during low pressure region would lead to inaccurate referencing for the entire pressure data of that cycle. The effects of noise on the calculation of the cylinder pressure offset are shown in Fig. 5.1. Although the pressure offset shows the same tendency, its variation depends on the design referencing point.
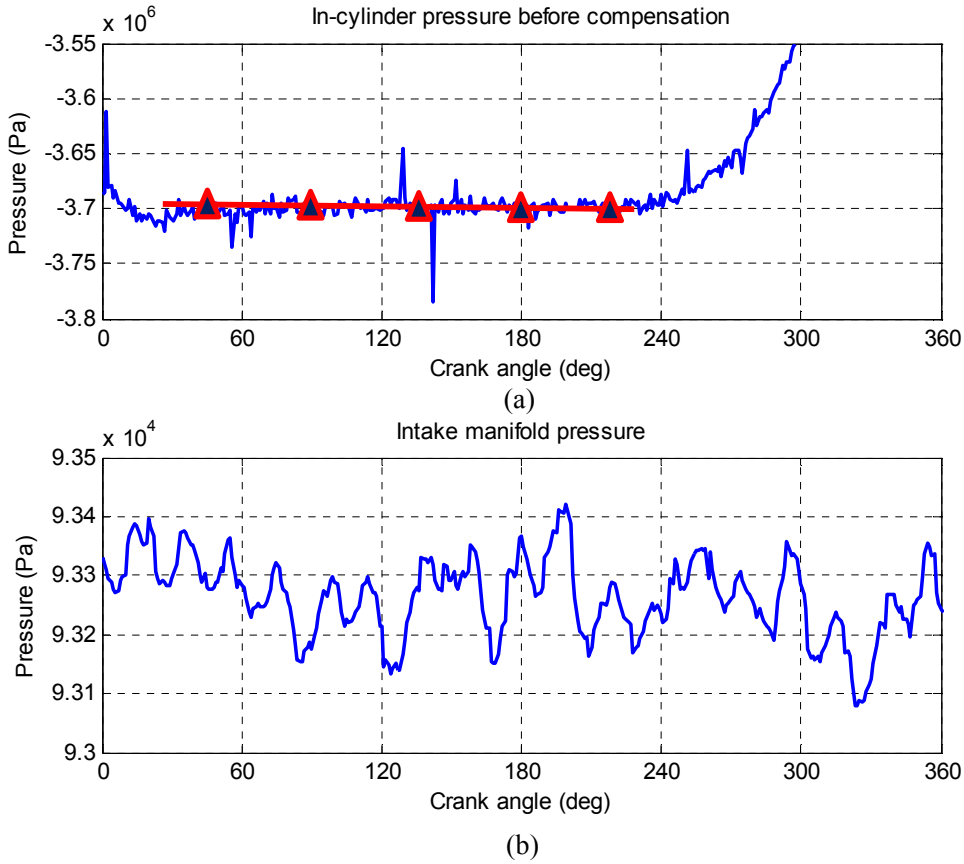
FIGURE 5.2: Referencing point idea: a) in-cylinder pressure b) intake manifold pressure

Considering the magnitude of the in-cylinder pressure during the intake valve opening, its variation is higher than the variation of the intake manifold pressure as indicated in Fig. 5.2(a) and (b). Hence, we focus on the in-cylinder pressure data and apply an idea to reduce the variation effect. The five average pressure referencing points for the pressure offset calculation are considered. The idea of the cylinder pressure average

and intake manifold pressure are shown in Fig. 5.2(a). This method will take the five cylinder pressure data during intake valves opening. Subsequently, the mean value of these pressure is calculated. Then, the cylinder pressure data at each point is compared with this mean value. If the absolute value of the cylinder pressure difference is higher than the predefined threshold, it will be set equal to the mean value. On the other hand, if the absolute pressure difference is lower than the threshold, it will be consider for pressure offset calculation.

In chapter 3, the in-cylinder pressure offset is calculated by least squares method with a constant polytropic exponent which is assumed to be known. However, for the compression heat transfer estimation, it is not reasonable to use the cylinder pressure data compensated from the previous method. This is because the value of the polytropic exponent corresponds to the compression heat transfer amount. Moreover, the estimated heat transfer will be utilized for the calculation of polytropic exponent variation. Hence, the compression heat transfer estimation should be considered independently from the assumption of constant polytropic exponent.
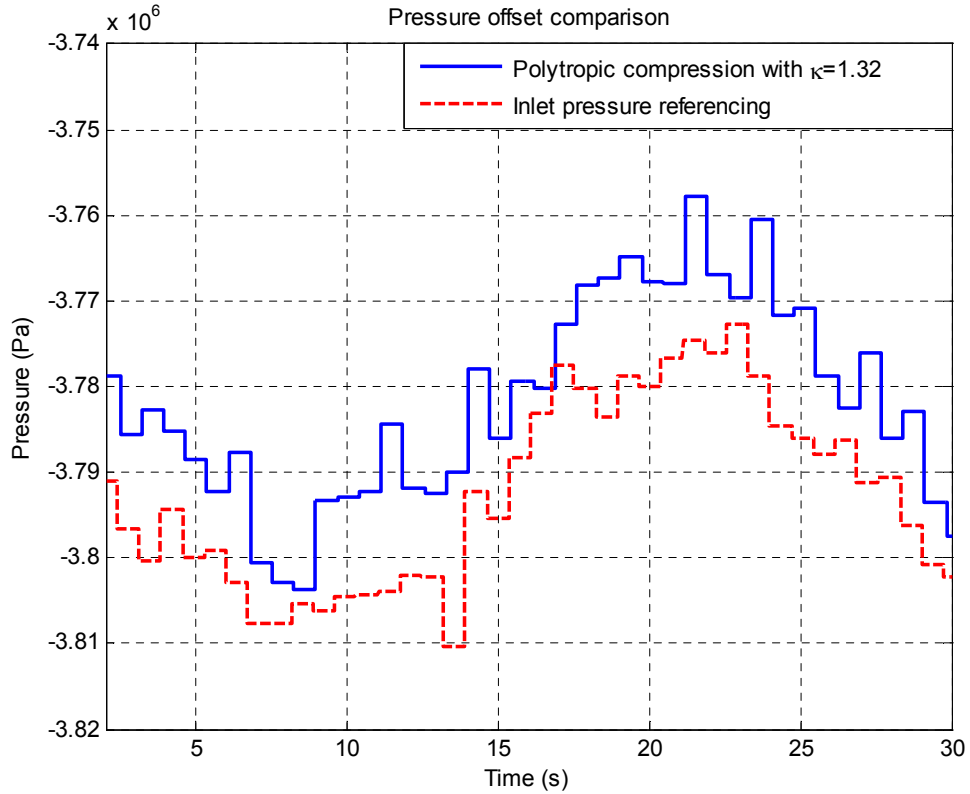
FIGURE 5.3: The pressure offset comparison

Based on the proposed idea and the pressure referencing method, the pressure offset is

71

calculated and compared with the previous compensation method cycle-by-cycle. The comparison results are exhibited in Fig. 5.3. From the presented results, the tendency of the pressure offset is similar, only the magnitude of the offset shows small different value. Additionally, the pressure referencing method show that the calculated pressure offset variation is lower than using the least squares method with a constant polytropic exponent. This is because the effects of average referencing points of the cylinder pressure during intake valves opening.

The measurement data at steady state operation, cylinder pressure after offset compensation and crank angle data are shown in Fig. 5.4(a) and (b), respectively.
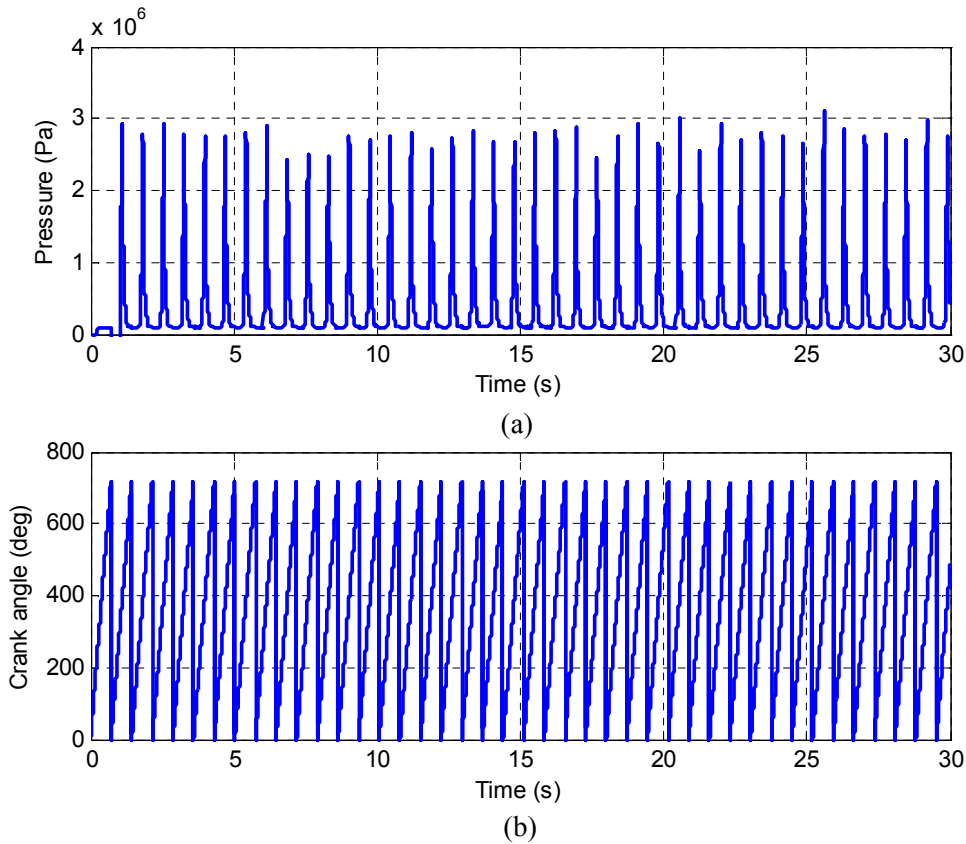
FIGURE 5.4: Measurement data: a) in-cylinder pressure, b) crank angle (at N=1000 rpm and T_L=180 Nm)

5.3 Compression Heat Transfer Modeling

We utilize the thermodynamic model presented in this section for compression heat transfer estimation. Using (2.30) and (2.35), the single zone thermodynamic engine

model account for heat transfer, and is represented as follows:

$$\dot{p}_c(t) = -\left(\frac{R}{c_v} + 1\right)\frac{\dot{V}(t)}{V(t)}p_c(t) - \frac{R}{c_v V(t)}\left(A_w(t)\omega p_c(t)\left(k_1 T(t) - k_0 T_w\right)\right)$$

$$\dot{T}(t) = -\frac{R}{c_v}\frac{\dot{V}(t)}{V(t)}T(t) - \frac{R}{c_v V(t)}\frac{T(t)}{p_c(t)}\left(A_w(t)\omega p_c(t)\left(k_1 T(t) - k_0 T_w\right)\right)$$

(5.1)

Considering the first relationship in the above equation, we can identify the heat transfer model parameters form this relation using some information obtained during compression. The considered equation can be rewritten as:

$$\dot{p}_c(t) = -\left(\frac{R}{c_v} + 1\right)\frac{\dot{V}(t)}{V(t)}p_c(t) - k_1 \frac{R\omega}{c_v V(t)}A_w(t)p_c(t)T(t)$$

$$+ k_0 \frac{R\omega}{c_v V(t)}A_w(t)p_c(t)T_w$$

(5.2)

The combustion process consists of four strokes, namely, intake, compression, combustion and exhaust. During the compression stroke, the heat transfer can be identified separately form the combustion heat release. Assuming that T_w is constant, and that the initial temperature at the intake valve close (IVC) is known (we use the coolant temperature at steady state $T_{ivc} = T_{cool}$), the state $T(t)$ can be calculated from the relationship between pressure and volume. Consider the ideal gas law

$$p_c(t)V(t) = mRT(t)$$

(5.3)

Note that during the compression stroke, both exhaust valves and intake valves are closed. Thus, if crevice effects are neglected, there is no mass transfer to or from the combustion chamber. From (5.3), the following relationship is obtained as

$$T = T_{ivc}\frac{p_c(t)V(t)}{p_{c,ini}V_{ini}}$$

(5.4)

where the subscript *ini* stands for an initial value of each variable. Using the previous model, and incorporating experimental data, we can calculate the compression temperature when the initial temperature is known. The engine geometries are used for the calculation of the cylinder volume. Using the least squares regression of the in-cylinder pressure and its derivative value at any points during the compression before ignition, the model parameters for heat transfer can be identified.

5.3.1 Least Squares Regression for Heat Transfer Identification

Let us consider again (5.2), where we can set up the model output

$$y = \varphi\theta \tag{5.5}$$

where

$$
\begin{aligned}
y &= \dot{p}_c(t) + \left(\frac{R}{c_v} + 1\right)\frac{\dot{V}(t)}{V(t)}p_c(t) \\
\varphi &= \left[-\frac{R\omega}{c_v V(t)}A_w(t)p_c(t)T(t) \quad \frac{R\omega}{c_v V(t)}A_w(t)p_c(t)T_w\right] \\
\theta &= [k_1 \quad k_0]^T
\end{aligned} \tag{5.6}
$$

Data can be obtained at any crank angle during compression. This yields

$$
Y = \begin{bmatrix} y_1 \\ \vdots \\ y_n \end{bmatrix} \tag{5.7}
$$

and

$$
\Phi = \begin{bmatrix} \varphi_1 \\ \vdots \\ \varphi_n \end{bmatrix} \tag{5.8}
$$

where Y is the output vector and Φ is the regressor matrix. Therefore, the closed-form solution of the least squares problems is

$$\hat{\theta} = (\Phi^T\Phi)^{-1}\Phi^T Y \tag{5.9}$$

5.3.2 Heat Transfer and Polytropic Exponent Relation

Based on the previous identification results, the application of compression heat transfer for the computation of the polytropic exponent variation is then presented. Using the first law of thermodynamics, we can obtain a differential equation describing the compression process

$$\frac{c_v}{R}V\,dp_c + \frac{c_p}{R}p_c\,dV - \delta Q_{th} = 0 \tag{5.10}$$

Note that the above equation can be expressed in the form that contains the specific heat ratio or adiabatic coefficients γ. If there is no heat transfer $\delta Q_{th} = 0$, the previous

equation can be rewritten as

$$\frac{dp_c}{p_c} = -\gamma \frac{dV}{V} \tag{5.11}$$

The relation of the coefficient is denoted by $\gamma = c_p/c_v$ and $R = c_p - c_v$, where c_p denotes the specific heat at constant pressure. Next, we will consider the effects of heat transfer during compression. Let us assume that the heat transfer can be defined by the condition

$$\delta Q_{th} = aV\,dp_c + bp_c dV \tag{5.12}$$

where a and b are constants that must be determined. Substituting (5.12) into (5.10) yields

$$\left(\frac{c_v}{R} - a\right)V\,dp_c + \left(\frac{c_p}{R} - b\right)p_c dV = 0 \tag{5.13}$$

which can be rewritten as

$$\frac{dp_c}{p_c} = -\kappa \frac{dV}{V} \tag{5.14}$$

with $\kappa = \left(\frac{c_p}{R} - b\right) / \left(\frac{c_v}{R} - a\right)$ is called the polytropic exponent which includes the effects of heat transfer. Subsequently, the compression heat transfer identification results, validation results, and the application for polytropic exponent variation calculation will be presented.

5.4 Compression Heat Transfer Identification

In this section, experimental data collection, identification procedure, identification results, and model validation will be presented.

5.4.1 Experimental Data Collection and Identification Procedure

The in-cylinder pressure and the crank angle position in the steady state experiment were recorded with 1 ms sampling time and were then transferred to the computer. The compression top dead center (TDC) for the cylinder pressure was set at 360 crank angle degree (CAD). The data were recorded and utilized for offline calculation of the compression heat transfer. During the experiment, the engine was fully warmed, the coolant temperature was controlled at 80°C, and the lubricant oil temperature was regulated at 70°C. Other control variables such as air-fuel ratio and fuel injection mode have controlled by ECU.
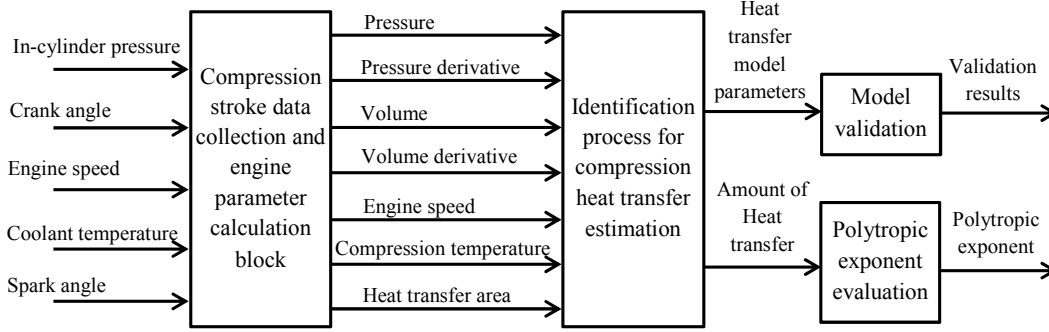
FIGURE 5.5: A block diagram of the identification process

A block diagram for the identification processes of the heat transfer model is expressed in Fig. 5.5. Four inputs, in-cylinder pressure, CAD, engine speed, and coolant temperature, are sent to the data collection block. This block, including the engine parameters, is also used for the calculation of some required model information. All the data are then arranged in a vector form and sent to the identification block. This block performs the system identification using the least squares regression. Finally, the model validation is investigated in the last process.

Based on the thermodynamic model and the reduced heat transfer model presented in chapter 2, the unknown heat transfer model coefficients can be estimated. The identification processes are as follows: first, the initial pressure and volume at 260 CAD are collected, and the initial temperature of the mixture and the coolant temperature are assumed to be equal. The model inputs and outputs are then sampled and recorded during the period from 260 to 355 CAD (the spark advance angle of this experiment is at 358.5 CAD). The output vector, regression matrix, and parameter vector, are then formed. Finally, the heat transfer model parameters are computed. Additionally, the parameters of the heat transfer model are updated at every cycle at approximately around TDC. The operating condition at low speed and high load is chosen for the identification (1000 rpm and the load of 180 N·m). At this condition, the spark angle is retarded (closed to TDC) and the valid identification period is longer than the case of low load condition. Therefore, we can obtain the low variation of the identification results.

5.4.2   Identification Results and Model Validation

This section presents the required information for the identification of the compression heat transfer model parameters, the identification results, and the model validation, during the compression period.
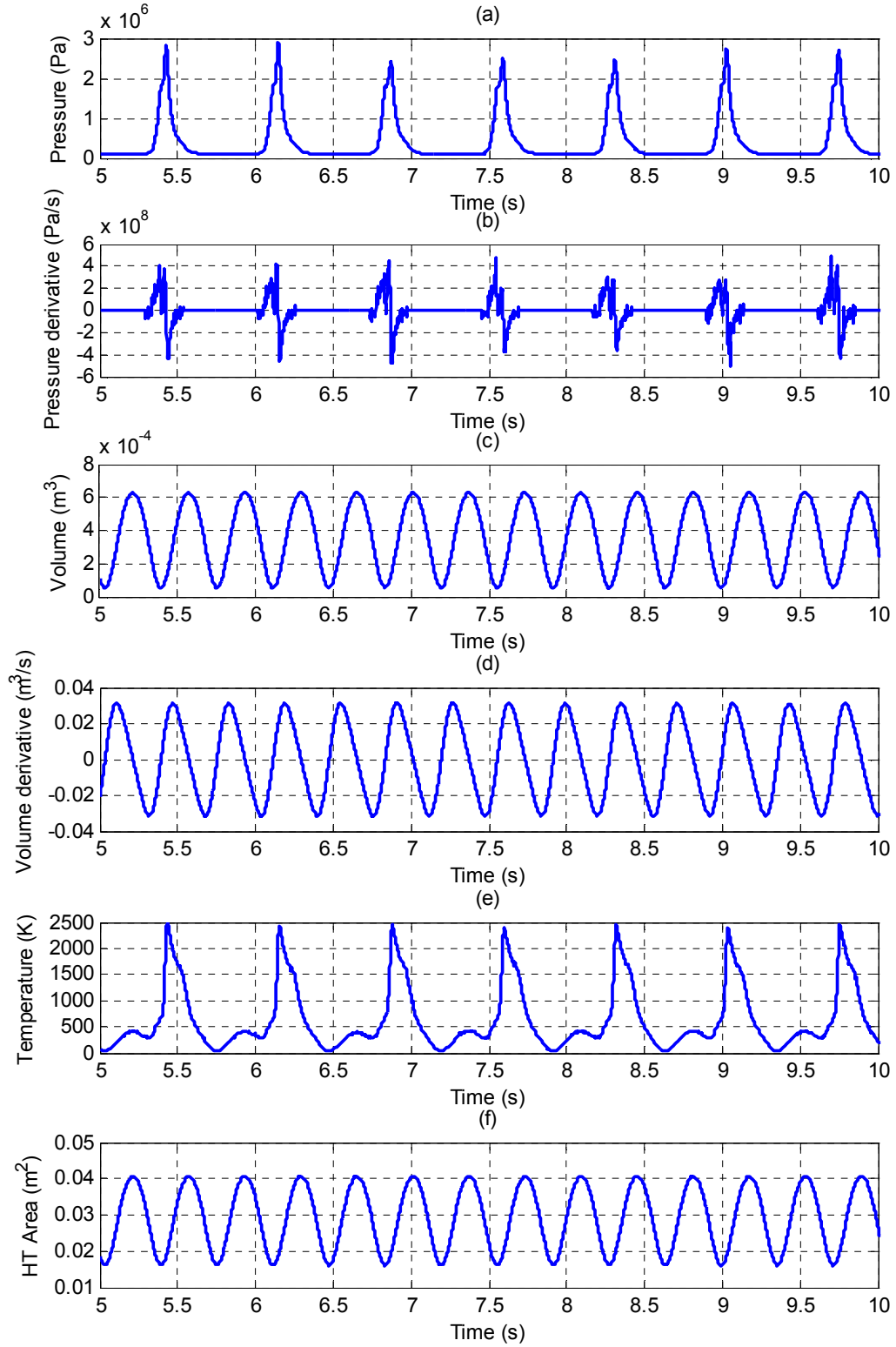
FIGURE 5.6: Calculated data for system identification: a) cylinder pressure, b) cylinder pressure derivative, c) cylinder volume, d) cylinder volume derivative, e) calculated in-cylinder temperature, and f) heat transfer (HT) area

Assuming T_w is constant and equal to 127°C (400 K) and the initial temperature at intake valve close (IVC) is equal 37°C (310 K). First, all required information for the compression heat transfer model identification, in-cylinder pressure, in-cylinder pressure derivative, cylinder volume, cylinder volume derivative, calculated temperature, and the area of heat transfer, are shown in Fig. 5.6.
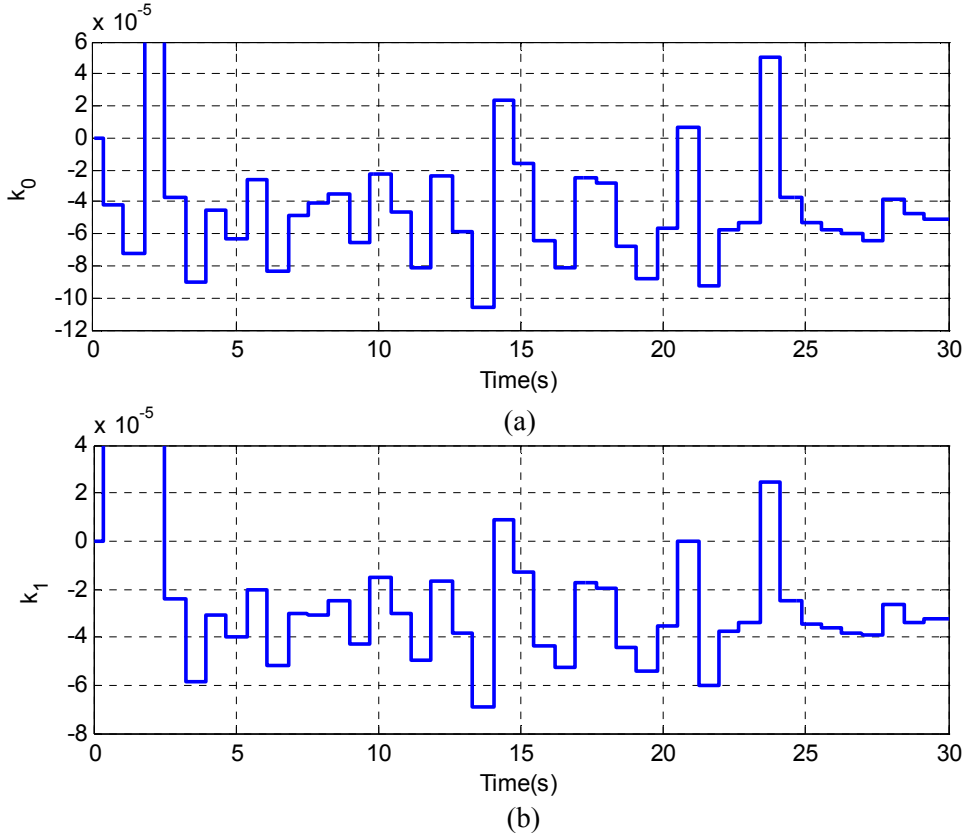
FIGURE 5.7: Identification results: a) model parameter k_0, b) model parameter k_1

The identification results of the reduced heat transfer model parameters (k_0 and k_1) are shown in Fig. 5.7. This identification algorithm requires some full cycles of data for initialization. Thus, we should ignore the results at the start of the calculation. The numerical heat transfer model parameters are computed after 355 CAD of each working cycle, and the values are kept constant until the updated results are obtained. The estimated model parameters variation is mostly from the cylinder pressure fluctuation. Considering the same cycle, the values of k_0 and k_1 show a similar sign. Nevertheless, the magnitude of these constants varies from cycle-to-cycle.

Subsequently, we used the parameters obtained from the identification for validation of the model based on the comparison of the pressure derivative during compression.
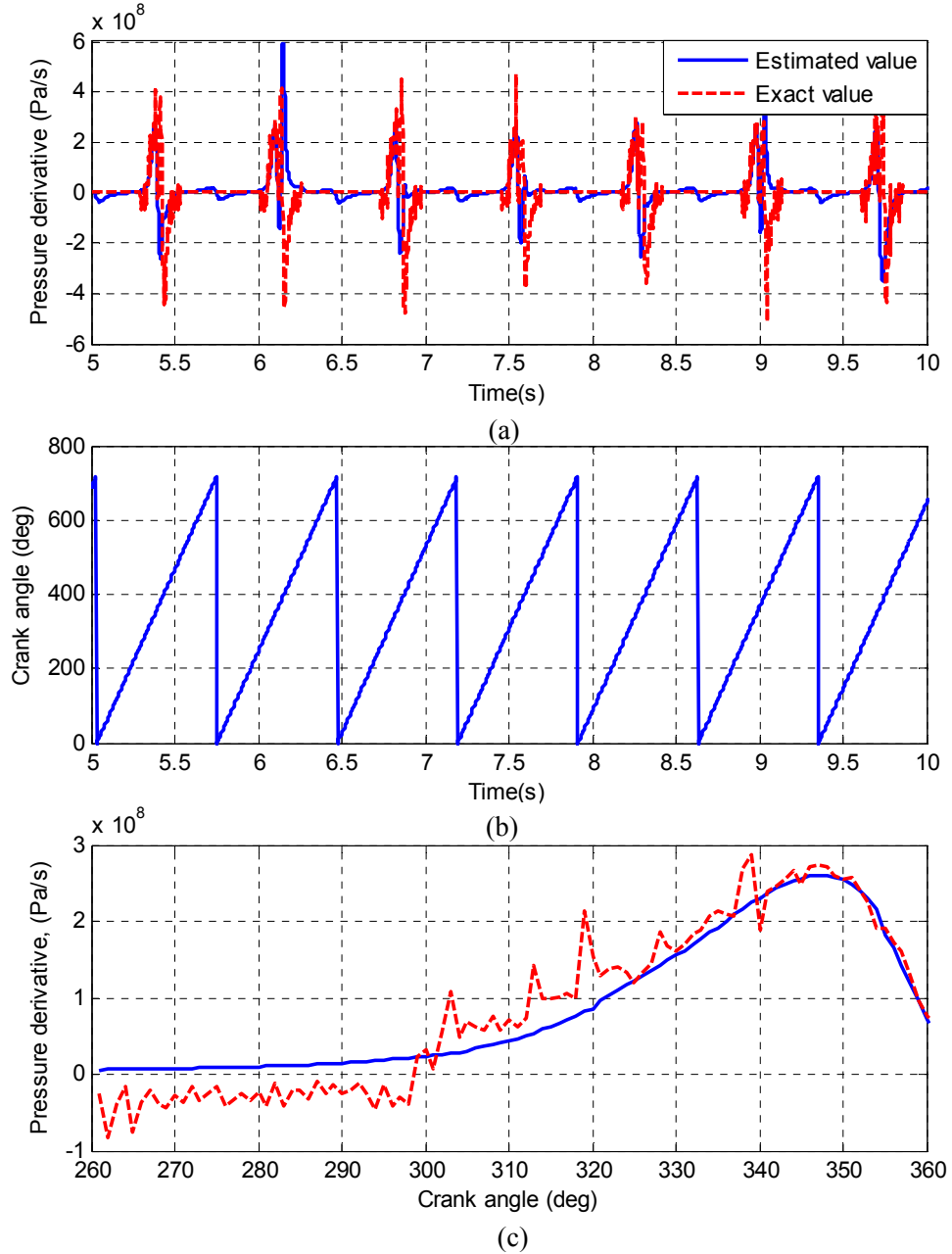
FIGURE 5.8: Validation results: a) actual and estimated pressure derivative, b) crank angle, and c) pressure derivative comparison with respect to crank angle

There is one cycle delay in this calculation. This means that the parameters calculated from the current cycle will be utilized in the next cycle. These validation results using the in-cylinder pressure derivative and the CAD cycle-by-cycle are shown in Fig. 5.8(a) and (b), respectively. In Fig. 5.8(c), the estimated in-cylinder pressure derivative is assigned to its fitted value during the identification period. The calculation program is enabled only from 260 to 355 CAD, and the calculation results are kept constant until

the next activation. This approach is used since the model that is used for identification does not include the heat release from combustion, rendering the model invalid during the combustion period. The heat transfer rate and heat transfer during the compression period are then investigated using the heat transfer model parameters obtained from the identification.

The value of heat transfer rate on cycle-by-cycle basis is presented in Fig. 5.9(a). The estimated compression heat transfer and heat release from combustion are compared in Fig. 5.9(b). Most identified cycles show that the direction of the calculated compression heat is transferred from the gases to the walls (positive value). Additionally, an example of enlarged identification results with respect to crank angle are presented in Fig. 5.9(c) and (d).

In the case of changing the engine speed while the engine torque is kept as a constant, it will affects the valid identification period directly because the spark angle is changed. In this identification experiment, we set the spark angle as a value given by ECU. Therefore, at low speed and high load, the valid identification period is longest. Additionally, the engine in this experiment is designed for late intake valve closing and we did not consider the effects of VVT.

5.5   Application of Estimated Compression Heat Transfer for Calculation of The Polytropic Exponent Variation

This section expresses an application of estimated compression heat transfer for calculation of the polytropic exponent variation. The difference between the polytropic exponent, κ, and the adiabatic coefficient, γ, is that it implicitly contains the information of the heat exchange of the gas-surroundings. The importance of the polytropic coefficient is even higher in the case of a cycle where fast compression and expansion processes follow one another, considering that it is compared to the adiabatic coefficient that only depends on the gas composition and temperature [78]. In this study, the effects of the uncertainties that affect the polytropic exponent determination are not considered. These uncertainties consist of three effects. First, cylinder pressure and volume functions are not well synchronized. Second, the reference pressure level along the cycle is not well estimated. Finally, the estimated volume function is not correct due to an imprecise calibration of the clearance volumetric. The details of the analyses can be found in Lapuetra [77].
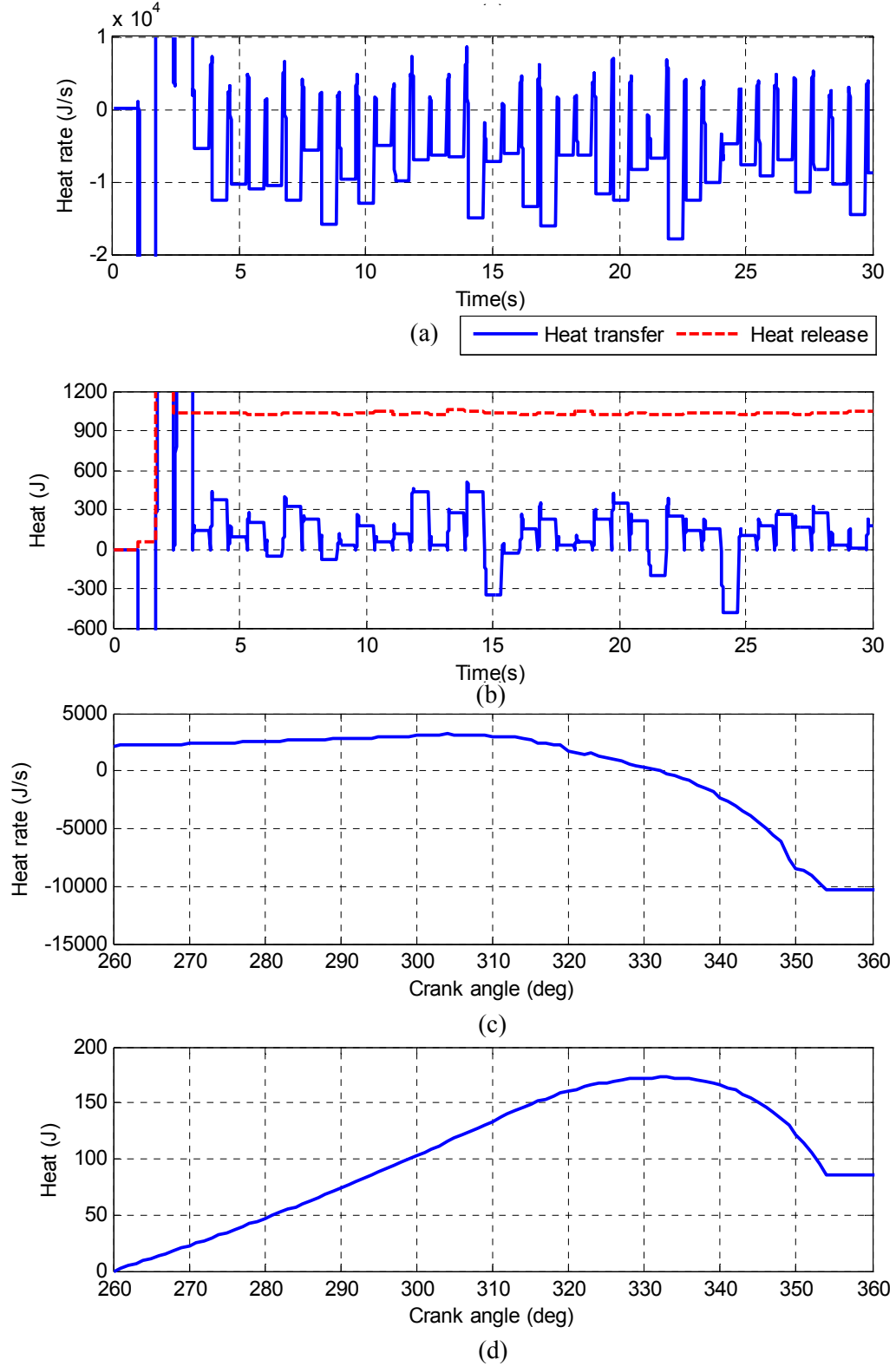
FIGURE 5.9: Heat transfer calculation results: a) heat transfer rate, b) heat release and heat transfer, c) enlarged heat transfer rate, d) enlarged heat transfer

Subsequently, use of the least squares regression allows the estimation of the values of constants a and b in equation (5.12). The heat transfer effects is then compensated for recalculation of the polytropic exponent. After the heat transfer estimation process is completed, its value is utilized again for computation of the polytropic exponent. The values of the compensated constants a and b are depicted in Fig. 5.10(a) and the value of the polytropic exponent after compensation with and without filter are shown in Fig. 5.10(b). In order to acquire robustness of estimation, we introduce a first-order auto regressive filter to determine the polytropic exponent variation. The equation for this filter is as follows:

$$\hat{\kappa}_i = c\hat{\kappa}_{i-1} + (1-c)\,\kappa_i \tag{5.15}$$

where i denotes the cycle index and c represents an auto-regressive coefficient.
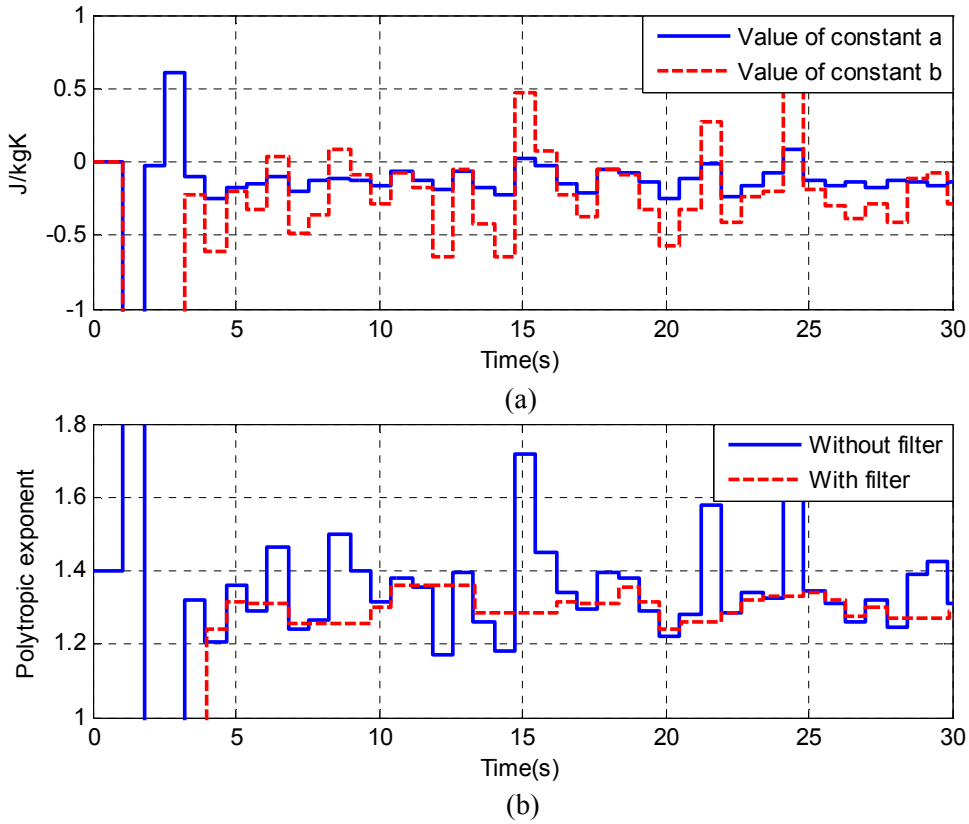
FIGURE 5.10: Compensation results: a) compensated constants, b) polytropic exponent

According to the work of Asad and Zheng (2014), the cylinder pressure, and the volume data during the compression and the expansion processes, can be described by the polytropic relation. The polytropic exponent is comparable to the average value of the specific heat ratio during the combustion phase, prior to combustion. However, the

increased heat transfer to the cylinder walls makes the polytropic exponent κ smaller than the corresponding value of γ. Based on the previous results, the heat transfer from the in-cylinder gases to the cylinder walls is considered negative sign, and the heat transfer from the walls to the in-cylinder mixture is positive. Hence, the variation of the polytropic exponent is depended on the direction and the amount of the compression heat transfer. The corresponding temporal variations of the compression heat transfer and polytropic exponent are depicted in Fig. 5.11.
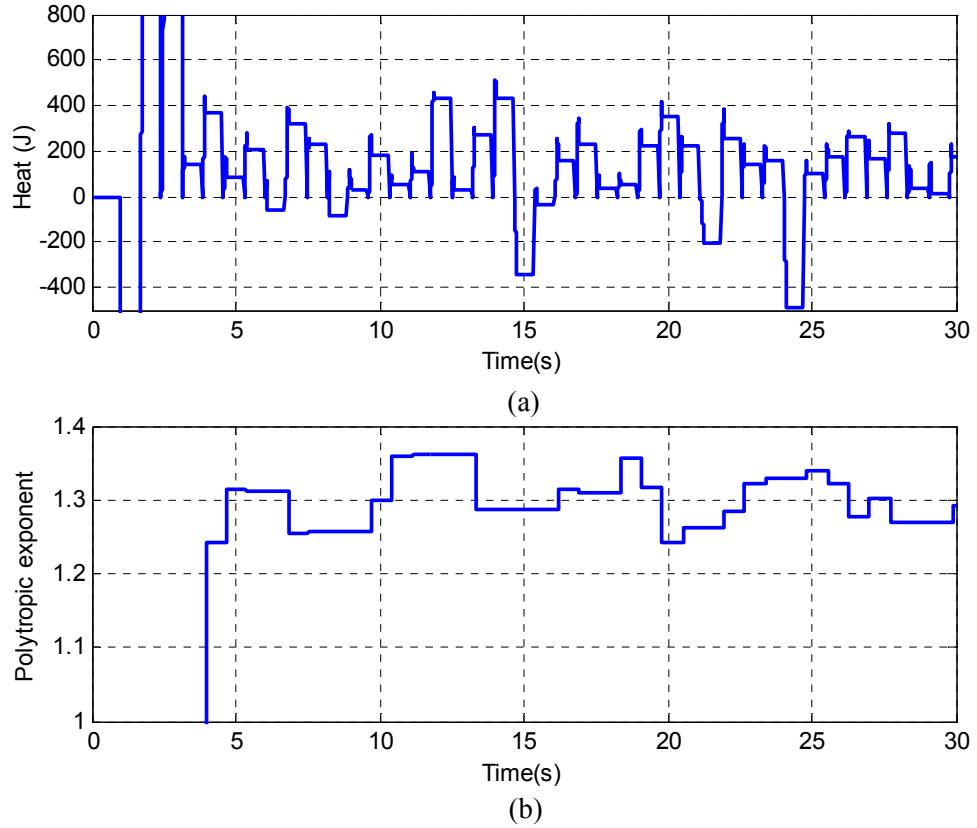
FIGURE 5.11: Temporal variations: a) heat transfer, and b) polytropic exponent

In these results, we can clearly observe the relation between the compression heat transfer and the polytropic exponent. On the other hand, the variation of this polytropic exponent appears to be rather high because of the operation of the engine at steady state condition. The results presented in previous section are analyzed and discussed in detail in the next section.

5.6   Analysis and Discussion

Based on the identification results, the amount of heat transfer and its direction varies from cycle-to-cycle. Most cycles show that the heat is transferred from the compressed gases to the cylinder walls. The value of evaluated polytropic exponent vary around 1.30. This value is reasonable for the compression process of SI engine with heat transfer consideration. On the other hand, in a few cycles, the heat is transferred from the cylinder walls to the mixture. These effects depend on the measured pressure and on some assumptions posed during the identification period. In this case, we consider that if the wall temperature is constant at 127°C (400°K), then the heat transfer direction will be changed if the mixture temperature is lower than that at the cylinder walls. To confirm the results, we present a comparison between the wall temperature and the calculated in-cylinder temperature in Fig. 5.12. These results show that the calculated in-cylinder temperature is lower than the wall temperature at the beginning of compression. After the initial compression period, the temperature of the compressed gases is continuously increased until it become higher than the cylinder wall temperature at the point before ignition. We can compare the results at the identified period (from 260 to 355 CAD). In the case where the temperature of the wall is changed, both the amount and direction of the heat transfer will be affected. Moreover, the calculation period is limited because the proposed model is valid only before ignition.
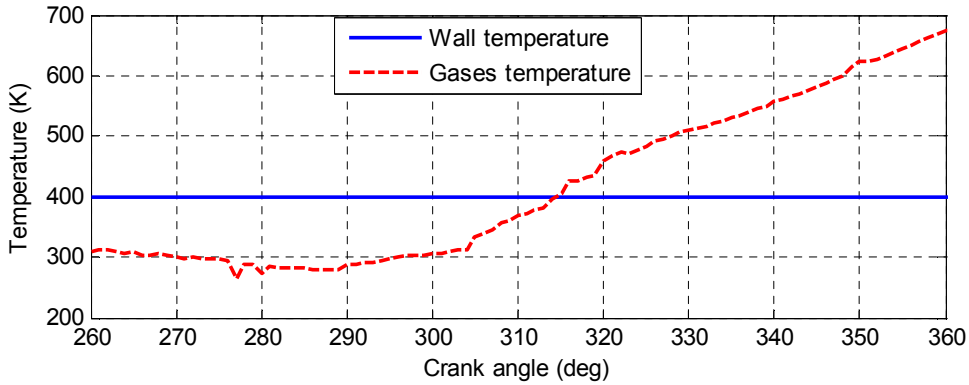
FIGURE 5.12:   Temperature comparison of the wall temperature and the calculated in-cylinder temperature

An important issue to the presented work is that the temperature of the cylinder walls is quite difficult to obtain precisely. Additionally, it does not have a uniform distribution. Many researchers, including [79] and [80] have studied the wall temperature measurement and estimation. Note that the wall temperature here refers to the average temperature of the cylinder surface, including the cylinder head, piston, and liner. The value of the wall

temperature directly affects the direction and the amount of the heat transfer during the compression stroke. In this study, we have assumed a constant wall temperature that may not be accurate in the heat transfer analysis. This temperature is mainly affected by the burnt gas and the variability of the combustion. Therefore, increasing the accuracy of the cylinder wall can improve the precision of the heat transfer estimation.

In this work, we have considered the surrounding temperature of the combustion chamber to choose the wall temperature for the compression heat transfer estimation. The in-cylinder temperature can be estimated from total heat release caused by combustion. The maximum temperature can be up to $2700°C$ (about $3000°K$). The coolant temperature is obtained from measurement and it is maintained at $80°C$ (about $353°K$). The limitation of material temperature is also considered for setting the estimated wall temperature during the compression stroke. The temperature limitation for cast iron (engine block) is about $400°C$, for aluminum (cylinder head) is about $300°C$. Moreover, the temperature which can maintain the liner (oil film) is about $200°C$. Therefore, based on the available information, the estimated combustion chamber wall temperature during the compression stroke can be defined. On the other hand, we can consider to combine the wall temperature with the heat transfer model parameter (k_0) for the system identification. Based on this idea, we can identify the model without the wall temperature assumption but the model structure is a little bit modified.

However, there are many issues that should be considered in this calculation. First, the temperature during compression is computed based on an adiabatic assumption and the validity of ideal gas law. In fact, the model requires the measured temperature at every point of sampling process including the heat transfer effects. Second, we have considered the compensated in-cylinder pressure for the heat transfer calculation. In according to the results by Heywood [35], as the mean charge temperature increases during the compression and combustion, and as it decreases during expansion, γ, should vary. Hence, it may not reasonable to use the compensated in-cylinder pressure for the heat transfer computation in the proposed model. Third, during the compression period, it is only possible to perform the heat transfer estimation when a heat transfer to, or from, the combustion chamber walls occurs. On the other hand, the pressure in the combustion chamber during the onset of the compression stroke is quite low, compared to the pressure during combustion. Therefore, the effects of noise should be considered for these measurements. Finally, the variation of the in-cylinder pressure derivative is primarily caused by the noise effects. Given the many limitations of the data, the obtained model parameters are valid only in the compression process.

In addition, the values of the gas constant and specific heat of the real mixture should also be considered. In-cylinder gases during compression generally consist of three main substances: fresh air, gaseous fuel, and residual gas fraction (RGF). This RGF also influences combustion phasing and variation, fuel consumption, and air-mass prediction for fuel control, as presented by [80]. Therefore, the composition of these substances affects the properties of the in-cylinder mixture. The gas constant and specific heat can be calculated from their components and their respective mass fractions. Furthermore, in this identification algorithm, there is an inevitable one-cycle delay for the calculation. This means that the currently estimated parameters of the heat transfer model are used for the calculation of the heat transfer in the next cycle. We should consider this delay, especially during transient responses. Furthermore, the parameters obtained from the calculation may be invalid for the entire combustion period because we only use the data during the compression stroke to identify the heat transfer model parameters.

5.7 Conclusion

The results show that the proposed method, based on some assumptions, can be used to estimate the in-cylinder heat transfer and its direction by using the information during the compression stroke. The heat transfer showed a variation both magnitude and direction. Most cycles show that the heat is transferred from the compressed gases to the combustion chamber walls. In practical applications, the estimated heat transfer can be used for the calculation of the polytropic exponent variation during the compression period. The variation of estimated polytropic exponent can be reduced using the first-order auto regressive filter with the specified threshold. The mean estimated value of the polytropic exponent is about 1.30. Hence, this value is reasonable for the compression process of gasoline engine (theoretical value is about 1.31). This is possible because the compressed gas temperature is changed from one cycle to the next. However, the heat transfer calculation should be improved because of the required assumptions and limitations of the data.

Chapter 6

Conclusions and Future work

This chapter presents the summary of this thesis and the future work. The main idea of this work is the SI engine AFR estimation with a cylinder pressure sensor and its application for SAC control based on obtained AFR estimation. Additionally, the results of the compression heat transfer analysis based on in-cylinder pressure data and polytropic exponent variation are summarized. Finally, the future of engine control and analysis based cylinder pressure measurement is presented.

6.1   Summary

This research has proposed the method for estimation of the in-cylinder AFR of SI engine using cylinder pressure measurement. First, from the physical definition of AFR, the relation between model inputs and in-cylinder AFR has investigated. The AFR model has four inputs, intake manifold pressure, engine speed, total heat release (in one cycle), and rapid burning angle. The first two inputs affect directly the amount of fresh air mass flow rate through the combustion chamber. For the total heat release and rapid burn angle, their values depend on the amount of fuel injection into the cylinder. Second, the structure of AFR model has designed by consideration of the variation of model inputs. The changing of intake manifold pressure and engine speed are rather slow then we applied the linear structure. On the other hand, the variations of total heat release and rapid burn angle are rapidly changed cycle-by-cycle. Therefore, the polynomial structure is utilized for these two inputs. Third, the model identification has performed on steady state condition with toque constant mode. We use the average 500 cycles for static model identification. The model parameters are calculated by using ridge regression.

Forth, the AFR model is validated at the same conditions as identification experiment. We obtain the AFR estimation model which can replace the AFR sensor. With the proposed model, the feedback AFR control can be performed with in-cylinder pressure sensor. Finally, for the AFR control, SAC has selected because it has high efficiency for control the fuel injection. The control performance of SAC with the proposed AFR model has investigated. The results show that this proposed AFR model can work as the virtual AFR sensor and SAC can control AFR of port injection SI engine. The controller can track the reference AFR and reject some disturbances.

However, the proposed model has some limitation. First, this model is only static one because we cannot measure the AFR cycle-by-cycle. This is because the signal obtained from AFR sensor contains some delay. Second, the experimental conditions for identification are rather limited. Hence, the high load condition cannot be performed. Third, because of combustion variation, the cycle moving average and the low-pass filter are required. Therefore, the estimated AFR contains some delay which affects control performance of SAC. Finally, the AFR estimation efficiency depends on the operation environment and experimental set-up.

For the heat transfer estimation and its application, we have applied the model presented in chapter 2. Based on the proposed model and some assumptions, the off-line calculation with the experimental data shows that the proposed method can be used to estimate the compression heat transfer. Using these calculation results, we can evaluate the variation of polytropic exponent cycle-by-cycle. The polytropic exponent variation included in the compression heat transfer effects are expected to be used for the improvements of the combustion parameter calculation. On the other hand, there are many issues of this proposed strategy that should be considered because of the limitations of measured data and some ideal required assumptions.

6.2 Conclusion

The SI engine control and analysis using in-cylinder pressure measurement have presented in this thesis. First, the AFR model based in-cylinder pressure measurement. This proposed model can be replaced the AFR sensor in feedback control of AFR control system. Second, SAC with the proposed model shows high performance for control AFR of port injection SI engine. Additionally, for the heat transfer analysis, the proposed estimation method and its application have expressed. Both the amount of heat transfer and its direction can be identified with the proposed method. This results can

be implemented for calculation of the polytropic exponent variation that can be applied for the improvements of combustion parameter calculation.

6.3 Future Work

There are many issues of this research should be considered. First, the measurement method for in-cylinder pressure can be improved by changing the method for obtaining the data. This is because we have applied the time based devices for cylinder measurement then the signal quality may not suitable for high engine speed operation. Therefore, use of the trigger based device is more appropriate. Second, the AFR is calculated using combustion parameters. Hence, the accuracy of the combustion parameters affects directly to the AFR estimation. Finally, the AFR output delay directly affects the controller performance while the adaptive control is applied. Consequently, the control strategy that can deal with the delay system should be considered.

Theoretically, some important information for engine control and analysis may be derived from the in-cylinder pressure data. Its measurement might allow replacing part of the existing sensors, with a potential reduction of system complexity and production cost. The proposed AFR model introduced in this research is one of the possible applications. In the future, if we can obtain the AFR cycle-by-cycle, the dynamic model for AFR estimation can be developed. Based on the precise model identification which cover all engine operating range, the virtual AFR sensor for SI engine can be obtained. Therefore, the AFR sensor might be replaced by the cylinder pressure sensor. The virtual sensor will has faster response compared with the standard AFR sensor because it uses the in-cylinder information. Moreover, we can perform the combustion analysis and estimate the AFR simultaneously.

Additionally, the results on the effects of compression heat transfer for investigation of the polytropic exponent variation can be implemented for increasing of the combustion parameter calculation accuracy. However, the precision of the compression heat transfer estimation should be improved because of the limitations of measured data and some required ideal assumptions. For example, we should continue to improve the accuracy of in-cylinder temperature calculation and include the effects of all mixture component in the calculation. This leads to enhancement of the heat transfer estimation accuracy and the variation of polytropic exponent calculation precision.

Currently, there are a few researchers work on the engine heat transfer analysis. This is because of large effort-little effect. From thermodynamic theory, the effects of heat transfer are well known but it is difficult to obtain the precise information of heat transfer under practical conditions. Therefore, in this work, we only propose one of the possible ways to analyze the effects of heat transfer using the existing measured information with some ideal assumptions.

Appendix A

Pressure Offset Identification with Known Polytropic Exponent

Tunestal et al. (2000), have presented the method to estimate and remove the offset from the cylinder pressure measurements. The method amounts to solving the nonlinear least-squares problem of fitting the measured pressure data to a polytropic compression curve. The method is applicable to any least-squares problem for which the residual function shows a nonlinear dependence on exactly one of the parameters. The problem formulation is as follows: first, assuming that cylinder pressure measurements have an unknown but constant offset Δp,

$$p_{c,m} = p_c + \Delta p \qquad (A.1)$$

where $p_{c,m}$ is measured pressure and p_c the exact value of in-cylinder pressure. From the relationship between pressure and volume for an isentropic process.

$$\frac{p_c}{p_{c,ini}} = \left(\frac{V}{V_{ini}}\right)^{-\kappa} \qquad (A.2)$$

where subscript ini stands for an initial value of each variable. Combining (A.2) and (A.1) yields

$$p_{c,m} = \Delta p + CV^{-\kappa} \qquad (A.3)$$

where

$$C = p_{c,ini}V_{ini}^{\kappa} \qquad (A.4)$$

Appendix A. *Pressure Offset Identification with Known Polytropic Exponent*

Note that in this analysis, in order to emphasize the generality, a polytropic compression process is assumed and hence, γ is replaced by κ. Further assume that κ is known. Posing the problem as a system identification problem

$$y = \varphi\theta \tag{A.5}$$

where y is known as the output, φ the regressor vector, and θ the parameter vector. Here,

$$y = p_{c,m}, \quad \varphi = [1 \quad V^{-\kappa}] \tag{A.6}$$

and

$$\theta = [\Delta p \quad C]^T \tag{A.7}$$

Let assume that crank angle resolved data is available for cylinder pressure and combustion chamber volume during the compression stroke, and form

$$Y = \begin{bmatrix} (p_{c,m})_1 \\ (p_{c,m})_2 \\ \vdots \\ (p_{c,m})_n \end{bmatrix} \tag{A.8}$$

$$\Phi = \begin{bmatrix} \varphi_1 \\ \varphi_2 \\ \vdots \\ \varphi_n \end{bmatrix} \tag{A.9}$$

Combining (A.5), (A.8), and (A.9) yields,

$$Y = \Phi\theta \tag{A.10}$$

The least squares solution for the parameter vector θ is

$$\hat{\theta} = (\Phi^T\Phi)^{-1}\Phi^T Y \tag{A.11}$$

This method of solving for θ is highly intuitive, and serves a good way to remember the expression for the least-squares solution.

Appendix B

Brief Outline of Stability Proof of Simple Adaptive Control

Barkana [64] has presented the proof of the simple adaptive control. First, let the plant be the square, multiple-input-multiple-output, system with realization

$$\dot{x}(t) = Ax(t) + Bu(t) \tag{B.1}$$

$$y(t) = Cx(t) \tag{B.2}$$

where x is the n_p-dimensional state vector, u the m_p-dimensional input vector and y the m_p-dimensional output vector, and A, B, and C are matrices of corresponding dimensions. The plant is required to asymptotically track the output of the model

$$\dot{x}_m(t) = A_m x_m(t) + B_m u_m(t) \tag{B.3}$$

$$y_m(t) = C_m x_m(t) \tag{B.4}$$

where x_m is the n_m-dimensional state vector, u_m the m_m-dimensional input vector of desired arbitrary magnitudes that excite the model and y_m the m_m-dimensional output vector, and A_m, B_m, and C_m are matrices of corresponding dimensions. The deterministic tracking problem assumes that there exists an ideal control input to the plant

$$u^*(t) = \tilde{K}_x x_m(t) + \tilde{K}_u u_m(t) \tag{B.5}$$

that could keep the plant along an ideal trajectory perfectly. In other words, the ideal plant

$$\dot{x}^*(t) = Ax^*(t) + Bu^*(t) \tag{B.6}$$

$$y^*(t) = Cx^*(t) \tag{B.7}$$

moves along ideal trajectories such that

$$y^*(t) = y_m(t) \tag{B.8}$$

We assume that the underlying LTI problem is solvable and thus, that some ideal gains $\tilde{K}_x$ and $\tilde{K}_u$ exist in the work of Barkana [27]. The plant is allowed to be of possibly very large order while the model can be of possibly very low order just sufficiently large to create the desired output command. Because the plant and the model may posses different dimensions, the following error is defined to be the difference between the ideal and the actual plant state.

$$e_x(t) = x^*(t) - x(t) \tag{B.9}$$

and correspondingly

$$
\begin{aligned}
e_y(t) = y_m(t) - y(t) &= y^*(t) - y(t) \\
&= Cx^*(t) - Cx(t) = Ce_x(t) \tag{B.10}
\end{aligned}
$$

Differentiating $e_x(t)$ gives:

$$
\begin{aligned}
\dot{e}_x(t) = \dot{x}^*(t) - \dot{x}(t) \\
&= Ax^*(t) + Bu^*(t) - Ax(t) - Bu(t) \\
&= Ae_x(t) - Bu(t) + Bu^*(t) \tag{B.11}
\end{aligned}
$$

For the control input, when one cannot assume full knowledge about the plant parameters, an adaptive algorithm is used to implemented the control gains. The constant gains are replaced with time-varying adaptive gains that are generated by an adaptive algorithm as follows:

$$u(t) = K_e(t)e_y(t) + K_x(t)x_m(t) + K_u(t)u_m(t) \tag{B.12}$$

The adaptive law is defined by

$$K_e(t) = K_e(0) + \int_0^t e_y(t)e_y^T(t)\Gamma_e dt, \tag{B.13}$$

$$K_x(t) = K_x(0) + \int_0^t e_y(t)x_m^T(t)\Gamma_x dt, \tag{B.14}$$

and

$$K_u(t) = K_u(0) + \int_0^t e_y(t)u_m^T(t)\Gamma_u dt \tag{B.15}$$

Here, Γ_e, Γ_x, and Γ_u are just constant matrix coefficients that control the rate of adaptation. Hence,

$$\dot{e}_x(t) = Ae_x(t) - B\left(K_e(t)e_y(t) + K_x(t)x_m(t) + K_u(t)u_m(t)\right) + B\left(\tilde{K}_x x_m(t) + \tilde{K}_u u_m(t)\right) \tag{B.16}$$

Adding and subtracting $B\tilde{K}_e e_y(t) = B\tilde{K}_e C e_x(t)$ above gives

$$\dot{e}_x(t) = \left(A - B\tilde{K}_e C\right)e_x(t) - B\left(K(t) - \tilde{K}\right)r(t) \tag{B.17}$$

where $r(t)$, $\tilde{K}$, $K(t)$ are defined by

$$r(t) = \begin{bmatrix} e_y(t) \\ x_m(t) \\ u_m(t) \end{bmatrix}, \tag{B.18}$$

$$\tilde{K} = \begin{bmatrix} \tilde{K}_e & \tilde{K}_x & \tilde{K}_u \end{bmatrix}, \tag{B.19}$$

and

$$K(t) = \begin{bmatrix} K_e(t) & K_x(t) & K_u(t) \end{bmatrix}, \tag{B.20}$$

respectively. Assuming that the Lyapunov function is chosen as

$$V(t) = e_x^T(t)Pe_x(t) + tr\left[W\left(K(t) - \tilde{K}\right)\Gamma^{-1}\left(K(t) - \tilde{K}\right)^T\right] \tag{B.21}$$

where $W = S^T S$, here, S is any non-singular matrix. P is a positive definite symmetric (PDS) matrix, Γ is an adaptation gain vector,

$$\Gamma = \begin{pmatrix} \Gamma_e & & \\ & \Gamma_x & \\ & & \Gamma_u \end{pmatrix}, \tag{B.22}$$

and $\tilde{K}$ is a set of ideal gains that could perform perfect model following if the parameters were known. The time derivative of the Lyapunov function (B.21),

$$
\begin{aligned}
\dot{V}(t) = {} & e_x^T(t)P\dot{e}_x(t) + \dot{e}_x^T(t)Pe_x(t) \\
& + tr\left[W\dot{K}(t)\Gamma^{-1}\left(K(t) - \tilde{K}\right)\right] \\
& + tr\left[W\left(K(t) - \tilde{K}\right)\Gamma^{-1}\dot{K}(t)^T\right]
\end{aligned}
\tag{B.23}
$$

Any linear time-invariant system with state-space realization $\{A, B, C\}$, with the $m \times m$ transfer function $T(s) = C\left(sI - A\right)^{-1}$, is called "W-almost strictly positive (WASP)" and its transfer function "W-almost strictly positive real (WASPR)," if there exist three positive definite symmetric (PDS) matrices, P, Q, and W, and a positive definite gain $\tilde{K}_e$ such that the following two conditions are simultaneously satisfied [64]:

$$
P\left(A - B\tilde{K}_eC\right) + \left(A - B\tilde{K}_eC\right)^T P = -Q
\tag{B.24}
$$

where Q is a positive definite symmetric (PDS) matrix

$$
PB = C^TW^T
\tag{B.25}
$$

Using relations (B.24)-(B.25) gives

$$
\begin{aligned}
\dot{V}(t) = {} & x^T(t)\left[PA_K + A_K^TP\right]x(t) \\
& - x^TC^TW\left(K(t) - \tilde{K}\right)Cx + x^TC^TW\left(K(t) - \tilde{K}\right)Cx \\
& - x^TC^T\left(K(t) - \tilde{K}\right)WCx + x^TC^T\left(K(t) - \tilde{K}\right)WCx
\end{aligned}
\tag{B.26}
$$

where A_k is defined as $A_k = A - B\tilde{K}_eC$. The last two terms in (B.26), originating in the derivative of the adaptive gain terms in $V(t)$, cancel the previous, possibly troubling, non-positive, terms and thus lead to the Lyapunov derivative

$$
\dot{V} = -e_x^T(t)Qe_x(t)
\tag{B.27}
$$

The Lyapunov function (B.21) is positive definite. The Lyapunov derivative (B.27) only includes the state error e_x and is only negative semi-definite. Lyapunov theory tells us that the system is stable, but not necessarily asymptotically stable. All state errors and adaptive gains are bounded, yet it may happen that the final error is not zero.

In practical applications, the integral gains (B.13) increases whenever the tracking error is not perfectly zero, because the argument under the integral is always positive.

The adaptive gains may slowly and continuously increase beyond any bound, thus even leading the adaptive system to instability. Therefore, the basic algorithm has been adjusted such that the integral gains contain a 'leakage' term that does not allow the gain to increase without bound even in the most difficult environments [25]. The new SAC adaptive gain was thus:

$$\dot{K}(t) = e_y r(t)^T \Gamma - \sigma K(t) \tag{B.28}$$

The efficiency of the modified algorithm in preventing gain divergence has been widely show in the application of SAC. Initially, the SAC has used the σ-term with all adaptive gains, so the σ-terms that were added to the control gains $K_x(t)$ and $K_u(t)$ add some negative terms in the Lyapunov derivative. Thus, one can prove boundedness of the system in all environments. However, these additional terms had some unfortunate effects that perfect tracking could not be achieved.

In [27], it was shown that the adaptive control gains $K_x(t)$ and $K_u(t)$ actually perform a steepest descent minimization of the tracking error and they would not diverge, unless the error becomes unbounded for other reasons. Moreover, if the operational conditions change, the feedforward gains $K_x(t)$ and $K_u(t)$ would also change, fitting the right values to the right situation. The argument earlier leads to the idea of separation of treatment of the main loop gain, $K_e(t)$, which is in charge of the guarantee of stability, and the control gains, $K_x(t)$ and $K_u(t)$ that must facilitate asymptotically perfect tracking. We will therefore use the algorithm

$$\dot{K}_e(t) = e_y e_y^T \Gamma_e - \sigma K_e(t), \tag{B.29}$$

$$\dot{K}_x(t) = e_y x_m^T \Gamma_x, \tag{B.30}$$

$$\dot{K}_u(t) = e_y u_m^T \Gamma_u \tag{B.31}$$

Here, we make an observation that allow further modifying the adaptive controller and lead towards good, or even perfect, tracking under ideal conditions. The proof of stability must deal with (B.29)-(B.31) and (B.11), see also [25], one gets

$$\dot{V}(t) = -e_x^T(t) Q e_x(t) - 2\sigma\, tr\left[W\left(K_e(t) - \tilde{K}_e \right) \Gamma^{-1} \left(K_e(t) - \tilde{K}_e \right)^T \right]$$
$$- 2\sigma\, tr\left[W\left(K_e(t) - \tilde{K}_e \right) \Gamma^{-1} \tilde{K}_e^T \right] \tag{B.32}$$

Because the ASPR plant becomes SPR via static output feedback, if an appropriate minimal gain can actually be chosen and used priory to the implementation of SAC, then the newly controlled plant could satisfy the passivity conditions even for $\tilde{K}_e = 0$. In this case, (B.32) becomes

$$\dot{V} = -e_x^T(t)Qe_x(t) - 2\sigma\,tr\left[WK_e(t)\Gamma^{-1}K_e(t)^T\right] \tag{B.33}$$

The adaptive gain $K_e(t)$ obtained from (B.29) is positive definite. Now, the Lyapunov derivative is negative definite and does guarantee asymptotically perfect tracking of the adaptive system. Moreover, although (B.32) contains terms that are not negative definite, they may affect perfect tracking only as long as the main adaptive gain $K_e(t)$ is far from any appropriate $\tilde{K}_e$.

Appendix C

Air-Fuel Ratio Sensor Calibration

In this appendix, the AFR sensor calibration results installed at the mixing point for both sides of the engine are presented. The AFR sensors are manufactured by Denso Auto Part and the model number is DOX-0222. The sensor output is corresponded to the AFR value at the detecting point. We focus on the linear operating range of the sensor (around AFR = 12 to 18).
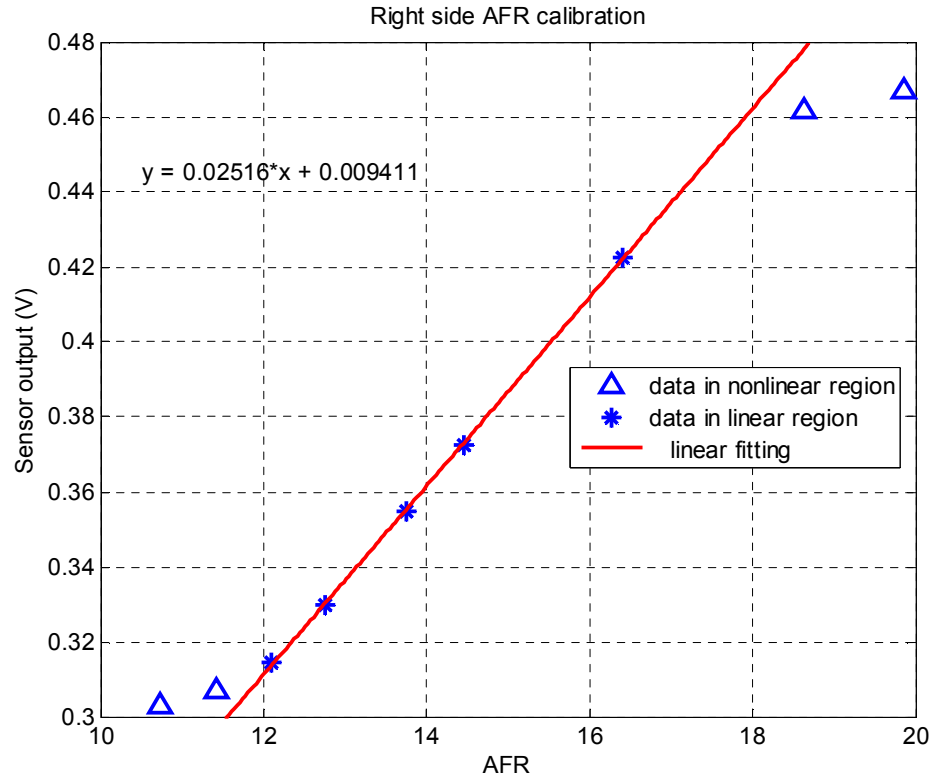

FIGURE C.1: Right side AFR voltage chart

The relation between the outputs voltages of the sensor are plotted with respect to the AFR value measured by the AFR meter. Because of the engine is V-type then both side of the sensor should be calibrated. The relationship between the AFR sensor output installed at the mixing point on the right side of the exhaust manifold and the measured AFR obtained from the AFR meter is shown in Fig. C.1. Subsequently, the calibration results for the AFR sensor installed on another side are exhibited in Fig. C.2.
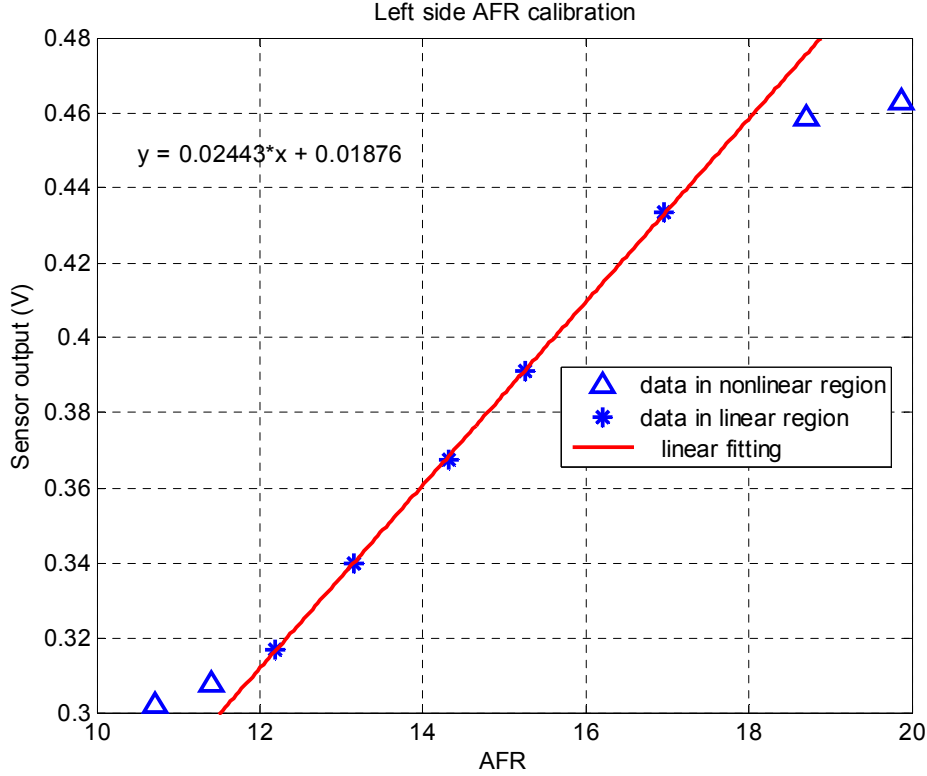
FIGURE C.2: Left side AFR voltage chart

Based on the presented results, the AFR sensor for the experiment shows the linear property over the operating range for the AFR measurement. Therefore, the sensors are applicable for the AFR model identification and model validation.

Note that the AFR measured output for this research is obtained from the sensors which have the estimated linear measurement range from 12 to 18. If the AFR is over the specified range, we cannot obtain the precise AFR for the system identification and model validation.

Bibliography

[1] L. Guzzella and C. H. Onder, *Introduction to Modeling and Control of Internal Combustion Engine Systems.* Springer-Verlag, 2nd Edition, 2010.

[2] P. Tunestal, *The Use of Cylinder Pressure for Estimation of the In-cylinder Air/-Fuel Ratio of an Internal Combustion Engine.* Ph.D. Thesis, University of California, Berkeley, 2000.

[3] U. Kiencke and K. Nielsen, *Automotive Control Systems: For Engine, Driveline, and Vehicle.* Springer-Verlag, 2nd edition, 2005.

[4] G. M. Rassweiler and L. Withrow, "Motion pictures of engine flames correlated with pressure cards," *SAE Transactions 380139*, 1938.

[5] N. C. Blizard and J. C. Keck, "Experimental and theoretical investigation of turbulent burning model for internal combustion engines," *SAE Transactions 740191*, 1974.

[6] J. A. Gatowski, E. N. Balles, K. M. Chun, F. E. Nelson, J. A. Ekchian, and J. B. Heywood, "Heat release analysis of engine pressure data," *SAE Technical Paper 841359*, 1984.

[7] P. Wibberley and C. Clark, "An investigation of cylinder pressure as feedback for control of internal combustion engines," *SAE Technical Paper 890396*, 1989.

[8] G. W. Pestana, "Engine control methods using combustion pressure feedback," *SAE Technical Paper 890758*, 1989.

[9] P. Li, T. Shen, J. Kako, and K. Liu, "Cyclic moving average control approach to cylinder pressure and its experimental validation," *Journal of Control Theory and Applications*, vol. 7(4), pp. 345–351, 2009.

[10] J. Yang, T. Shen, and X. Jiao, "Air-fuel ratio control with stochastic l_2 disturbance attenuation in gasoline engines," *Journal of Control Theory and Applications*, vol. 11(4), pp. 586–591, 2013.

[11] J. C. Gilkey and J. D. Powell, "Fuel-air ratio determination from cylinder pressure time histories," *Journal of Dynamic Systems Measurement and Control-Transactions of the ASME*, vol. 107(4), pp. 252–257, 1985.

[12] R. S. Patrick, *Air-Fuel Ratio Estimation in an Otto Cycle Engine: Two Methods and Their Performance*. Ph.D. Thesis, Stanford University, Mechanical Engineering Department, 1989.

[13] W. E. Leisenring and S. Yurkovich, "Comparative analysis of closed loop afr control during cold start," in *Proceedings of American Control Conference, Philadelphia: IEEE*, pp. 1377–1382, Jun, 21-26 1998.

[14] J. Aseltine, A. Mancini, and C. Sarture, "A survey of adaptive control systems," *IEEE Transaction on Automatic Control*, vol. 3(1), pp. 102–108, 1958.

[15] W. Caldwell, "Control system with automatic response adjustment," *American patent, 2,517,081. Filed 25, April 1947*, 1950.

[16] P. Ioannou and B. Fidan, *Adaptive Control Tutorial (Advances in Design and Control)*. Siam, 2006.

[17] P. A. Ioannou and J. Sun, *Robust Adaptive Control (Dover Books on Electrical Engineering)*. Courier Corporation, 2012.

[18] H. Whitaker, J. Yamron, and A. Kezer, *Design of Model Reference Adaptive Control Systems for Aircraft*. Report R-164, Instrumentation Laboratory, M. I. T. Press, Cambridge, Massachusetts, 1958.

[19] P. Osburn, A. Whitaker, and A. Kezer, "New developments in the design of model reference adaptive control systems," *Paper No. 61-39, Institute of the Aerospace Sciences*, 1961.

[20] R. Kalman, "Design of a self optimizing control system," *Transaction of the ASME*, vol. 80, pp. 468–478, 1958.

[21] I. Barkana and H. Kaufman, "Model reference adaptive control for time-variable input commands," in *Proceedings of Conference on Informational Sciences and Systems Princeton, New Jersey*, pp. 208–211, 1982.

[22] I. Barkana, H. Kaufman, and M. Balas, "Model reference adaptive control of large structural systems," *American Institute of Aeronautics and Astronautics (AIAA) Journal of Guidance*, vol. 6(2), pp. 112–118, 1983.

[23] J. Glower and D. Carpenter, "Model-reference adaptive control for systems with D matrices," in *Proceedings of the American Control Conference*, pp. 165–166, 1991.

[24] R. Turin and H. Geering, "Model-reference adaptive A/F-ratio control in an SI engine based on kalman-filtering techniques," in *Proceedings of the American Control Conference*, vol. 6, pp. 4082–4090, Jun, 21-23 1995.

[25] I. Barkana, "Robustness and perfect tracking in simple adaptive control," *International Journal of Adaptive Control and Signal Processing*, 2015.

[26] I. Barkana and H. Kaufman, "Global stability and performance of an adaptive control algorithm," *International Journal of Control*, vol. 42(6), p. 14911505, 1985.

[27] I. Barkana, "Gain conditions and convergence of simple adaptive control," *International Journal of Adaptive Control and Signal Processing*, vol. 19(1), pp. 13–40, 2005.

[28] H. S. Soyhan, H. Yasar, H. Walmsley, B. Head, G. T. Kalghatgi, and C. Sorusbay, "Evaluation of heat transfer correlations for HCCI engine modeling," *Journal of Applied Thermal Engineering*, vol. 9(2-3), pp. 541–549, 2009.

[29] K. Huber, G. Woschni, and K. Zeilinger, "Investigations on heat transfer in internal combustion engines under low load and motoring conditions," *SAE Paper 905018*, 1990.

[30] G. Woschni, "A universally applicable equation for the instantaneous heat transfer coefficient in the internal combustion engine," *SAE Technical Paper 670931*, vol. 76, 1967.

[31] G. F. Hohenberg, "Advanced approaches for heat transfer calculations," *SAE Technical Paper 790825*, vol. 88, 1979.

[32] B. S. Han, Y. Chung, Y. J. Kwon, and S. Lee, "Empirical formula for instantaneous heat transfer coefficient in spark-ignition engine," *SAE Technical Paper 972995*, vol. 1306, pp. 219–226, 1997.

[33] C. S. Wang and G. F. Berry, "Heat transfer in internal combustion engines," *ASME Winter Annual Meeting, Florida, Paper No. 85–WA/HT–23*, 1985.

[34] L. Eriksson, "Requirements for and a systematic method for identifying heat-release model parameters," *SAE Technical Paper 980626*, 1998.

[35] J. B. Heywood, *Internal Combustion Engine Fundamentals*. McGraw-Hill, 1988.

[36] C. Aquino, "Transient A/F control characteristics of a 5 liter central fuel injection engine," *SAE Technical Paper 810494*, 1981.

[37] A. Balluchi, L. Benvenuti, M. D. Benedetto, T. Villa, H. Wong-Toi, and A. Sangiovanni-Vincentelli, "Hybrid controller synthesis for idle speed management of an automotive engine," in *Proceedings of American Control Conference, IEEE, vol. 2*, p. 11811185, Jun, 28-30 2000.

[38] X. Jiao, J. Zhang, T. Shen, and J. Kako, "Adaptive air-fuel ratio control scheme and its experimental validation for port-injected spark ignition engines," *International Journal of Adaptive Control and Signal processing*, vol. 29(1), pp. 41–63, 2013.

[39] J. S. Souder and J. K. Hedrick, "Adaptive sliding mode control of air-fuel ratio in internal combustion engines," *International Journal of Robust and Nonlinear Control*, vol. 14(6), pp. 525–541, 2004.

[40] S. Choi, M. Won, and J. K. Hedrick, "Fuel-injection control of S.I. engines," in *Proceedings of the 33rd IEEE Conference on Decision and Control*, pp. 1609–1614, Dec, 14-16 1994.

[41] X. Jiao and T. Shen, "Lyapunov-design of adaptive air-fuel ratio control for gasoline engines based on mean value model," in *Proceedings of the 30th Chinese Control Conference*, pp. 6146–6150, Jul, 22-24 2011.

[42] K. Huber, G. Woschni, and K. Zeilinger, "Investigations on heat transfer in internal combustion engines under low load and motoring conditions," *SAE Technical Paper 905018*, 1990.

[43] L. Eriksson and L. Nielsen, *Modeling and Control of Engines and Drivelines*. John Wiley and Sons, 2014.

[44] P. Tunestal and J. K. Hedrick, "Cylinder air/fuel ratio estimation using net heat release data," *Control Engineering Practice: Advances in Automotive Control*, vol. 11(3), pp. 311–318, 2003.

[45] M. Rivas, *Modeling and control for Euro VI Spark Ignited SI Engine*. Ph.D. Thesis, Universite de Grenoble, 2013.

[46] P. Tunestal, *Estimation of the In-cylinder Air/Fuel Ratio of an Internal Combustion Engine by the Use of Pressure Sensors.* Ph.D. Thesis, Lund Institute of Technology, Sweden, 2001.

[47] P. M. Smith, *Crevice Volume Effect on Spark Ignition Engine Efficiency.* Master Thesis, Massachusetts Institute of Technology, Mechanical Engineering, 2013.

[48] B. Johansson, "Cycle to cycle variations in S.I. engines - the effects of fluid flow and gas composition in the vicinity of the spark plug on early combustion," *SAE Technical Paper 962084*, 1996.

[49] M. R. Belmont, M. S. Hancock, and D. J. Buckingham, "Statistical aspects of cyclic variability," *SAE Technical Paper 860324*, 1986.

[50] D. D. Brehob and C. E. Newman, "Monte carlo simulation of cycle-by-cycle variability," *SAE Technical Paper 922165*, 1992.

[51] G. Grunefeld, V. Beushausen, P. Andresen, and W. Hentschel, "A major origin of cyclic energy conversion variations in SI engines: Cycle-by-cycle variations of the equivalence ratio and residual gas of the initial charge," *SAE Technical Paper 941880*, 1994.

[52] C. S. Daw, C. E. A. Finneyz, J. B. Green, M. B. Kennely, J. F. Thomasy, and F. T. Connolly, "A simple model for cyclic variations in a spark-ignition engine," *SAE Technical Paper 962086*, 1996.

[53] P. Aleiferis, A. Taylor, J. Whitelaw, K. Ishii, and Y. Urata, "Cyclic variations of initial flame kernel growth in a honda vtec-e lean-burn spark-ignition engine," *SAE Technical Paper 2000-01-1207*, 2000.

[54] F. A. Ayala and J. B. Heywood, "Lean SI engines: The role of combustion variability in defining lean limits," *SAE Technical Paper 2007-24-0030*, 2007.

[55] N. Ozdor, M. Dulger, and E. Sher, "Cyclic variability in spark ignition engines a literature survey," *SAE Technical Paper 940987*, 1994.

[56] M. Kang, *Receding Horizon Optimal Control of Gasoline Engines.* Ph.D. thesis, Department of Engineering and Applied Sciences, Sophia Unicersity, 2014.

[57] M. A. Ceviz, B. avusoglu, F. Kaya, and I. V. Oner, "Determination of cycle number for real in-cylinder pressure cycle analysis in internal combustion engines," *International Journal of Energy Engineering*, vol. 36(5), pp. 2315–3618, 2011.

[58] R. Cremers, *Beginning for Cylinder Pressure Based Control.* Eindhoven University of Technology, Report No. WVT 2007.16, 2007.

[59] A. T. Lee, M. Wilcutts, P. Tunestal, and J. K. Hedric, "A method of lean air-fuel ratio control using combustion pressure measurement," *JSAE Paper 20014491*, vol. 22(4), 2001.

[60] J.-S. R. Jang, C.-T. Sun, and E. Mizutani, *Neuro-Fuzzy and Soft Computing: A Computational Approach to Learning and Machine Intelligence.* Prentice Hall, 1997, 1st Edition.

[61] Y. Yildiz, A. Annaswamy, D. Yanakiev, and I. Kolmanovsky, "Adaptive air fuel ratio control for internal combustion engines," in *Proceedings of American Control Conference, Seattle: IEEE*, pp. 2058–2063, Jun, 11-13 2008.

[62] K. J. Astrom and B. Wittenmark, *Adaptive Control.* Addison-Wesley, 1995, 2nd Edition.

[63] I. Barkana and H. Kaufman, "Simple adaptive control of uncertain systems," *International Journal of Adaptive Control System and Signal Processing*, vol. 2(2), pp. 133–143, 1988.

[64] I. Barkana, "Simple adaptive control-a stable direct model reference adaptive control methodology-brief survey," *International Journal of Adaptive Control System and Signal Processing*, vol. 28(7-8), pp. 567–603, 2013.

[65] A. E. Hoerl and R. W. Kennard, "Ridge regression: Biased estimation for non-orthogonal problems," *Technometrics*, vol. 12, pp. 55–67, 1970.

[66] T. Hastie, R. Tibshirani, and J. Friedman, *The Elements of Statistical Learning: Data mining, Inference and Prediction.* Springer-Verlag, 2nd Edition, New York, 2008.

[67] R. Tibshirani, "Regression shrinkage and selection via the lasso," *Journal of the Royal Statistical Society, Series B*, vol. 58, pp. 267–288, 1996.

[68] J. Maindonald and W. J. Braun, *Data Analysis and Graphics Using R an Example-Based Approach.* Cambridge Series in Statistical and Probabilistic Mathematics 3rd Edition, 2010.

[69] P. A. Ioannou and K. S. Tsakalis, "A robust direct adaptive control," *IEEE Transaction on Automatic Control*, vol. 31(11), pp. 1033–1043, 1986.

[70] J. Hou, X. Qiao, Z. Wang, W. Liu, and Z. Huang, "Characterization of knocking combustion in HCCI DME engine using wavelet packet transform," *Journal of Applied Energy*, vol. 87(4), pp. 1239–1246, 2010.

[71] H. Machrafi, S. Cavadias, and J. Amouroux, "A parametric study on the emissions from an HCCI alternative combustion engine resulting from the auto-ignition of primary reference fuels," *Journal of Applied Energy*, vol. 85(8), pp. 775–764, 2008.

[72] U. Asad and M. Zhen, "Diesel pressure departure ratio algorithm for combustion feedback and control," *International Journal of Engine Research*, vol. 15(1), pp. 101–111, 2014.

[73] L. Eriksson, "Requirements for and a systematic method for identifying heat-release model parameters," *SAE Technical Paper 980626*, 1998.

[74] K. H. T. Zar, N. Uchiyama, T. Unno, S. Sano, S. Noda, and Y. Fujita, "Diesel engine dynamics modeling considering fuel injection period based on combustion heat release rate identification," *Journal of Thermal Science and Technology*, vol. 8(1), pp. 58–73, 2013.

[75] N. P. Komninos, "Modeling HCCI combustion: Modification of a multi-zone model and comparison to experimental results at varying boost pressure," *Journal of Applied Energy*, vol. 86(10), pp. 2141–2151, 2009.

[76] N. P. Komninos and G. M. Kosmadakis, "Heat transfer in HCCI multi-zone modeling: Validation of a new wall heat flux correlation under motoring conditions," *Journal of Applied Energy*, vol. 88(5), pp. 1635–1648, 2011.

[77] M. Lapuerta, O. Armas, and S. Molina, "Study of the compression cycle of a reciprocating engine through the polytropic coefficient," *Journal of Applied Thermal Engineering*, vol. 23(3), pp. 313–232, 2003.

[78] M. Lapuerta, O. Armas, and J. J. Hernandez, "Diagnostic of DI diesel combustion from in-cylinder pressure signal by estimation of mean thermodynamic properties of the gas," *Journal of Applied Thermal Engineering*, vol. 19(5), pp. 513–529, 1999.

[79] F. Yan and J. Wang, "Engine cycle-by-cycle cylinder wall temperature observer-based estimation using cylinder pressure signals," *Journal of Dynamic Systems, Measurement, and Control*, vol. 134(6), 061014-1, 2012.

[80] C. Wilhelmsson, A. Vressner, P. Tunestal, B. Johansson, G. Sarner, and M. Alden, "Combustion chamber wall temperature measurement and modeling during transient HCCI operation," *SAE Technical Paper 2005-01-3731*, 2005.